CHAPTER VII

WATER MASSES AND CIRCULATION IN THE TROPICAL INDIAN OCEAN

The Indian Ocean is the smallest and the least explored ocean of the world. It occupies approximately 20% of the world ocean (73.6 x 10^6 sq. Km). The Indian Ocean is bounded to the north by Iran, Pakistan, India and Bangladesh; to the west by Africa and Arabia; to the east by Myanmar (Burma), Malayan Peninsula, Thailand, Indonesia and Australia; to the south by the Antarctic continent. The Indian Ocean connects to the Atlantic Ocean near the southern tip of South Africa; it connects to the Pacific Ocean through the straits and marginal seas, such as Sunda straits, the Timor and Java Seas and the Great Australian Bight.

The Indian subcontinent divides the northern Indian Ocean into two marginal seas - the Arabian Sea to the west and the Bay of Bengal to the east. The Mediterranean Sea, the Persian Gulf and the Red Sea, join the Arabian Sea. The chain of Andaman and Nicobar islands separate the Andaman Sea from the Bay of Bengal. A hydro-chemical front located along 10°S (Wyrtki, 1973b) is generally taken as the boundary between the south and north Indian Oceans. Wind reversals due to the monsoons are seen primarily to the north of this latitude.

The Indian Ocean is used to be the least known among the world oceans prior to 1960’s. The International Indian Ocean Expedition (IIOE) conducted from 1962 to 1965 with participation of 20 countries and 40 research vessels led to the collection of a vast amount of oceanographic data and increased our knowledge immensely. Subsequent to IIOE, several field experiments designed for monsoon related and process oriented studies in Indian Ocean viz.(Indo Soviet Monsoon Experiment (ISMEX) (1973), MONSOON (1977), Monsoon Experiment (MONEX) (1979), Indian Experiment (INDEX) (1979-80), Monsoon Trough Boundary Layer Experiment (MONTBLEX) (1990), World Ocean Circulation Experiment (WOCE) (1990-1997) Joint Global Ocean Fluxes Studies (JGOFS) for the Indian Ocean (1992-1997), Indian Ocean Experiment (INDOEX) (1998 and 1999), Joint Air-Sea Monsoon Interaction Experiment (JASMINE) (1999) and the Bay of Bengal Monsoon Experiment (BOBMEX) (1998 -1999) and Arabian Sea Monsoon Experiment (ARMEX) (2002 - 2003) under International Climate Research Program (ICRP) were conducted and a vast amount of data were collected. The Indian research vessels RV Gaveshani (commissioned in 1976) and ORV Sagar Kanya (commissioned in 1983) played significant role in the data collection under these programs. For the last few years, satellites with dedicated sensors for ocean parameters like SST, sea surface winds, waves, topography, and ocean colour are providing a wealth of data contributing to the studies of ocean processes of the Indian Ocean. The MISMO (Mirai Indian ocean cruise for the Study of the MJO-convection Onset)(2006) and CERENE are the recent process oriented experiments conducted in the equatorial Indian Ocean by the Japan and France.

On the basis of the circulation system, the Indian Ocean is divided into three regions viz., i) the seasonally changing monsoon gyre, ii) the southern hemisphere subtropical anticyclonic gyre and iii) the Antarctic waters with the circumpolar current.

The general circulation showing different warm and cold currents are shown in Fig.7.1a.

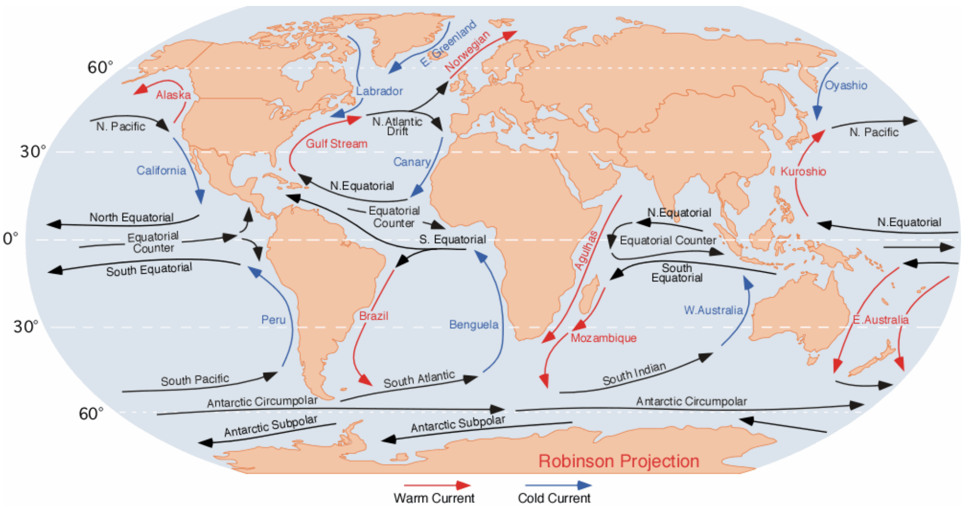

Fig.7.1a.Major circulations in the oceans

Oceans are not just bodies of stagnant water. Ocean water moves from one place to another. Waters at different depths move in different directions and at different speeds. Surface waters move because of wind. Waters at different depths also move due to differences in density which in turn depends on temperature and salinity. Such movements of ocean water are called currents. Currents are like rivers in the oceans. They can carry enormous amounts of water. For example, the Antarctic Circumpolar Current can transport 100 million cubic metres of sea water per second (100 Sverdrups)! Fig.7.1b corresponding to table 7.1 shows the major currents of the world ocean. Brick red arrows show warmer and purple arrows show warm and navy blue shows cold currents.

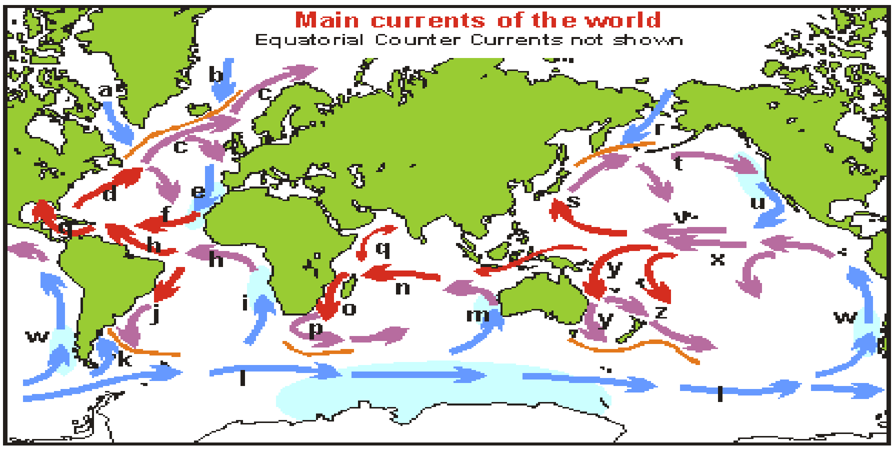

Fig.7.1b.Major currents in the oceans

a Labrador Current	n South Equatorial C.
b East Greenland C.	o Mozambique C.
c North Atlantic Drift	p Agulhas C.
d Gulf Stream	q Monsoon Drift
e Canary C.	r Kamchatka C./Oya Shio
f North Equatorial C.	s Kuro Shio C.
g Caribbean C.	t North Pacific Drift
h South Equatorial C.	u California C.
i Benguela C.	v North Equatorial C.
j Brazil C.	w Peru/ Humboldt C.
k Falkland C.	x South Equatorial C.
l West Wind Drift	y East Australia C.
m West Australian C.	z East Auckland C.

Table 7.1 major current systems of the world oceans

In the oceans the general circulation of the ocean comprises of gyres, Equatorial current system, and western and eastern boundary currents. A combination of four forces viz., surface winds, the sun's heat, the coriolis effect and gravity makes the ocean surface to circulate clockwise in the Northern Hemisphere(N.H) and counter clockwise in the Southern Hemisphere (S.H) are called gyres. These gyres are called the back bone of the circulation as shown in Fig.7.1c. The equatorial current system comprises of westward flowing North and South equatorial currents, eastward flowing equatorial counter current, equatorial jets and eastward flowing equatorial under current. While western boundary currents are swift, eastern boundary currents are in general weak. Indian Ocean circulation is different from that of the other major oceans.

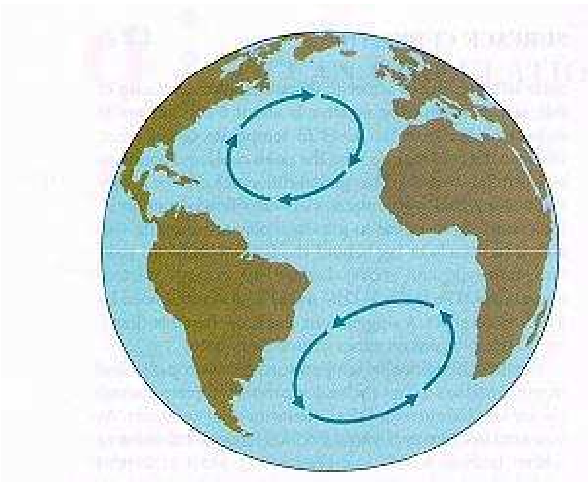

Fig.7.1c. The clockwise and anticlockwise gyres in the northern and southern hemispheres- the back bone of the circulation.

The surface circulation of the Indian Ocean resembles that of the other major world oceans (the Atlantic and the Pacific oceans) during the boreal (Northern Hemispheric) winter season and undergoes drastic change during boreal summer season only in the north Indian Ocean leaving the south Indian Ocean unaltered.

This change in the circulation north of the equator is largely controlled by the prevailing monsoon winds (Fig.7.2). The south Indian Ocean circulation is characterized by a subtropical anticyclonic gyre. The westward flowing South Equatorial Current (SEC) in the 10^oS-20^oS

latitudinal belt forms the northern boundary of the gyre. The poleward flowing Agulhas Current lies west (Fig.7.1b), the eastward flowing Antarctic Circumpolar Current (ACC) lies south and the equatorward flowing West Australian Current lies east of SEC (Fig.7.1b).

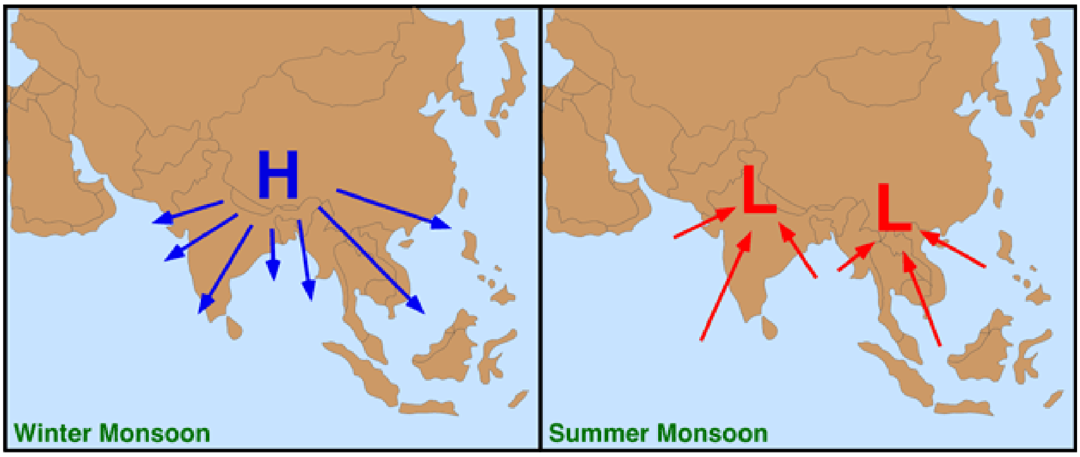

Fig. 7. 2. Reversal of wind direction during winter to summer monsoon. 'H' indicates High pressure and 'L' indicates Low pressure

7.1. Main features of Indian Ocean circulation:

The surface circulation system north of about 10°S undergoes drastic seasonal changes under the influence of the seasonally reversing wind system (Fig.7.3). During the winter monsoon season, northeast trade winds bring cool, dry continental air, while during the summer monsoon season, the strong southwest winds bring humid maritime air into the northern Indian Ocean and to the Indian sub continent. In response to these wind systems, the surface circulation undergoes seasonal changes (Fig.7.4) in the north Indian Ocean, the details of which are given in the following pages. South of 10°S the seasonal changes of winds are smaller, and therefore, the variability of the ocean circulation in the southern part of the Indian Ocean is also smaller.

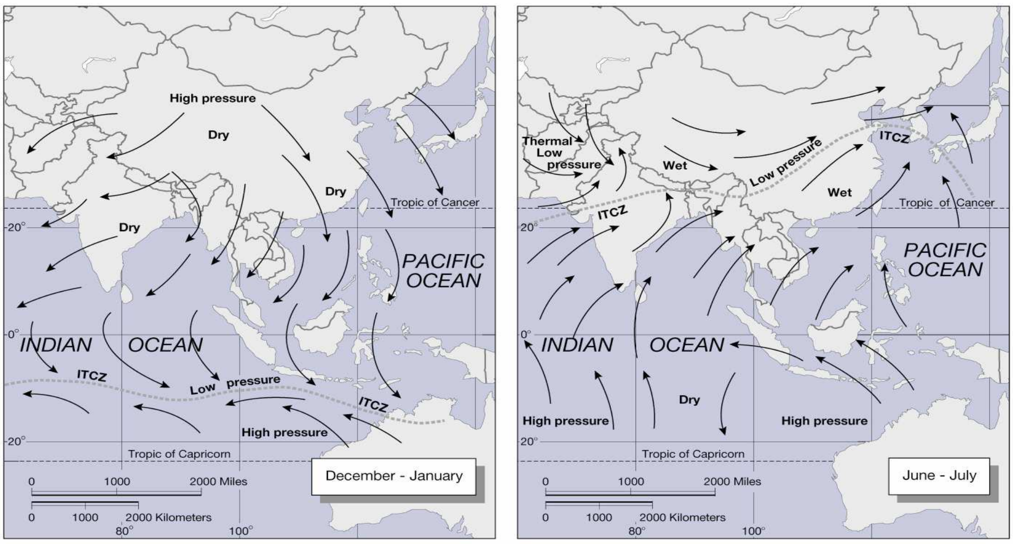

Fig.7. 3 wind and pressure distribution during winter (a : Dec-Jan) and summer (b: June-July).ITCZ is shown as dotted wavy curve.

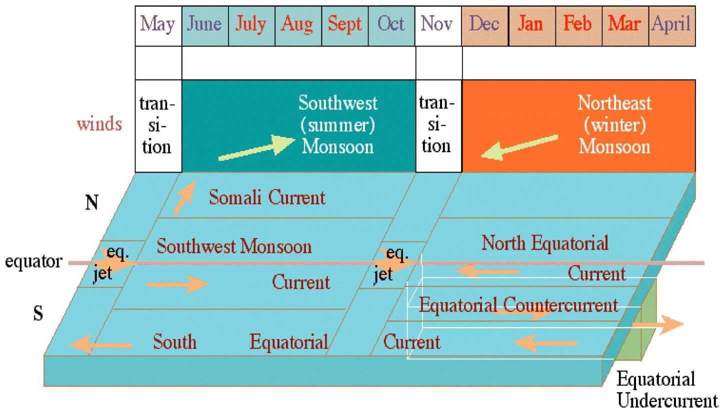

Fig.7. 4. plan view of different surface currents in Indian Ocean with respect to two different monsoons (by courtesy from www.indianocean.free.fr/ref.2.html#tomczak)

7.1.1. Surface circulation during the northeast monsoon season (December-March):

The seasonal reversal of the surface wind field over the tropical Indian Ocean is more dramatic than in the other regions of low latitudes, and these reversals have profound effects on the upper hydrospheric structure and seasonal variations of surface current system. The northeast monsoon starts in December and reaches its maximum strength during January-March. The wind direction is from northeast north of the equator, northerly at the equator and northwesterly south of it. The surface wind field provides the major mechanical forcing for the basin wide upper ocean circulation.

The current patterns in the tropical Indian Ocean during winter can be characterized as two counter rotating gyres extending across the entire basin (Fig.7.5). The southern gyre rotates clockwise (cyclonic) and is bounded on the south by the South Equatorial current (SEC) and on the north by the Equatorial Counter Current (ECC). The axis of this gyre appears at about 10°S across the basin. The SEC extends from 20°S to 10°S, while the ECC is observed between 10°S and equator. The North Equatorial Current (NEC) represents the northern boundary of the counter clockwise rotating northern gyre. This gyre is bounded on the south by the ECC. The axis of this gyre is located approximately on the equator. Both gyres are closed on the west by the equatorward flowing boundary currents along the African coast, namely, the East African Coastal Current (EACC) and the Somali Current (SC). The SEC feeds the EACC, which separate from the boundaries south of the equator. The SC is fed by the retroflection of NEC at the coast and exhibited continuous southward flow along the boundary from about 8°N to 3°S. As a further extension of SEC, there are two southward flowing boundary currents, namely, the Mozambique Current (MZC) (Fig.7.1b) and the East Madagascar Current (EMC) (Fig.7.5). In the northern Arabian Sea, the circulation is not well defined during this season. One branch of NEC circulates around the islands of Laccadives and flows along the west coast of India as poleward flowing West India Coastal Current (WICC). A prominent feature of circulation in the Bay of Bengal is the equatorward flowing East India Coastal Current (EICC) (Fig.7.5).

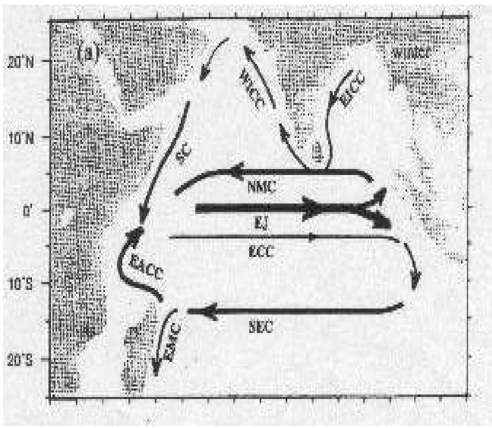

Fig.7. 5 Schematic diagram of major surface currents in the TIO during winter and pre - monsoon. The thick and bold arrow along the equator represents the Equatorial Jet during pre- and post-monsoon seasons.

7.1.2. Surface circulation during pre-monsoon season (April-May):

In April-May, during the transition period between northeast and southwest monsoon seasons, the winds north of the equator get weakened and moderate eastward winds blow along the equator. An anticyclonic wind gyre is found over the Bay of Bengal, broadly overlying the anticyclonic ocean gyre.

The most dramatic circulation feature in the spring season is the development of intense eastward Equatorial Jet (EJ) (Fig.7.5) driven by the semiannual eastward winds. The EJs occur in a narrow band, trapped within 2°-3°of equator, mostly in the central and eastern parts with a speed of nearly 1.5 m/s during May. At the western boundary of the Indian Ocean, the Somali Current flows southwestward and meets northward flowing EACC near the equator.

In early May, the Somali Current responds rapidly to the onset of local southwesterly winds, reverses its direction and flows northward as continuation of EACC near the equator. There are hardly any changes in the current pattern in the southern tropical Indian Ocean.

7.1.3. Surface circulation during the southwest monsoon season (June – September):

During the southwest monsoon season (June- September) (Fig.7.6), the southeast trades of the southern hemisphere crosses the equator, change direction and sweeps as south-westerlies over the entire north Indian Ocean. The surface circulation south of the monsoon regime, ie, 10°S does not show much seasonal variability. The SEC and EACC feed the northward flowing SC. It then crosses the equator, and a part turns offshore at about 4°N, flows southward and re-circulates across the equator as the Southern Gyre (SG). With the onset of intense southwest monsoon winds in June, a strong anticyclonic gyre (clock wise) forms, called the 'Great Whirl' that develops in the north between 4°N and 10°N (Fig.7.6b). A 'Socotra Eddy' is also observed in summer monsoon northeast of Socotra (right of Fig.7.7g). In August-September, the southern cold wedge propagates northward along the coast and meets the northern one and the Somali Current appears as a continuous current from the equator up to 10°N. In some years this circulation pattern exhibits inter annual variability.

In the Arabian Sea, the Somali Current feeds the eastward flowing low latitude monsoon current known as the Southwest Monsoon Current (SMC). The equatorward flowing WICC joins SMC and much of the SMC turns northward into the Bay of Bengal, flowing around the cyclonic

Sri Lanka Dome (SD). In the northern Bay of Bengal, north of 15°N, the eastward currents which are already set during April -May remain until August.

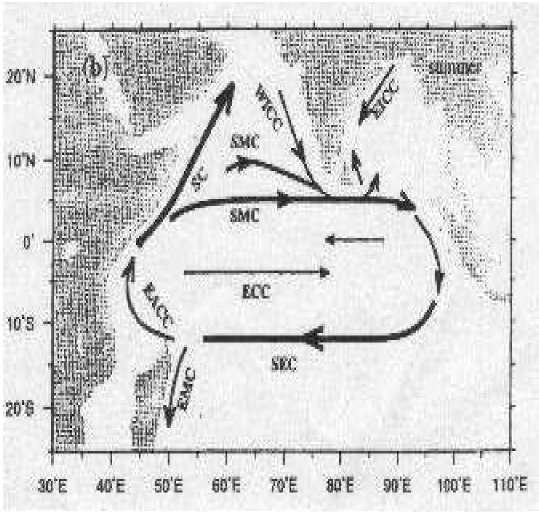

Fig.7. 6 a Schematic diagram of major surface currents in the TIO during the southwest (summer) monsoon. The thickness of arrows represents the relative magnitudes of the currents. (Adapted from Shenoi et al., 1999a)

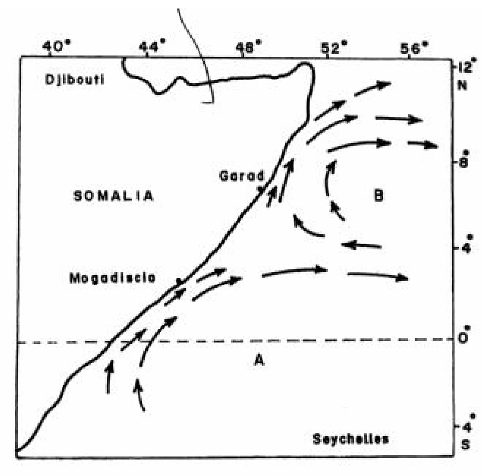

Fig.7. 6 b The two gyres of Somali current.

7.1.4. Surface circulation during the post monsoon season (October-November):

October-November corresponds to the second transition period between the end of southwest and the beginning of northeast monsoon. At the equator, moderate eastward winds blow in strength slightly higher than the pre-monsoon season and the wind vanishes north of the equator. The equatorial circulation is dominated by eastward Equatorial Jet (EJ) within 2°-3° of

the equator (Fig.7.5) with strength higher than the pre-monsoon EJs. The strong SC observed during southwest monsoon decreases in its strength and continues to flow northward. The EACC continues to flow equatorward. There are no changes in the circulation pattern in the southern tropical Indian Ocean.

7.2. Arabian Sea Circulation:

The Arabian Sea is one of the few tropical basins that has limited northern extent and is forced by the seasonally reversing monsoon winds. These winds regulate various physical processes including the upper ocean circulation. The most prominent and the best documented variations of upper ocean circulation can be seen off the coast of Somali.

7.2.1. The Somali Current:

It is the western boundary current in Indian Ocean (Fig.7.7A,a_2) with a volume transport comparable to that of the Gulf Stream and reverses in an annual cycle in response to the changes between the northeast and southwest monsoon seasons. It flows northeastward during the summer (Fig.7.7a_2) and southwestward during the winter (Fig.7.7a_3). At its peak, during the southwest monsoon season, surface currents with magnitudes ranging from 3 to 4m/s have been reported, and its volume transport has been estimated to be 70 million tons per second.

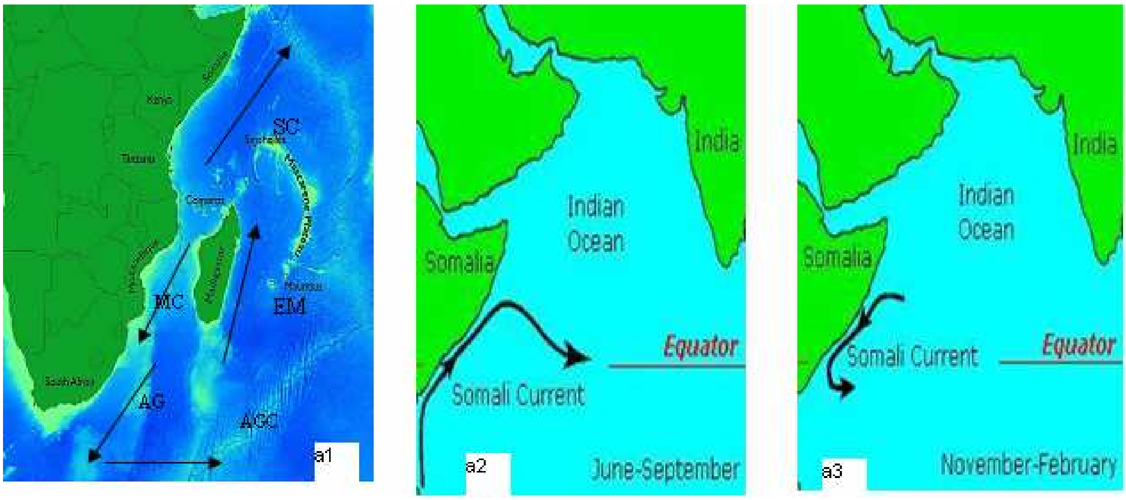

Fig.7.7A (**Left**)Different Currents in the Somali / Mozambique / Aghulas Basin , SC-Somali current; MC-Mozambic current; EM- East Madagascar current; AG- Agulhas Current; AGC- Agulhas Counter Current (Retroflection) (a_1); (**Center**) Somali current during Southwest monsoon (a_2); (**Right**)) Somali current during Northeast monsoon (a_2).

The first survey of the circulation of the Somali Current was carried out by Swallow and Bruce (1966) during the IIOE period. From the hydrographic measurements of Somali Current between equator and 12°N, during the southwest monsoon of 1970, Bruce (1973) identified two upwelling areas off Somalia (Fig.7.7 b), each being associated with a branch of the current that turned eastward offshore. More evidence for the existence of a two-gyre circulation pattern (Fig.7.7 C) was provided by measurements during 1975-1978 with XBT's from tankers running from the Persian Gulf to South Africa. These studies showed that a large eddy first formed in the Somali region approximately between 4 °N and 12°N during late May or early June (Fig.7.7 d& red spot in 7.9a). Bruce (1979) called it as the 'Prime eddy' because it appears to be first formed in the region upon the commencement of the southwest monsoon. Prime eddy was considerably larger and more energetic than the other eddies formed during the season and it has been observed

to remain in this location at least for 3 months after the cessation of the southwest monsoon. A smaller eddy associated with the Prime eddy was observed each year (1975-76) off Socotra between 12°N and 15°N. Also during another year (1976), a southern eddy was observed south of about 5°N and adjacent to the southern boundary of the prime eddy to the east of African coast. Observations indicate that northeastward flowing Somali Current is clearly part of the eddy field.

Large areas of cold waters along the Somali Coast (Fig.7.8) were observed between 5°N and 10°N during June and July. The cold waters associated with the northern and southern eddy systems could be traced several hundred kilometers off shore. By late August, the cold wedge at 5°N translated north eastward up to 10°N with a speed of 15 to 30 m/sec indicating a coalescence of the systems. Further observations say that the Somali Current system contained two clockwise gyres, one south of 5°N, the other between 5°N and 10°N for at least part of June. They have presented evidence suggesting that the southern gyre appeared within a week or two of the onset of local south-westerly winds and that the northern gyre was well developed within two weeks of the appearance of the strong southwesterly wind off northeastern Somalia.

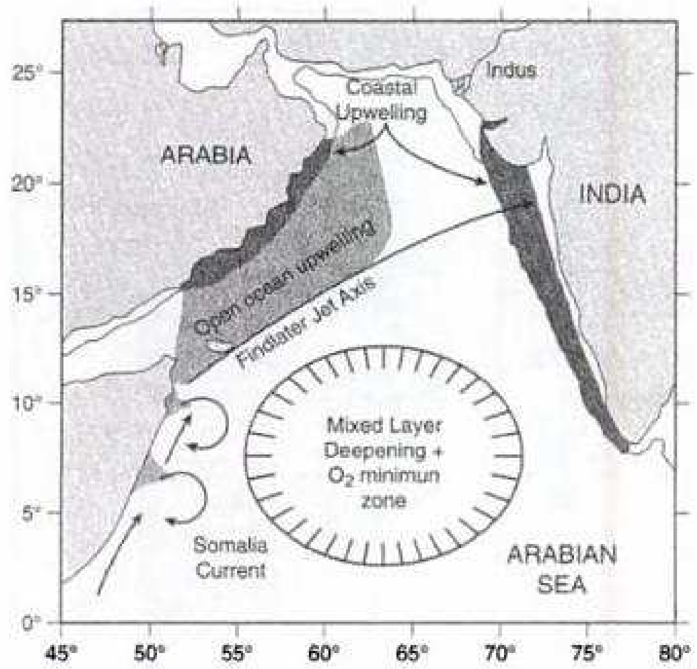

Fig.7. 7 b.Depicting coastal upwelling (black patch) along the coasts of Arabia, Somalia and west coast of India resulting from the influence of Findlater jet and upward Ekman pumping . (Adapted from Summerhayes,C.P etal., Eds., upwelling in the Ocean: Modern Processes and ancient records. John Wiley & Sons. Chichester.1995.422)

Fig.7.7c shows the circulation characteristics in the vertical (upwelling) in the North West Indian Ocean. Open arrows show the lateral advection from the Somalia and Arabia upwelling system, which transports nutrient–rich waters to the central Arabian Sea. Thin dark arrows show the prevailing flow in summer. Long open arrow with the bold face is the atmospheric Find later jet, which extends from the tip of Somalia to Gujarat, India. The positive (negative) wind stress curl north (south) of this jet drives the cyclonic (anticyclonic) circulation in the sea, which is indicated by the anticlockwise (clockwise)arrow; the dark, short arrows out of (into) it show the associated divergence (convergence). The right hand side of the box shows the climatological mean thermal structure for August along 64^{O}E, based on Levitus data, which show the northward shoaling of the isotherms (shallowing of thermocline).

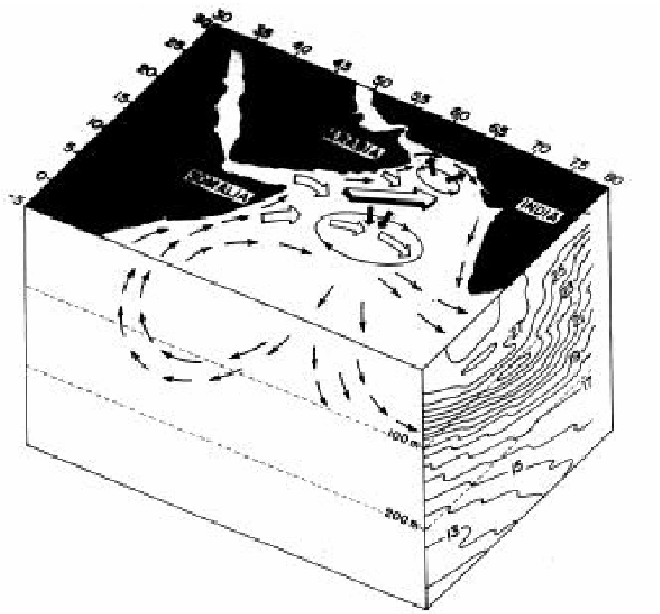

Fig.7. 7 c. Schematic representation of the flow regimes and the physical forcing that fertilizes the central Arabian Sea during summer – Two gyre circulation pattern (Adapted from Prasannakumar et al. 2001).

In short, the observed high biological production in the central Arabian Sea is mediated by a combination of processes that vary from north to south of the axis of the Findlater Jet (Fig.7.7d). In the northern region, upward Ekman pumping and entrainment driven by basin-wide winds along with advection of upwelled waters from the coastal region of Arabia (Fig.7.7b), supply nutrients to the upper layers. In the southern region, nutrients advected from the Somali upwelling region lead to fertilization. Figure 7.7b shows the schematics of the above-mentioned physical processes that are responsible for making the central Arabian Sea biologically productive during summer.

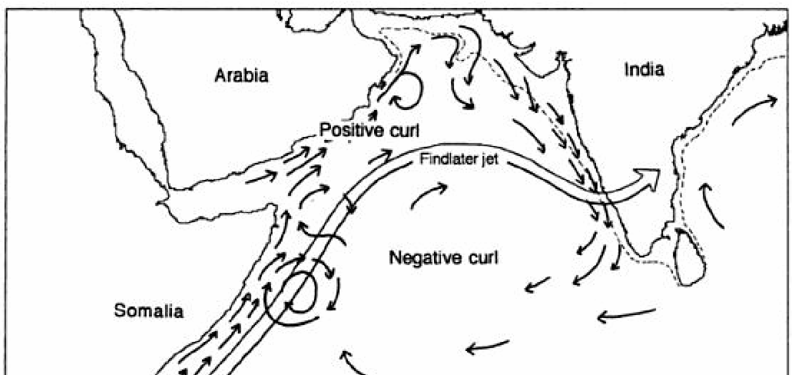

Fig.7. 7 d. The effect of Findlater jet of the low level atmospheric circulation which crosses off the coast of Somalia (solid line). To the south of the jet, negative curl of the wind stress deepens the mixed layer, to the north positive curl causes the mixed layer shoal and it is an important factor in coastal upwelling. Note the anticyclonic features of the Great whirl and the Socotra eddy off Somalia and the similar eddy east of Arabia.

The Findlater Jet forces cold, nutrient-rich water to upwell along the coast of Somalia and Arabia and makes it one of the most productive oceans in the world (Fig.7.7 e). The jet has been thought of as a broad, smooth and continuous flow in the beginning (Fig.7.7 d). But analyses of recent satellite data reveal that it is disrupted by some eddies created by differences in SST and wind shear (Fig.7.7f). During the summer monsoon, the jet drives the northward Somali Current and creats several stationery eddies, among them the Great Whirl (I) is famous (left panel of Fig.7.7g). Together with the coastal upwelling, these eddies form patches of cold surface water in the warm Arabian Sea. These cold patches slow down the Findlater Jet. It may be noted in the right panel of Fig.7.7g, wind speed is less than 10 m/s over the cold filaments south of Socotra Island (<21^{o}C) and increases to nearly 15 m/s over the warm waters east of the island (>24^{o}C). The red letter 'H' indicates the regions of high winds of the Findlater Jet and the red arrow indicates the Socotra Island. This surprising covariation between SST and wind is an example of SSTs and winds that correlate positively in regions of warm-cold ocean fronts (Xie, 2004).

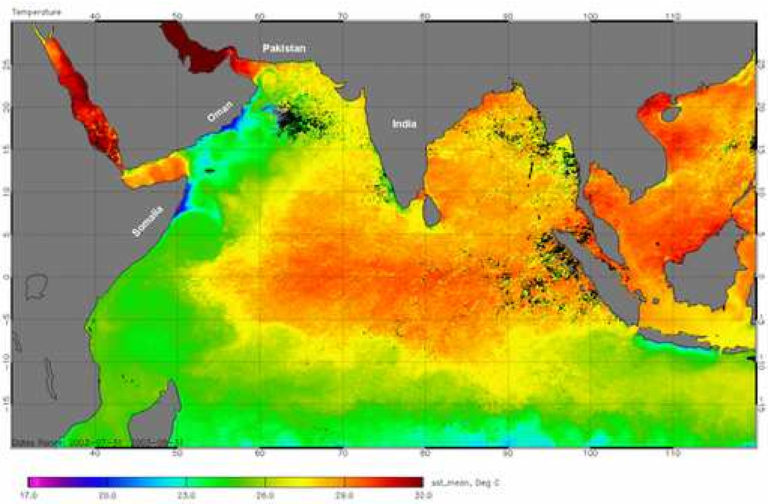

Figure 7. 7e. MODIS 11 µm SST from the month of July, 2003. This is the peak time for the southwest Indian monsoon. Somali current is well established towards north and shows in the image as vast areas of cold waters (green color) off the east coast of Africa due to upwelling (www.daac.gsfc.nasa.gov./oceancolor/scifocus/modis/indianmonsoon-Fig.3.png)

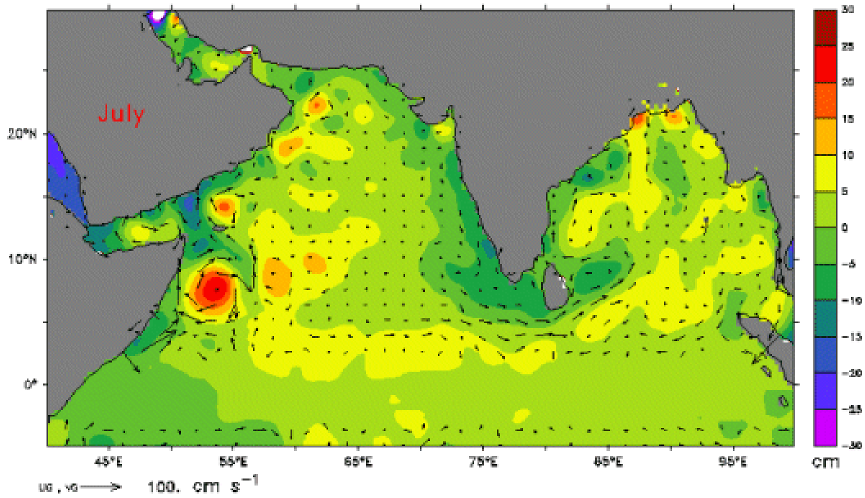

Fig. 7. 7f. North Indian Ocean circulation during July. See the Great whirl or Prime eddy off Somalia (red spot). The color code indicates the height of sea level. Note the low sea level along west coast of India (By courtesy of NOAA) & (Credits Topex/Poseidon, National Institute of Oceanography, Goa, India).

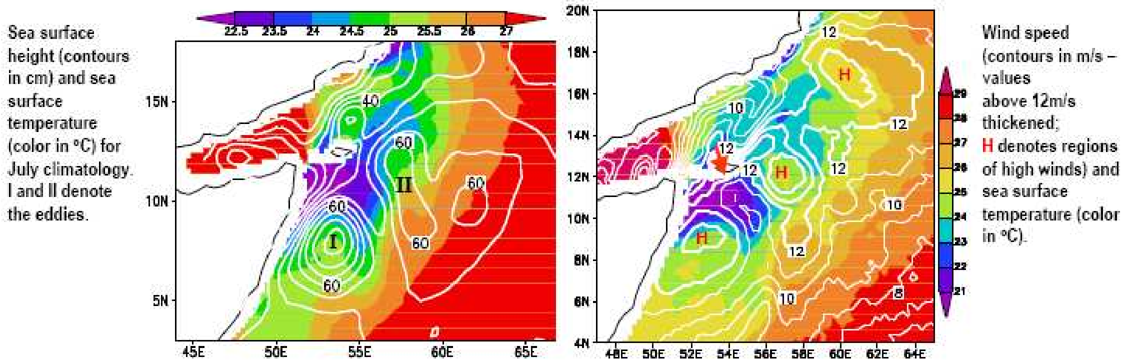

Fig.7. 7g Sea surface height (cm), SST (^{O}C) and wind speed off Somalia during July.The red arrow in the right figure indicates Socotra island (Vecchi, G.A., S.P. Xie, and A.S. Fischer, 2004, *J. Climate*; S.-P.Xie, 2004, *Bull. Amer. Meteor. Soc*.)

Directly north of the Mozambique Channel, the northward setting current along the coast of the African continent is called the Zanzibar Current (ZC) (Fig7.8). It has its main source the northern part of the westward flowing South Equatorial Current (SEC). During the north east monsoon season the Zanzibar Current is opposed by the southward flowing Somali Current and this meeting point usually shifts southward as the season progresses. It is only the surface expression of the Zanzibar Current that is prevented from moving northward. At subsurface depths this ZC continues as an undercurrent below the Somali Current. The north east monsoon occurs during the months of November-February, and is the strongest in February.

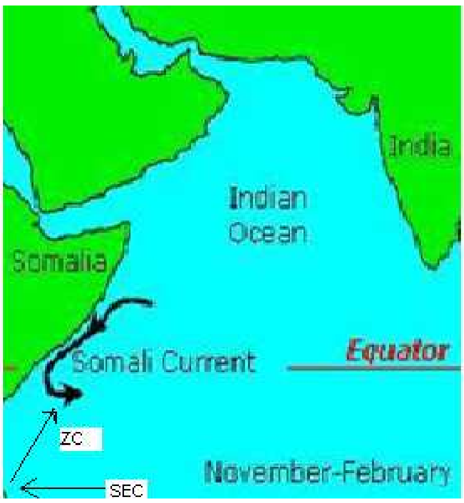

Fig.7.8. The flow of Zanzibar Current (ZC), South Equatorial Current (SEC) and Somali current during North East monsoon season.

During the opposite wind phase, the south west monsoon season (June to October, maximum in August), the Zanzibar Current is strengthened considerably forming as a tributary to the Somali Current carries water northward as an intense coastal jet (Fig.7.7a$_2$). Speeds in this jet may reach up to 3.5 m/s. The southern part of the current is shallow. The northward flow of the Somali Current during the south west monsoon season is not simply alongshore. The flow turns

offshore at about 3°N. North of this point a strong upwelling cell has been observed (Fig.7.7b). Two coastal gyres (Left -Fig.7.7g) are then created at the sides of this upwelling cell. These gyres seem characteristic of the flow during the beginning of this season. As the season advances, these upwelling gyres shift northward, join together and by the time of the most intense part of the south west monsoon in August, the Somali Current is established as a continuous western boundary current from the Zanzibar Current in the south to the East Arabian Current in the north.

The monsoonal wind patterns vary year to year and so in consequence of this, the Somali Current also varies. This inter-annual variability may have a decisive influence on the shelf circulation, on the marine ecosystem of the region and also on the success of the local fisheries.

In the Somali basin during southwest monsoon, the low salinity water (< 35.1‰) of the SEC get mixed up with the high salinity (> 35.3 ‰) surface waters of the Arabian Sea. During the late summer monsoon, after the collapse of the two gyre system, the Somali Current flows as a continuous current carrying low salinity waters from south of equator to 10°N latitude. Somali Current is not continuous before the onset of northeast monsoon. Instead, cross-equatorial flows with low surface salinity are joined to turn offshore south of 2°N, and between 6°N and 11°N, large anticyclonic gyre (Great whirl) with high surface salinity are observed.

Using shipboard current profile, Leetma (1982) measured the transport in the Somali Current system during March-July 1979 in the top 100m (Fig.7.9 A). He found that just south of the equator the transport is 10-15 Sv and is east-west t. Quadfasel and Schott (1983) carried out current meter measurement near 5°N off Somali coast for a period of 2½ years and reported the existence of permanent southward subsurface current in the depth range of 150 to 600 m with a speed of 15 cm/s (Fig.7.9 B,c-e). They have estimated the annual mean southward transport of Somali Current to be around 5 Sv. Schott (1986) found that the southward Somali Current during the winter monsoon season extended up to 150m and northward flow occurred up to 400m, followed again by southward flow underneath.

Schott et al., (1990) found that current structure during the summer monsoon season between 4°S and 12°N (Fig.7.9A,a) is similar to western boundary current, while the profile in winter consist of a thin surface layer of southward flow(Fig.7.9A,d), a northward undercurrent between 120m and 400m depth (Fig.7.9 B) and below that a reverse flow again to southward. He has computed the summer mean transport close to zero and the annual mean transport in the upper 500m is 10Sv northward. Fisher et al., (1996) found that the monsoon circulation was confined to the upper 300m depth, with intense surface currents up to 2.2m/s and 1.4 m/sec in the Great Whirl and Socotra Gyre regions respectively. Moored array observation during WOCE 1995-96 and shipboard sections of winter 1997/98 conducted off the south of Socotra and Socotra passage by Schott and Fisher (2000) showed that the northern Somali Current during that time was characterized by an inflow from the east, causing a divergence at the coast somewhere near 6-8°N, with northward surface flow north of these latitudes and equatorward flow south of them. The northward surface flow passes through the Socotra passage, but also veers eastward along the southern banks off Socotra. From the moored array studies, Dengler et al., (2002) concluded that the depth of monsoon response of the Great Whirl was less than 1500 m.

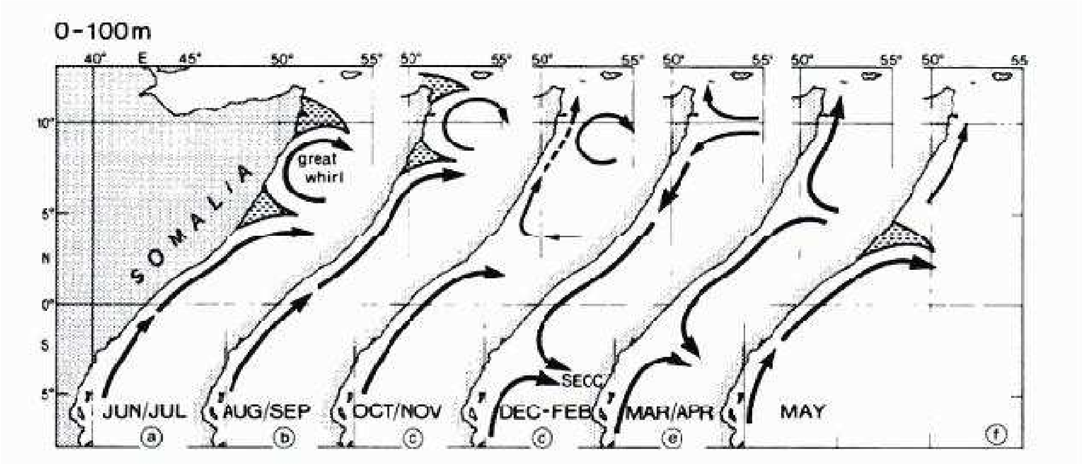

Fig. 7. 9 A. Somali current pattern during different seasons for top 100m. Hatched areas shows upwelling cells.The bottom most arrow shows Zanzbar cuurent and the northern arrow shows the Somali Current Adapted from Schott et al. (1990)

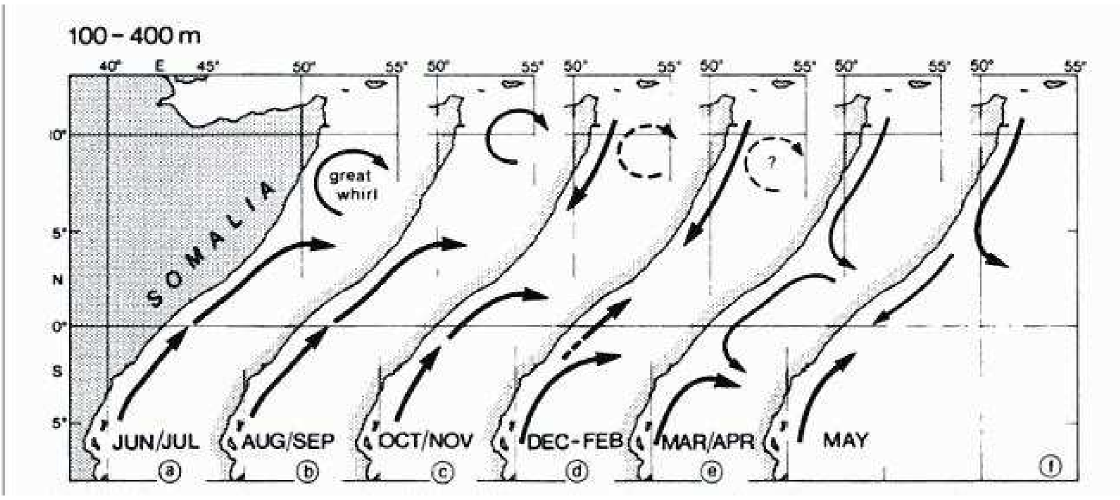

Fig. 7. 9 B. Somali current pattern during different seasons for 100-400m. Adapted from Schott et al. (1990)

Three Somali undercurrents (5^oS-0^o, 0^o- 5^oN, 5^oN-10^oN) have been observed at different locations and at various times during the year (Fig.7.9 B). In April to early June, a southward undercurrent between 5^oN-10^oN (Fig.7.9 B, c to f) develops just beneath the northward surface flow (Fig.7.9 A, c to f) in a depth range from about 100m to 300m. Leetma et al., (1982) has estimated the maximum instantaneous speed of this undercurrent to be 60cm/s.

The second undercurrent was observed during fall and winter flowing southward underneath the northward flowing branch of Somali Current in the region 8-12°N (Quadfasel and Schott, 1983). They measured southward velocities of about 30cm/s below 100m in the passage between Socotra and the mainland in January 1998.

A third cross-equatorial northward undercurrent was observed during the winter season in a depth range of 150-400m. Studies of Schott et al., (1990) showed that the transport of this northward undercurrent almost balances the southward surface flow of the Somali current.

7. 3. Monsoon Currents:

The zonal monsoon circulation between Sri Lanka and equator is a crucial link for the exchange of water between the Arabian Sea and the Bay of Bengal. Cutler and Swallow (1984) showed that this circulation reverses with the change of monsoons. It flows eastward as southwest monsoon current (SMC) from June to September (Fig.7.6a) and westward as the Northeast Monsoon Current (NMC) from December to March (Fig.7.5).

7.3.2. Southwest Monsoon Current (SMC):

The Southwest Monsoon Current (SMC) flows eastward south of India, turns around Sri Lanka and enters into Bay of Bengal (Fig.7.10). According to Shenoi et al., (1999) & Unnikrishnan et al., (2001) a part of SMC appears to flow southeastward between 80°E-88°E and crosses the equator near Sumatra. The SMC thus transports Arabian Sea high salinity water into the Bay of Bengal.

The first direct measurement of the seasonal variation of monsoon currents was carried out by Schott et al., (1994). The moored and shipboard ADCP (Acoustic Doppler Current Profiler) measurements revealed that the strength of SMC decayed very quickly with depth. The eastward SMC transport between 4-6°N was estimated to be 8.4 Sv with 70% in the top 100m. The current and mass transport also exhibited strong intra-seasonal variability. The eastward core of SMC was observed near 4°N and was separated from the eastward equatorial flow by a zone of weak currents. The intrusion of SMC into the Bay of Bengal was studied by Vinayachandran et al., (1999a). They have estimated the mean seasonal (May- September) transport of SMC into the Bay of Bengal to be 10 Sv.

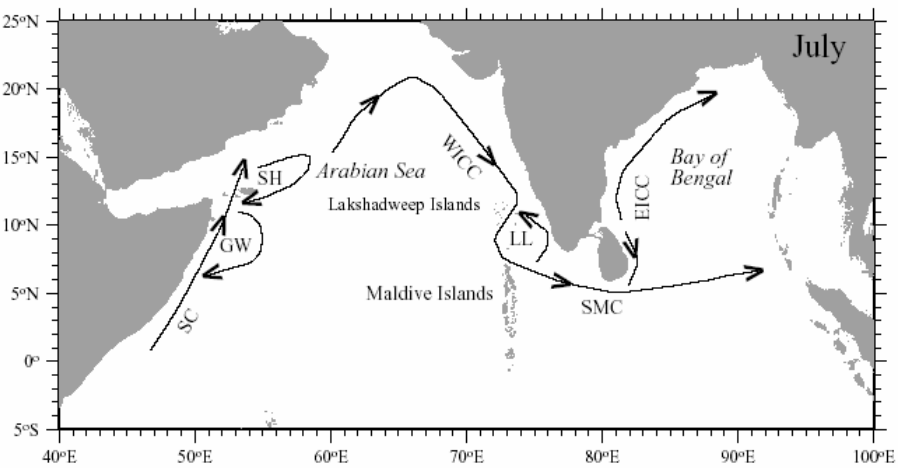

Fig.7.10 . Coastal circulation along Peninsular India during southwest monsoon. LL: Lakshadweep Low, WICC: West India Coastal Current, SMC: South west Monsoon Current, EICC: East India Coastal Current, SC: Somali Current , GW: Great whirl, SH: Socotra High (Vinayachandran and Yamagata, 1998)

7.3.3. Northeast Monsoon Current (NMC):

The surface currents (Fig. 7.11a) (Rao et al., 1989) show a westward flow south of Sri Lanka during the winter monsoon, partly continuing westward at low latitude and partly flowing around Laccadive High (LH) (red spot in Fig.7.11a & 7.11b) and into the west India coastal current (Fig7.12b). This current is referred to as the Northeast Monsoon Current (NMC). The

NMC transports low salinity waters of the Bay of Bengal into the eastern Arabian Sea (Fig.7.16) and flows along the Indian west coast as the WICC .Using Moored and shipboard ADCP measurements, Schott et al., (1994) estimated the transport of NMC to be 12 Sv in early 1991 and 10Sv in early 1992.

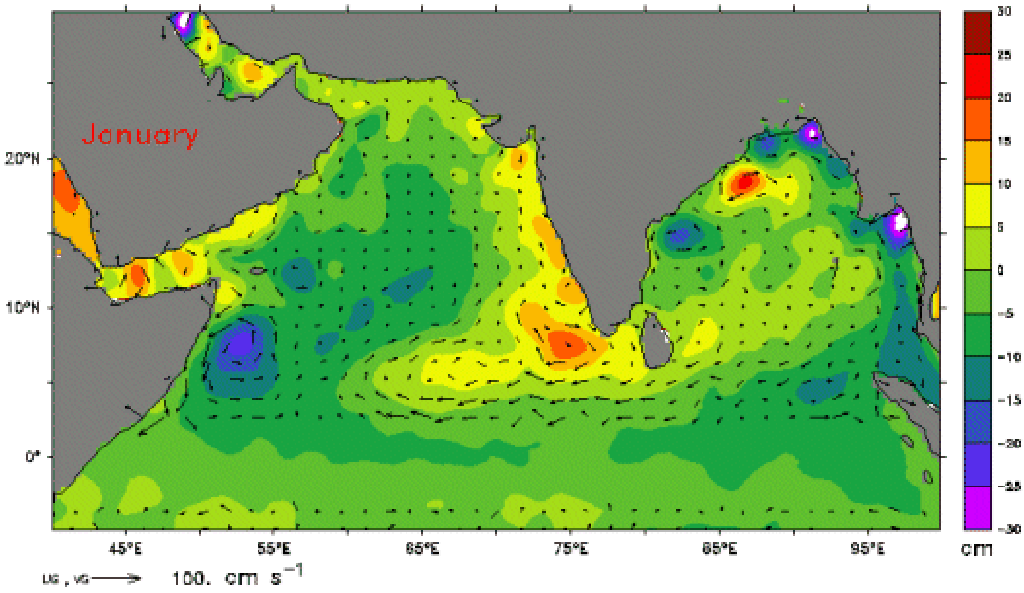

Fig. 7.11a North Indian Ocean circulation during January .Note the LH (red spot) and GW(blue spot) like a mirror image (By courtesy of NOAA) & (Credits Topex/Poseidon, National Institute of Oceanography, Goa, India).

7.3.4. West India Coastal Current (WICC):

During the last few years there have been important advances in our understanding of the working of large scale seasonal currents in the North Indian Ocean, in general, and the coastal currents around India, in particular. This was made possible by a number of studies (Potemra et al 1991; Yu et al 1991; Mc Creary et al 1993, 1996; Shankar et al 1996; Vinaychandran et al 1996 etc.

The west India Coastal Current (WICC) flows northward during November-February (Fig.7.11b) and southward during April-September (Fig.7.10). At the time of formation of the northward phase of the current, a high sea level and the Lakshadweep High (LH) forms off southwestern India and migrates westward across the Arabian Sea. Similarly at the time of southward phase of this WICC, a low in sea level and the Lakshadweep Low (LL) forms off southwestern India.

The west coast of India forms the eastern boundary of the Arabian Sea basin. A striking feature along the west coast of India is the shallowing of the thermocline (Fig.7.7f) and the development of an equatorward surface current and a weak poleward current during spring (Fig.7.11b). Cutler and Swallow (1984) show that the southward flow appears along the west coast of India in March, reaches peak strength in July and vanishes by October. This current is known as the West India Coastal Current.

Later studies showed that the southwest monsoon is the time of upwelling, with the WICC flowing equator ward (Fig 7.10) during southwest monsoon and poleward during northeast

monsoon (Fig 7.11b). The local winds are the important forcing mechanism of the WICC. Johennessen et al., (1981) noted that up-sloping along the coast started in the month of March or April and the seasonal variation was repetitive from year to year. Though the wind is an important driving force from February onwards, the upwelling is not only associated with the local wind, but also with more large scale monsoonal condition which drive the anticyclonic Arabian Sea monsoon gyre.

Antony (1990) observed a northward (poleward) flowing undercurrent at the time of upwelling along the west coast of India along 15°N in the eastern Arabian Sea because an upward tilt of isotherms towards the coast from April to September was noticed. Shetye et al., (1990) later confirmed the presence of this undercurrent along the coastal region off western India during June-August 1987. They have computed the dynamic topography relative to 1000db at various locations along the coast and pointed out that, during the southwest monsoon, there is an equatorward coastal current and poleward undercurrent with its core at 150 m or below. The T-S analysis showed that the undercurrent carried low salinity waters of southwestern Bay of Bengal.

During the northeast monsoon season, Shetye et al., (1991a) described the poleward surface current (Fig. 11b) and a southward moving undercurrent along the west coast of India. They concluded that it is the alongshore pressure gradient which drives the currents along the west coast of India during northeast monsoon season, where as currents are driven by winds during the southwest monsoon season.

Stramma et al., (1996) found a northward surface current against the prevailing winds at a speed of 40cm/s and a poleward undercurrent with its core at 100m depth. The total transport was estimated to be 4.7 Sv from surface to 300m. Water mass properties indicated that waters at the shelf edge were a mixture of low salinity water of the Bay of Bengal around Sri Lanka and high salinity waters of the Arabian Sea. Another interesting feature observed was the presence of a narrow westward current just south of Sri Lanka from 5.5°N to 6°N.

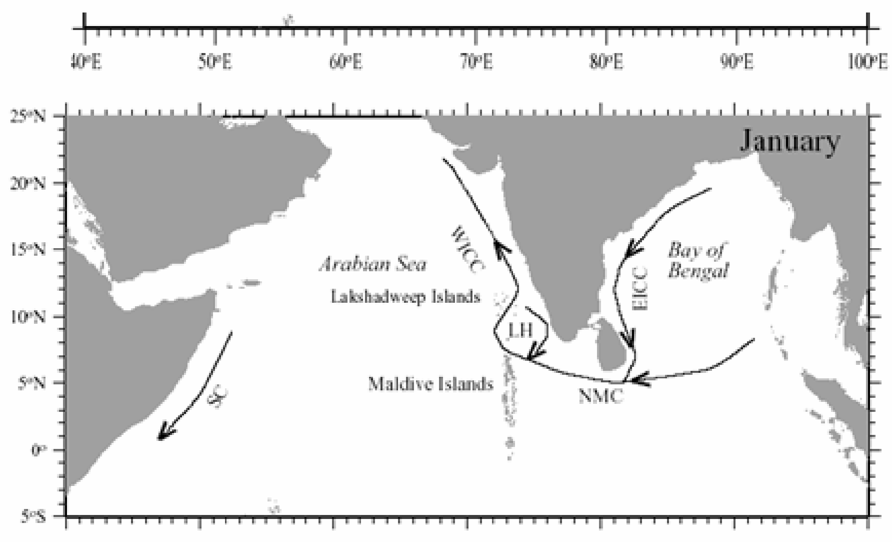

Fig.7.11b Coastal circulation along Peninsular India during Northeast monsoon. LH: Lakshadweep High, WICC: West India Coastal Current, NMC: Northeast Monsoon Current, EICC: East India Coastal Current, SC: Somali Current (Vinayachandran and Yamagata, 1998)

According to Shetye (1998), the WICC reverses seasonally (Fig.7.12). It is essentially a surface flow, the velocity being restricted to the upper most few hundred meters. The core of the current is on the continental slope, i.e., close to the 1000 m isobath. The WICC flows equatorward when the southwest monsoon (April-September) winds are active (Fig.7.12b) , and

is best developed when the winds reach the peak during July-August (Fig.7.12c). At this time the current is strongest along the southwest coast of India, weaker in the middle part of the coast, and is hardly noticeable off the northwest coast. The transport of the current has been estimated to be about 4 sv near the southwestern part of the coast in July (Fig.7.12c).

The poleward phase of the WICC occurs during the northeast monsoon (November-February). This phase sets in when the equatorward current at the east coast of India, the East India Coastal Current (EICC), turns around Sri Lanka and starts flowing poleward along the west coast of India against the weak winds of this season (Fig.7.12a). The low salinities near the Sri Lanka coast clearly indicate that this water originates in the Bay of Bengal (Fig.7.14 & 7.20) and brought by equatorward EICC. The current is about 40 km wide jet-like flow along the continental slope off the northwest coast of India, where the transport has been estimated to be 7 Sv and is wider in the south (Shetye etal 1991).Thus the poleward phase of the WICC is better developed during north east monsoon season (Fig.7.12a) than the equatorward phase during south west monsoon season (Fig.7.12c), though the winds during the northeast monsoon are weaker.

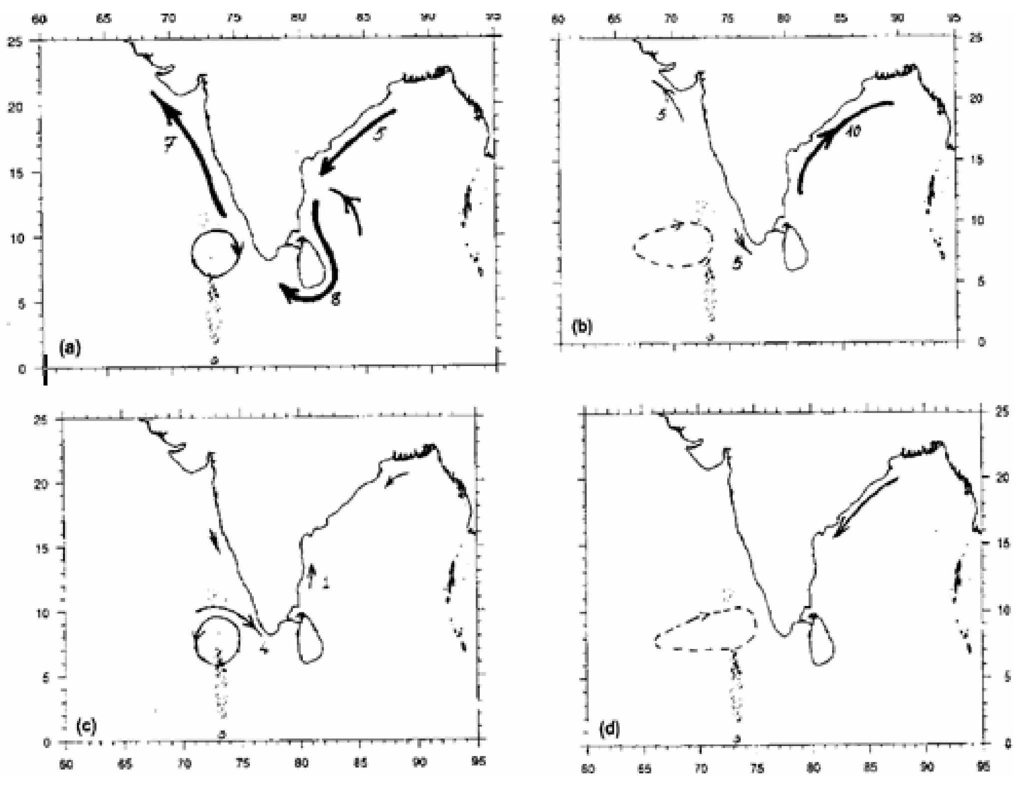

Fig. 7.12. WICC & EICC in (**a**) January (**b**) April **(c)** July and (**d**) October . The numbers at the arrows indicate the transport of currents in Sverdrups ($\times 10^6$ m^3 S^{-1}) (Adapted from Shetye, 1992)

7. 3. 5. Laccadive High (LH) and Low (LL):

Associated with the seasonal cycle of WICC, there are seasonal changes that occur offshore. Sea level starts rising at the southwest coast of India with the formation of the poleward phase of the WICC. By early January, positive anomalies of sea level spread offshore and northward along the west coast, and a circular 'high' (Fig.7.12a) in sea level forms to the east of the Lakshadweep islands called 'Lakshadweep High (LH)'. From February to June this high is no

longer circular (Fig.7.12b). It stretches westward and by July it becomes cyclonic. Later it becomes anticyclonic again.

Bruce (1994), using hydrography and satellite altimetry sea level observations, discovered the presence of an anticyclonic eddy in the upper 300-400m of the eastern Arabian Sea during the northeast monsoon period (December-April). They called this as the 'Laccadive Eddy'or Laccadive High (LH) (red spot in Fig.7.11a & 7.12). Its center is located at 10°N, 70°E to the west of the north south Laccadive Island chain. It grows rapidly from late November to late December at 10°N and then propagated westward in January and died in the mid basin. The LH appeared as the mirror like counterpart to the 'Great Whirl' (GW) (blue and red spots in Fig. 7.11a) found off the Somali Coast during the southwest monsoon season. Surveys and satellite altimetry measurements together with high resolution numerical simulation by Bruce et al., (1998) indicated that LH is comprised of multiple eddies. They hypothesized that in addition to local and remote seasonal forcing; the Laccadive High region is influenced by an intra seasonal signal that originates in the Bay of Bengal.

Evolution of the Lakshadweep Low (LL) proceeds in a fashion similar to that of the High (LH). The sequential events are like this. First, the sea level drops at the southwest coast of India in June, when the WICC is equatorward. Second, the negative anomalies spread offshore and along the coast, and a circular low forms to the east of the Lakshadweep islands in July-August. Third, the LL stretches westward and by the end of October, negative anomalies in sea-level occur all over the Arabian Sea (Fig.7.12d).

The interior of the Arabian Sea is filled with mesoscale eddies. The relation between Laccadive High and Low (LH/LL) and the interior Arabian Sea was studied by Brandt et al., (2002) and Stramma et al., (2002). They analyzed the WOCE ship section along 8°N during summer and winter monsoons in conjunction with Topex/Poseidon altimetry data. They concluded that much of the seasonal variability in the stratification and meridional circulation could be explained by the propagation of the Rossby waves from the west coast.

7.3.6. Long waves of the equatorial Indian Ocean and Coastal wave guides:

The currents in the equatorial Indian Ocean basin are primarily free and forced long waves of three kinds. They are equatorially-trapped Rossby and Kelvin waves and coastally trapped Kelvin waves (Shetye, 1998). All these waves are triggered by the monsoon winds. The equatorial region can support a variety of waves. To understand the circulation annual and semi-annual periods are needed to be considered. The wavelengths associated with these periods can be either short or long. As short waves tend to get dissipated quickly due to friction and do not contribute to large scale circulation, long waves only need to be considered for north Indian Ocean circulation.

It is clear now that the elements that lead to the formation of the WICC and LH/LL are these three waves. In its simplest form, the WICC is a coastally –trapped Kelvin wave and the LH/LL results due to Rossby waves radiated by the Kelvin wave. Thus to have the WICC and LH/LL two basic elements needed are 1) coastally trapped Kelvin waves along the east coast of India and 2) the periods of Kelvin waves must be large enough to have trapping length that can extend up to the region where the LH/LL form.

The EICC is forced by all winds on the equator, along the periphery of the Bay and in the open Bay (Shankar et al 1996; McCreary et al 1996). Each of these forcing functions has annual and semi-annual waves associated with them. It is the superposition of these forcing functions that forms the EICC which can be looked on as a sum of Kelvin waves with annual and semi-annual periods. When the Kelvin waves reach the west coast of India after turning around Sri Lanka, and make their way northward along the coast, they radiate annual and semi-annual Rossby waves. The Kelvin waves along the coast form the WICC, and the Rossby and Kelvin

waves together form the LH/LL. As the Rossby waves propagate westward, the LH/LL stretches westward.

7.3.6.1. Equatorially – trapped Kelvin waves:

These waves are trapped in the vicinity of the equator, with the trapping radius, the equatorial radius of deformation (R_e), given by $\left(c/2\beta \right)^{1/2}$. For the choice of 'c', R_e is about 200 km. the phase velocity of these waves is always eastward. The advective particle velocity associated with the wave is strictly along the equator and can be both eastward and westward. The cross equatorial advective velocity is zero. For these waves the equatorial regime acts as a wave guide centered on the equator, with a width of about 400 km (see Fig.)

7.3.6.2. Long equatorially-trapped Rossby waves:

These waves propagate westward approximately in a non-dispersive manner with wave speed $\sigma/k = -c/(2n+1)$ where σ is the frequency (= $2\pi/T$, T being the period), K is the zonal wave number ($2\pi/\lambda$, λ being the wave length) and n = 1,2,3…. (H=50 m and f=10 $^{-5}$ S^{-1} .Hence the waves propagate westward with a phase velocity that is at least three times slower than that of the Kelvin waves.The advective particle velocity can have both eastward and northward components. It can be shown that away from the equator a local dispersion relation can be written for these waves as

$\sigma/k = -c^2/\beta y^2$ which states that the local phase velocity increases as distance from the equator decreases.

The long equatorially-trapped waves have a trapping scale given by $y_c = c/2\sigma$

For the annual wave y_c is approximately equal to 56^o. For the semi-annual waves, it is 28^o. Hence the north Indian basin lays equatorward of turning latitudes of both these waves. However, for a wave with period of 60days, y_c is about 9^o, and hence the basin has regions both poleward and equatorward of the latitude up to which the waves get trapped (see Fig.7.13)

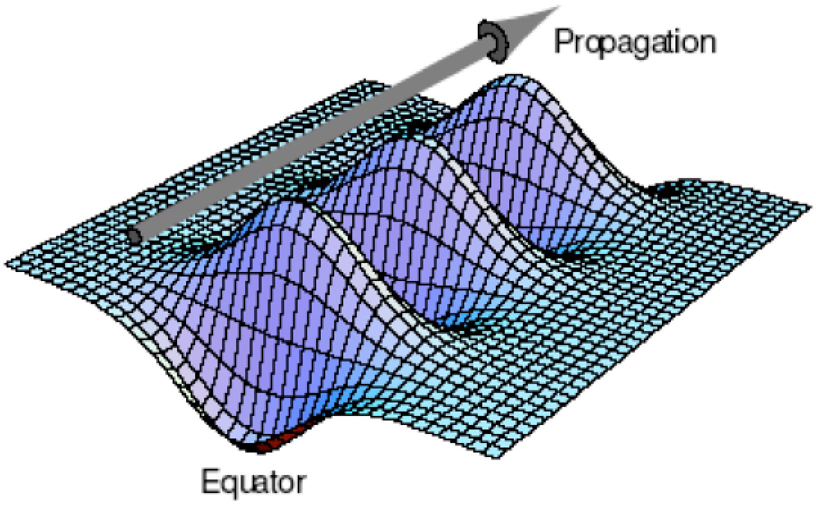

7.3.6.3. Coastally – trapped Kelvin waves:

The coastally-trapped Kelvin waves (fig.7.13a) propagate with the coast to their right in the northern hemisphere (Gill 1982). They are nondispersive and are trapped at the coast with a trapping scale, The Rossby radius of deformation R_c, given by c/f. The trapping makes the coastal zone a wave guide of these waves. Of course the width of the wave guide varies with latitude because f depends on latitude. Using the value of c, the value of R_c is about 75 km at 10^{o}N and 150 km at 5^{o}N. The advective velocity associated with these waves is along the coast and it can be either in the same direction as that of the phase propagation or opposite. The cross shore component of the advective velocity is always zero. If a Kelvin wave propagates along a meridional eastern boundary which is equatorward of critical latitude y_c, it radiates westward propagating Rossby waves and the coastal wave guide turns "leaky". In this case the Kelvin wave is not separable from the Rossby wave and the two remain coupled to form a mode. Annual and semi-annually coastal trapped Kelvin waves propagating along the eastern boundaries of the Bay of Bengal and the Arabian Sea fall in this category. The approximate extent of the coastal wave guide was marked in Fig.7.13

Coastal Kelvin Wave

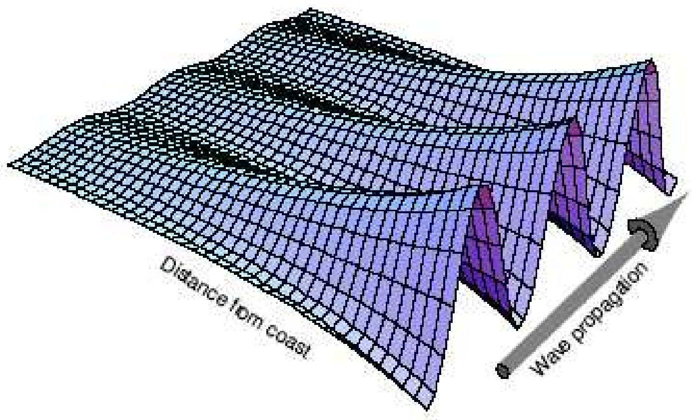

Fig.7.13a coatally trapped Kelvin wave

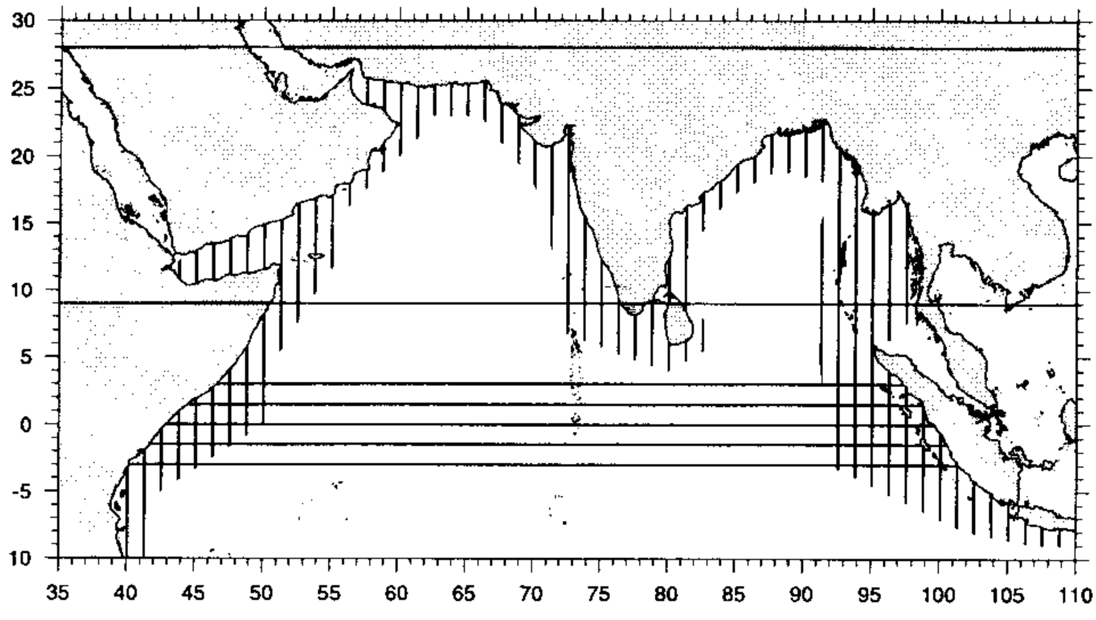

Fig.7.13a. Coastal and equatorial wave guides in the North Indian Ocean. The band between 3°N and 3°S shows the equatorial Kelvin wave guide. Vertical lines give the approximate extent of the coastal wave guide. Zonal lines between 28°N and 9°N gives y_c for waves with periods of 180 and 60 days respectively.

7.3.6. 4. Propagation of a disturbance in the north Indian Ocean:

Figure7.13a, can be used to know the propagation of any disturbance occurred in the north Indian Ocean. For example, the periodicity of the disturbance is semiannual (6 months) and

is located at 10°N, 60°E. As this location is outside the coastal or equatorial wave guide, it can excite only westward propagating Rossby waves. At 10°N their speed of propagation is 0.11 m S^{-1}.Hence in about 104 days the disturbance reaches the coast of Somalia. Off Somalia, coastally trapped Kelvin waves can only propagate towards the equator in the coastal wave guide. So the disturbance can travel much faster and takes 6 days to travel from Somalia to the northern edge of the equatorial wave guide. Once the disturbance travels eastward as an equatorially trapped Kelvin wave with velocity c, it takes 35 days to reach the coast of Sumatra. The Reflection of the equatorially trapped Kelvin wave from the coast of Sumatra produces coastally trapped Kelvin waves that move away from the equator and the westward moving Rossby waves. These coastally trapped Kelvin waves reach the northern tip of Sri Lanka from Sumatra in 28 days. During this time the slower Rossby waves travel with a velocity that is dependent on the latitude, hence they take 127 days to reach the north coast of Sri Lanka, i.e about 4 times longer than Kelvin waves to go around the bay of Bengal and this coast.

A coastally trapped Kelvin wave present on the east coast of Sri Lanka can bend around the island and reach approximately 10°N on the west coast of India in approximately 11 days. It can then travel all the way around the rim of the Arabian Sea and reach the coast of Somalia in 40 days.

Hence if a disturbance is generated along the coast of Somalia, the waves emanating from it can go around the North Indian Ocean in the coastal and equatorial wave guides and reach the original spot of disturbance in 4 months. This is true for both annual and semi-annual disturbances.

However, the spot of original semi annual disturbance we are examining is not in the coastal wave guide, but outside in the open Arabian sea. For the waves caused by this disturbance to reach the original location, they need to travel westward as Rossby waves from the west coast of India. The Rossby waves take about 140 days to travel from the coast of India to 60°E which is the original location of the disturbance. Hence the total time required for the waves to reach the original spot of generation after going around the basin is almost 330 days.

7.3.6. Ras Al Hadd Jet & Northern Arabian Sea circulation:

The northern Arabian Sea was extensively studied as part of the JGOFS (Joint Global Ocean Flux Studies) during 1994-1996. The observations consisted of repeated ship sections normal to the Oman coast, of special frontal surveys and satellite SST and altimetry. The AVHRR (Advanced Very High Resolution Radiometer) observations and Acoustic Doppler Current Profiler (ADCP) survey by Bohm et al., (1999) identified the existence of a northeastward coastal jet along the south coast of Oman in early May and persisting throughout the summer monsoon. It was called as the 'Ras Al Hadd Jet' as it flowed past Ras Al Hadd at the southeast corner of Oman (Fig.7.13b). Its maximum velocity was 1.0 m/s and maximum transport was estimated to be 2-8 Sv in September. The headlands cause filaments and jets of water to be expelled from the coastal region. Stirring of the coastal waters with waters farther offshore is evident. Two eddies on either side of Ras al Hadd are evident, as seen in the Fig.7.13b. Shi et al., (1999) determined time series of the alongshore flow from a combination of Topex/Poseidon altimetry, Joint Global Ocean Flux Studies (JGOFS) hydrography and Ekman transports for 1993-1995 in the northern Arabian Sea and found that the maximum eastward flow occurred earlier in monsoon and decreased strength from about 10Sv in 1993 to about 2 Sv in 1995 in correspondence to a decrease in monsoonal wind forcing between these years. The main reason for this northeastward flow was due to onshore pressure gradient established by the upwelling which reduces sea level near the coast by 30 cm.

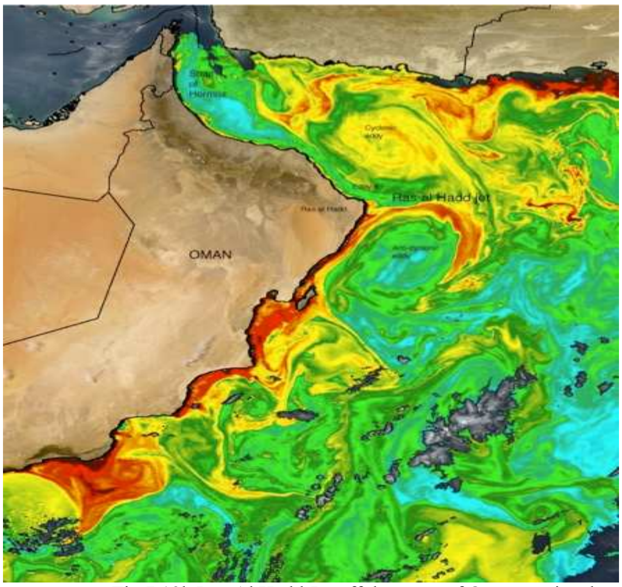

Fig.7.13b Ras Al Hadd Jet off the coast of Oman peninsula

7.4. Bay of Bengal circulation:

While the Arabian Sea is the northwestern arm of the Indian Ocean, the Bay of Bengal is the northeastern arm as both are completely separated by the Peninsular India. Though the Bay of Bengal and Arabian Sea are located in the same latitudinal belt and are influenced by monsoons, there are remarkable differences between these two basins. Unlike the Arabian Sea, a large quantity of fresh water enters the Bay of Bengal through river discharge and rainfall. Hence the surface waters in the Bay have low salinity (See Fig.7.14) and the stratification in the upper layers is often dominated by salinity gradients. The width of the Bay of Bengal is less than the Arabian Sea and the coastline is about 1.5 times shorter than that of Arabian Sea. These dimensions are relevant for the propagation of Rossby and coastal Kelvin waves in the two basins. The sea surface temperature of Bay of Bengal (Fig.7.15)is greater than 28°C which is favorable for the genesis of synoptic scale disturbances (cyclogenisis).

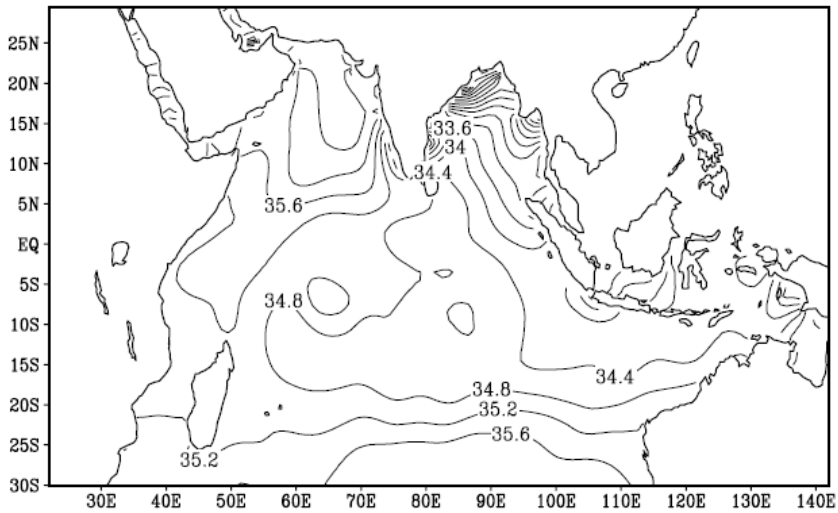

Fig.7.14 Surface salinity during July in Bay of Bengal & Arabian sea

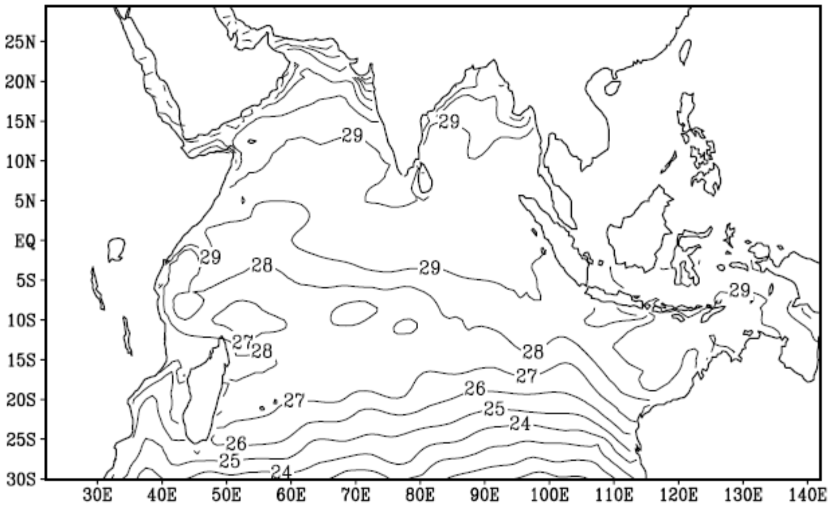

Fig.7.15 Surface temperature during April in Bay of Bengal & Arabian sea

Observations in the Bay Bengal started in the 19th century with the expedition of the NOVARA (1857-1859) and VALDIVIA (1898-1899). The data collected during the cruises of 'RMIS Investigator' were analyzed and documented by Sewell in various reports of Memoirs of the Asiatic Society of Bengal (Sewell, 1929). During IIOE, many cruises were conducted in the Bay of Bengal and the availability of the data increased tremendously. The voluminous data collected for the Indian Ocean during IIOE were analyzed and presented in the form of an atlas by Wyrtki (1971). Other sources of data in the Bay of Bengal are the atlases (KNMI, 1952; Deutsches Hydrographisches Institut, 1960; Cutler and Swallow, 1984) which give the surface currents of the Indian Ocean. Among these, the Cutler and Swallow (1984) atlas is particularly useful to study Bay of Bengal circulation because of the data coverage over a long period and better spatial resolution.

The winds over the Bay of Bengal are southwesterly during May- September (7.16a) and northeasterly during November-January (Fig.7.16b). The transition from SW to NE winds takes place during October (Fig.7.16d) and reverse transition takes place during February-April (Fig.7.16c). The wind possesses strong anticyclonic curl in the southern Bay during summer monsoon (Fig.7.16a) and strong cyclonic curl in the southern Bay during the northeast monsoon season (Fig.7.16b). In response to the winds, circulation in the Bay exhibits a seasonal cycle which is reflected in the surface currents and hydrography.

(a) (b)

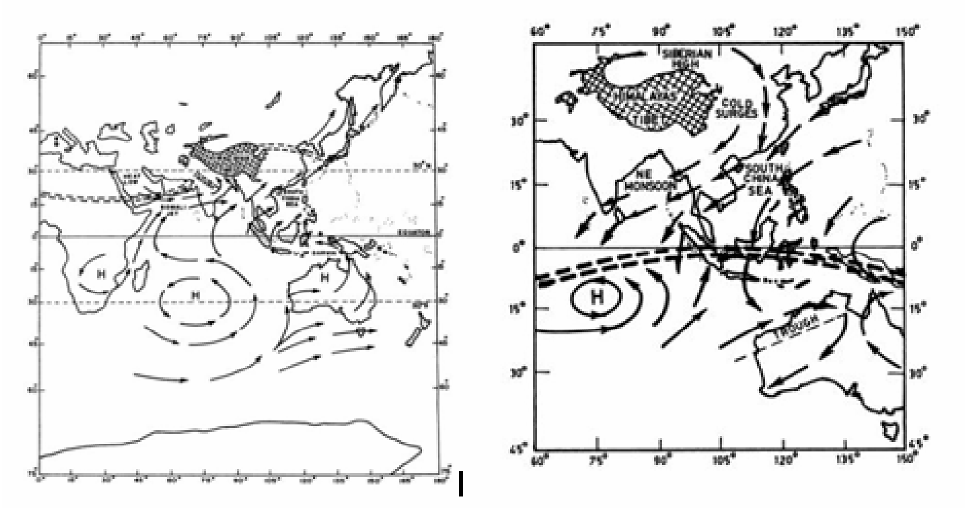

Fig.7.16 (a & b). Winds over Indian Ocean during May-Sept (a- **Left**) and during Nov-Jan (b-**Right**). The dashed curve indicates the position of ITCZ.

(c) (d)

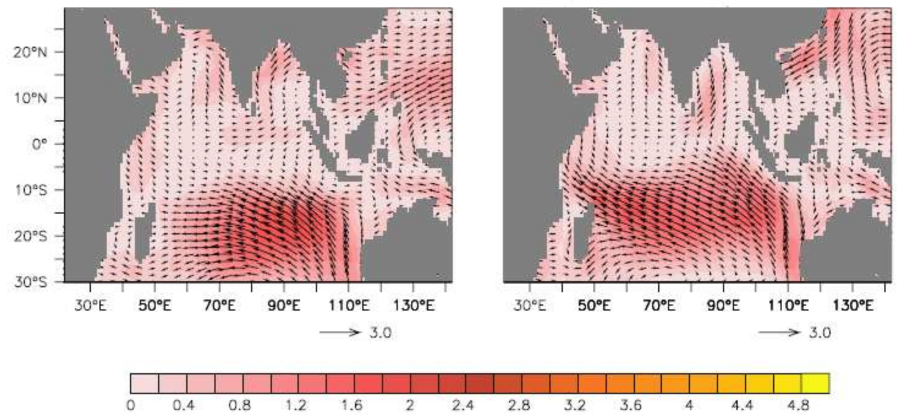

Fig.7.16 (c & d). NCEP reanalysis wind stress fields for different months (dynes cm^{-2}), (c) April and (d) October

The surface circulation in the interior of the Bay of Bengal is best organized during the transition period from NE to SW monsoon during Feb-May. Ship drift (Cutler and Swallow, 1984; Duing 1970), satellite tracked drifting buoys (Molinari et al., 1990) and dynamic topography computed from climatological temperature and salinity (Shetye et al., 1993) all suggest the presence of an anticyclonic gyre (G2 in Fig.7.17) during this period. The EICC flowing poleward forms the western boundary of this basin-wide anticyclonic gyre (left branch of G1 in Fig.7.17). EICC reverses direction twice a year, flowing northeastward from February to September (left branch of G1 in Fig.7.17b) with a strong peak in March- April (Fig. 7.17) and southwestward from October to January (left branch of G1 in Fig.7.17a) with a strong peak in November. Earlier hydrogaphic surveys which revealed the existence of EICC include the studies of La Fond 1957, and Scherbinin (1979).

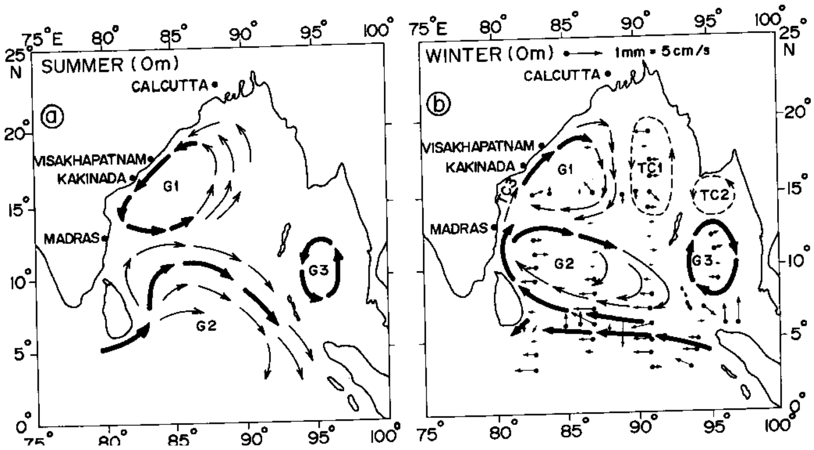

Fig.7.17. Reversal of circulation and EICC in summer (**a**) and winter (**b**) monsoons

With the onset of the SW monsoon, the anticyclonic gyre breaks up (Fig.7.17a). Gopalakrishna and Sastry (1985) pointed out that the flow in the South east coast of India is directed poleward during April-September (Fig.7.18a) and so strong upwelling takes place in the southern regions off the east coast of India.

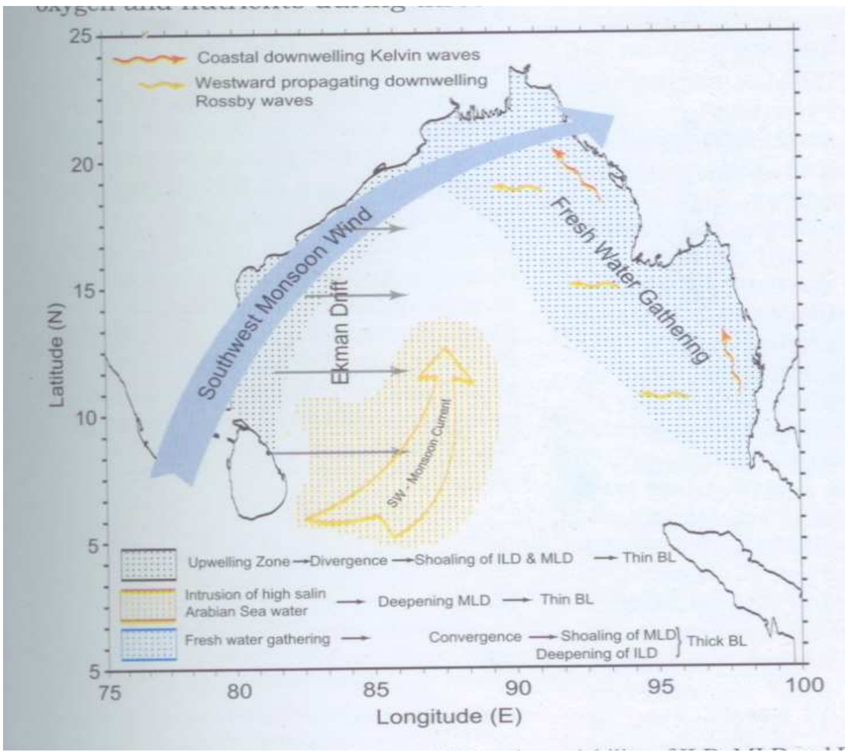

Fig.7.18a. The arrows show the Ekman drift and hatched portion show the upwelling area during southwest monsoon (June-Sept).

According to Shetye et al., (1991a) during SW monsoon season, active upwelling takes place along the eastern coast, with near surface isotherms and isopycnals tilting upward from the depths of about 80m within 40Km of the coast and deeper ones sloping downwards suggesting a southward undercurrent. In the northern Bay of Bengal flow is equatorward (Fig.7.17a) with the

freshwater plume from Ganges and Brahmaputra moving southward against local prevailing winds (south & southwest) and were located just outside the upwelling band. Because of this situation an eddy (G_1) is formed (Fig.7.17a &b). Studies of Babu et al., (1991) in the northwestern Bay of Bengal during July 1984 revealed the existence of a cold core subsurface eddy centered at 17 °40' N and 85° 19'E between 50 and 300 db. The flow along the northern Bay was southward due to the influx of freshwater and wind stress curl, and in the southwestern Bay the flow was northward (Fig.7.17a) due to the local winds. They proposed that the eddy (G_2) was generated due to the baroclinic instability at the interface of these two opposing boundary currents along the western Bay of Bengal.

Using ship drift currents and surface geostrophic flows derived from Topex/Poseidon, Eigeneheer and Quadfasel (2000) showed that at the height of summer monsoon there was a western boundary confluence near 10°N with the EICC flowing northward to the north of 10°N and southward south of it. Studies of Vinayachandran et al., (1999) showed that this confluence is mainly due to the Southwest Monsoon Current that circulates cyclonically about the Sri Lanka Dome at about 6°N (G2 in Fig.7.17a). Murthy et al., (1992a) studied the circulation pattern along the northwestern Bay of Bengal during the withdrawal phase of summer monsoon of 1983. The study revealed that local winds induced upwelling and that observed near surface salinity near the coast was an indicator of the Ekman processes of upwelling. Murthy et al., (1992b) studied the effects of freshwater flux, the wind forcing and Indian Ocean monsoon drift currents on the property distribution and the circulation in the Bay of Bengal during southwest monsoon season. They found that the northern freshwater influenced region is characterized by cyclonic circulation and the southern region is thermohaline driven. These studies also suggest the propagation of long period planetary waves from the southeastern Bay towards the southern Bay.

In the open Bay due to the intrusion of SMC into Bay of Bengal northeastward current is seen Vinayachandran et al., (1999, and 1998). Vinayachandran and Yamagata (1998) used the results from an OGCM to study the response of the oceanic region surrounding Sri Lanka to the monsoonal winds. They found that during the southwest monsoon season, a cold dome developed east of Sri Lanka (G2 in Fig.7.17a) which they called the Sri Lanka Dome (SLD). SLD is formed mainly due to the cyclonic curl in wind stress. The SLD decays after September and then this cold dome is called as Bay of Bengal Dome (BBD) which is developed north of Sri Lanka (G2 in Fig.7.17b). The source of cold water of the Bay of Bengal Dome was traced back to the SLD and upwelling zone along east coast of India.

During the northeast monsoon season, an equatorward current (Fig.7.18b) along the western boundary of the Bay of Bengal is present (Cutler and Swallow, 1984). The surface circulation relative to 1000db level surface indicates a northward flowing eastern boundary current north of 8°N off Sri Lanka and a cyclonic gyre to the west of it (Fig.7.18b). Shetye et al., (1996) could locate low salinity plume along the eastern coast of India and equatorward flowing EICC during the northeast monsoon. Shetye et al., (1996) calculated the transport of EICC north of 13°N with reference to 1000db level as 7.1Sv. The EICC flow southward along the east coast of India and its southern part, south of 13°N, a northwestward flow from the offshore meeting with the coastal current was observed.

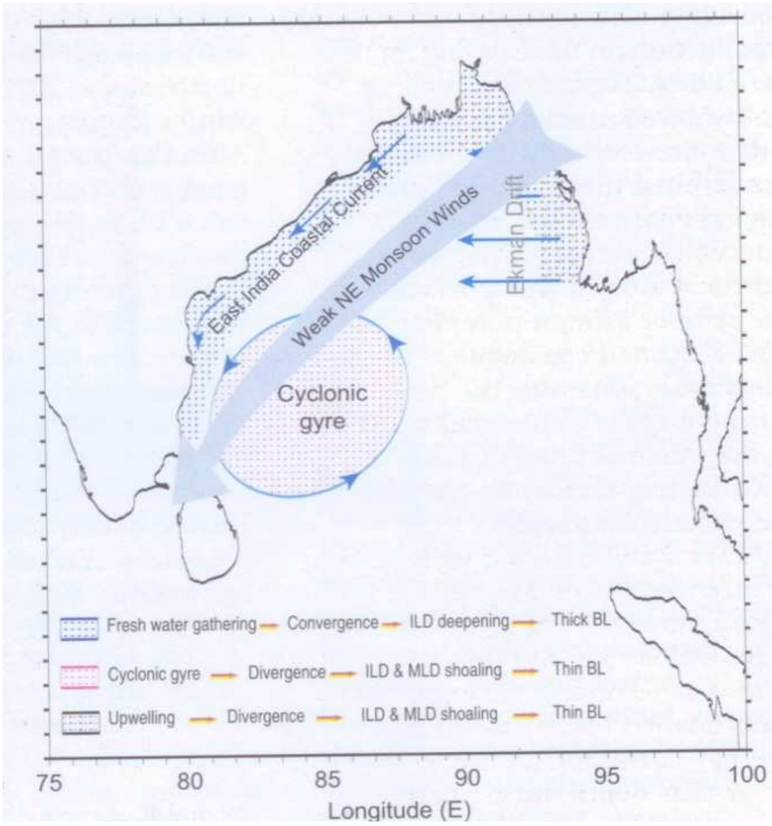

Fig.7.18b Equatorward flowing EICC and the cyclonic gyre east of it during NE monsoon (Nov-Dec).

Shetye et al., (1991a) during March-April 1991 showed the presence of poleward current along the western boundary of the Bay north of 10°N carrying warmer waters of southern origin. They proposed that this poleward current is the western boundary current of the seasonal anticyclonic subtropical gyre which forms in the Bay of Bengal during January and best developed during March-April and decays in June.

The most striking one is the northward flowing East India Coastal Current (EICC) (Shetye et al., 1993) during spring inter-monsoon (March-May) (Figure 7.20). Despite low wind speeds (~4 m/s) this current attains a peak velocity of ~100 cm/s. This is in direct contrast with the Arabian Sea where maximum current speeds are obtained during summer monsoon when the winds are stronger. This contrast is explained in terms of the role of remote forcing by the westward propagating Rossby waves and coastally trapped Kelvin waves (Fig.7.18a) in the establishment of this current (Potemra et al., 1991, Yu et al., 1991, Vinayachandran et al., 1996; McCreary et al., 1996; Shankar et al., 1996; Shankar et al., 2002). Studies indicate that this current is highly sheared in the vertical (Babu et al., 2003), which is an important aspect when dealing with the instabilities. During fall inter-monsoon (October), however, this current is equatorward. Another region of intense current is the southern Bay of Bengal (BOB) during summer when the southwest monsoon current flows into the BOB. This current flows around the Sri Lankan dome (SLD), a wind driven sea-level low (Vinayachandran et al., 1998), carrying cold and high-saline waters into the warm and less-saline southern BOB during summer monsoon. Presence of SLD and the warmer and less-saline water (Figure 7.19b) to the east of it gives a frontal characteristic to the southern BOB during summer monsoon.

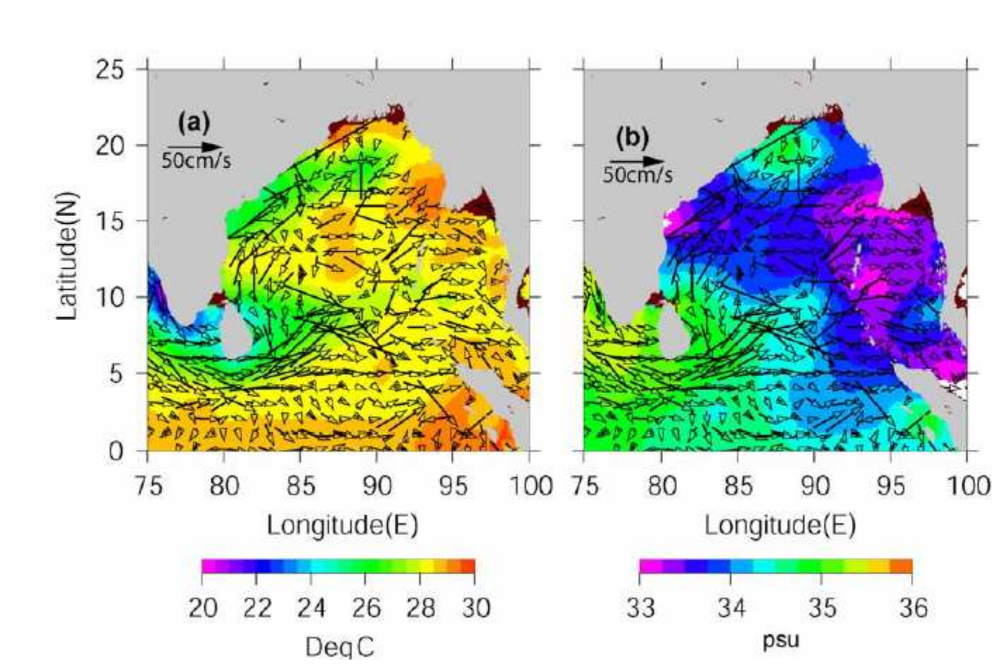

Fig 7.19. Monthly mean climatology of (a) temperature (^{O}C) and (b) salinity (psu) from WOA01 (Conkright et al 2002) overlaid with one-degree surface current vectors derived from NOAA ship drift data during July.

Fig.7.20. shows the coastal currents off the east and west coasts of India. The number against each arrow indicates the transport in sverdrups associated with it in the top 1000m of the water column.

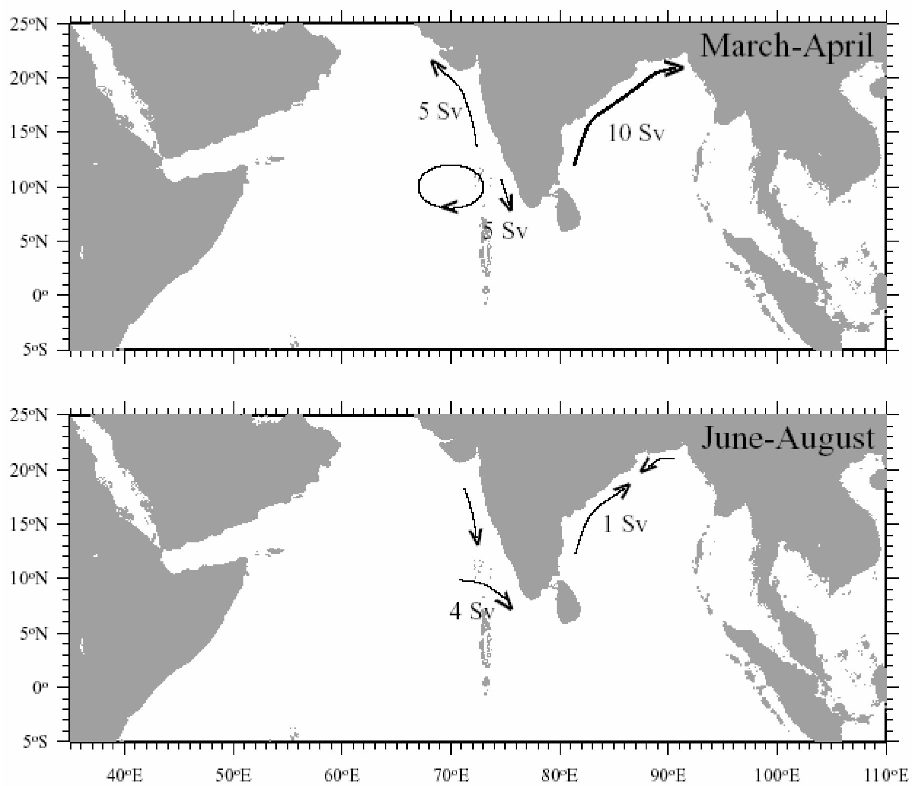

Fig.7.20. Coastal currents during (a) March-April & (b) June – Aug. The Number is transport in sverdrups (10^6 m^3 S^{-1})

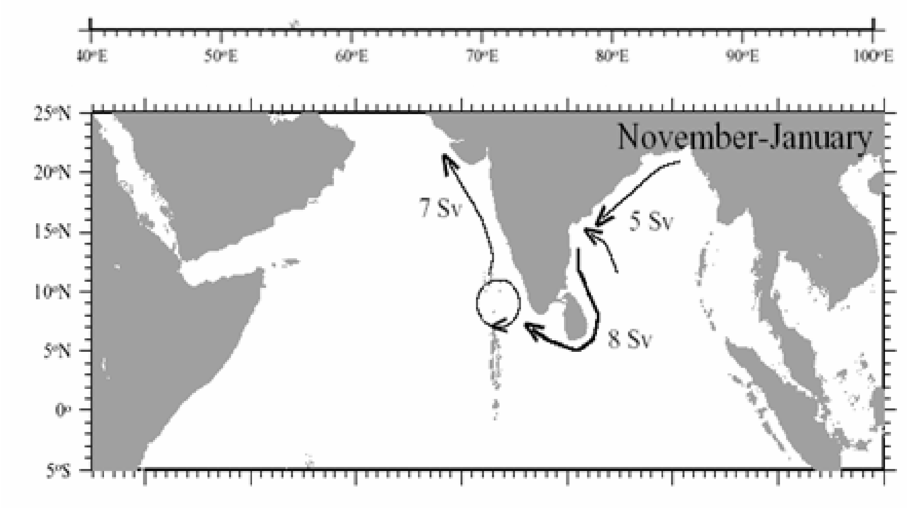

Fig.7.21. Coastal currents along the East and West coasts of India during November-January. The Number against each current vector is transport in sverdrups (×10^6 m^3 S^{-1})

7.5 Eddies in the Bay of Bengal:

The important characteristics of the BOB that emerged from earlier studies are the occurrence of intense currents along the western boundary and in the southern Bay, the high stratification arising from warm and low-salinity waters, presence of westward propagating Rossby waves and coastally trapped Kelvin waves. Apart from the above features of the BOB, there had been reports of occurrence of the eddy in the BOB way back in 1957. Ramasastry and Balaramurty (1957) reported the presence of an eddy off Vishakhapatnam along the western boundary of the BOB during March-April and October-November. They noticed strong cross-shore temperature gradients during these seasons. Subsequently, Rao and Sastry (1981) reported cyclonic and anti-cyclonic flows and linked the nutrient distribution with these flows. Though indications of a western boundary current was present in the earlier studies (eg, Ramasastry and Balaramurty, 1957 and La Fond, 1957) its presence was established by Legeckis (1987) based on satellite derived sea surface temperature (SST) data using Advanced Very High Resolution Radio meter (AVHRR) and delineated two warm core eddies in the central and northern Bay during February 1985. Based on remote sensing (altimetry) and *in situ* observations Gopalan et al. (2000) showed strong inter-annual variability in the spatial location and intensity of eddies (Table 1.1). Recent studies too indicated presence of eddies near the western boundary of the BOB during March-August (Babu et al., 1991; Murty et al., 1993; Shetye et al., 1993; Sanilkumar et al., 1997; Babu et al., 2003 ; Prasanna Kumar et al., 2004). The distribution of cold core(blue) and wam core (red) eddies in Bay of Bengal during June 2002 as illustrated by Murukesh (2007) is shown in Fig.7.22a

The *in situ* measurements show that these eddies mostly confine within the upper 500 m of the water column (eg. Babu etal 1991, Prasanna Kumar et al., 2004) and have horizontal dimensions of 200 to 300 km. A comparison of eddies at various locations all over the world is

given in the following table (Table 1.2). Though the presence of eddies in the BOB is revealed in many studies, very few of them have directly addressed their generation and evolution (Prasanna Kumar et al., 1992 and Babu et al., 1991).

The factors responsible for the generation of eddy in the open BOB could be (i) direct atmospheric forcing, (ii) topographic effect, and (iii) breaking of Rossby waves (La Casce and Pedlosky, 2004; Chelton et al., 2007). Since all the eddies discussed above were found to occur in the upper 500 m of the water column, well away from the influence of the bottom topography, the possibility of topographic effect in generating these eddies may be discounted.

Table 1.1.Details of eddies encountered along the central BOB(88°E track) during July 2001 to April 2003 (Adapted from Murukesh 2007)

Name of eddy	Time and year of formation	Location of formation	Type of eddy	Lifespan (months)
CESP3	January 2003	17.5°N, 93°E	Cyclonic	5
ACPS2	February 2003	15°N, 91.5°E	Anticyclonic	2
CESP1	April 2003	11°N, 91°E	Cyclonic	1
CESP4	April 2003	19.75°N, 89.5°E	Cyclonic	4
CES2	May 2001	15°N, 89.5°E	Cyclonic	3
CES3	May 2001	18.5°N, 91.5°E	Cyclonic	3
CES1	June 2001	9°, 87°E	Cyclonic	1
CEF3	June 2002	17°N, 91°E	Cyclonic	2
ACF2	August 2002	Western Andaman Sea	Anticyclonic	3
CEF1	September 2002	9.5°N, 87°E	Cyclonic	1

Table 1.2. Details of spatial scales associated with eddies observed at different geographic locations.

Region	Depth of sampling	Vertical extent of eddies	Horizontal dimension	Author
Gulf stream	2000 m 800 m	~ 2000 m ~ 800 m	~ 200 km ~200 km	Iselin, 1936, Richardson et al., 1978
Kuroshio	500 m	~500 m	~ 200 km	Bernstein et al ., 1977
East Australian current	900 m	~900 m	~ 200 km	Nilsson and Cresswell, 1980
Agulhas retroflection	?	> 2000 m	~ 200 km	Duncan, 1968
Somali Current	450 m	450 m	~400-600 km	Bruce, 1979
Bay of Bengal	1000 m 500 m	100-400 m 500 m	~ 350 km ~ 200 km	Babu et al., 1991 Sanilkumar et al, 1997

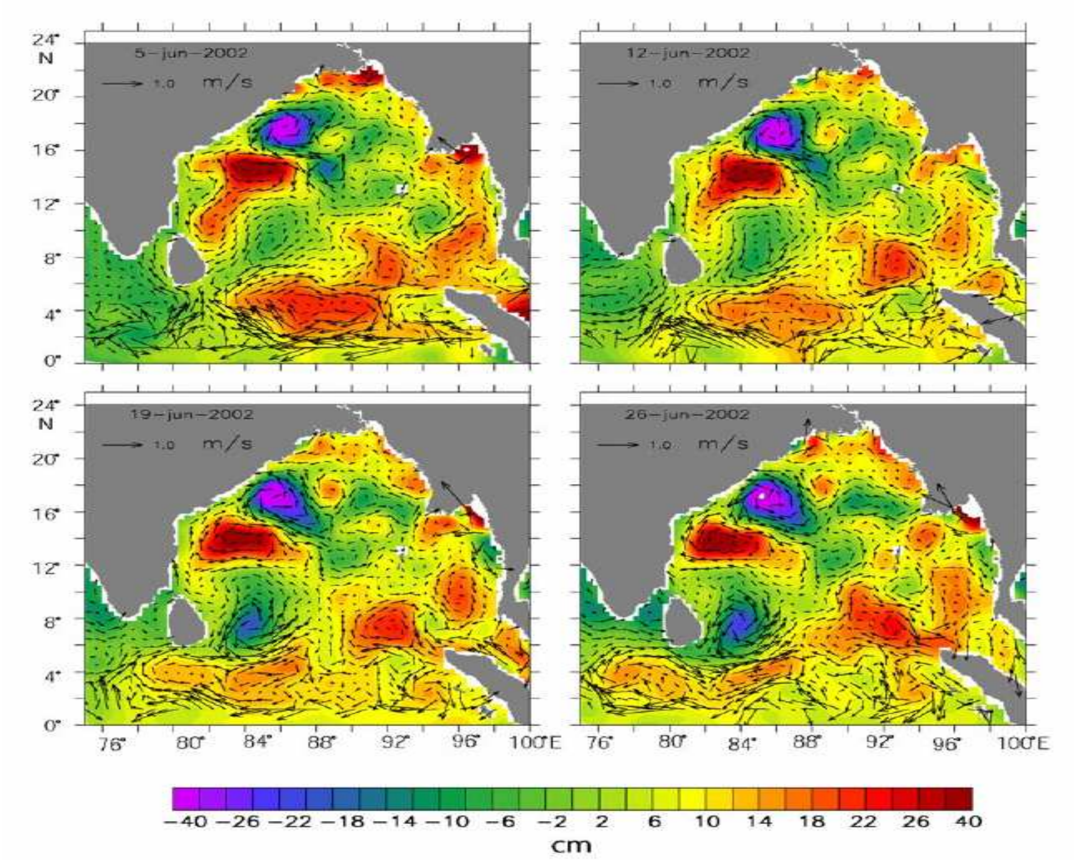

Fig.7.22 a. Seven day snap-shots of Topex/Poseidon ERS ½ merged sea-level anomalies overlaid with geostrophic velocities during June 2002 (Adapted from Murukesh, 2007)

These eddies changed the ambient temperature by about 2°C. However, the changes in the salinity field due to these eddies were much smaller, < 1 psu. The life span of eddies vary from a month as in the case of southern eddies to about 4-5 months as in the case of cyclonic eddy during spring and inter-monsoon in the north (Table 1.2). In general, they originated east of the central BOB transect and moved in a westward direction. However, the eddy encountered in the SLD region (blue spot near Sri Lanka), was found to be generated locally.

Results of Bay of Bengal Process Studies (BOBPS):

The signature of cold core eddies and their role in altering the biological productivity of the Bay of Bengal was examined using two hydrographic data sets collected along the central and western Bay of Bengal during fall (Sept-Oct, 2004) and spring (April-May 2003) inter monsoons under the Bay of Bengal Process Studies (BOBPS) program (Fig.7.22b). Based on the thermohaline structure and the satellite derived sea level anomaly maps nine cyclonic eddies were identified. Out of this nine, four cyclonic eddies such that two each along the central Bay and along the western boundary occurred during fall intermonsoon while five occurred such that three along the central Bay and two along the western Boundary occurred during spring intermonsoon.

The eddy depressed the temperature, which varied from 3^{o} to 7^{o}C at 120 m depth. Maximum depression of temperature was associated with spring time eddies in the northern Bay, where subsurface stability was low. The reduced water column stability in spring leads to greater eddy-pumping, thereby cooling the water to a greater extent. However, the cyclonic eddies were unable to break the stratification of the top 20 m layer, thereby curtailing their effects below this depth during both seasons. Eddy pumping not only cooled the water column but also enhanced the nutrient concentrations to1½ to 2 times. Thus eddy pumping of nutrients controls the biological productivity of the Bay of Bengal during both the seasons.

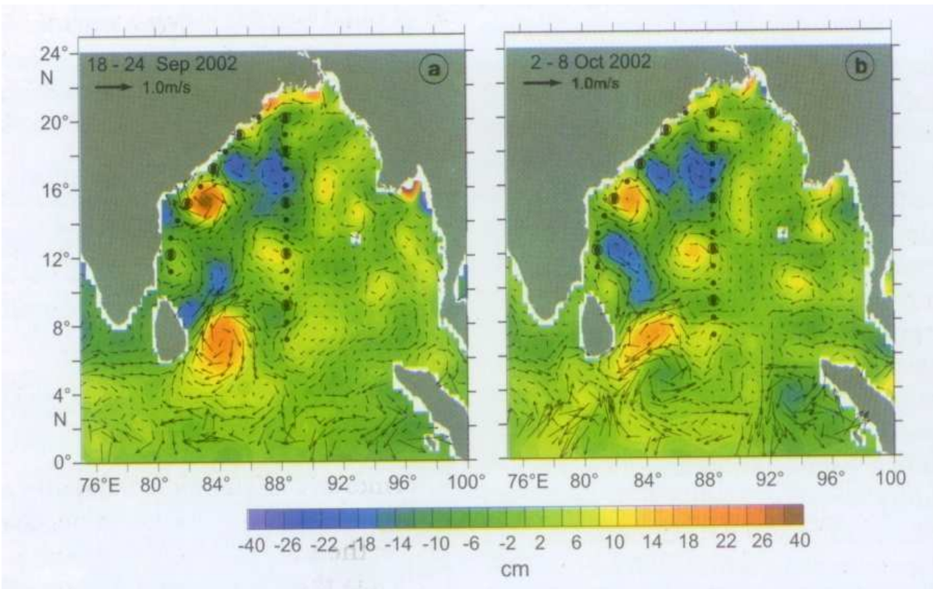

Fig.7.22b .7day snap shot of Topex/Poseidon ERS1/2 merged seal level Anomalies overlaid with geostrophic velocities during a) 18-24 Sept 2002 and b) 2-8 oct 2002. Dark circles indicate the CTD stations.

Eddies into the Gulf of Aden from the Arabian Sea:

Sea level anomalies from the satellite altimetry revealed the westward movement of mesoscale eddies into the Gulf of Aden (Fig.7.22c). Inside the Gulf the eddies move at a speed of 6.0 to 8.5 cm S^{-1}, comparable to the first mode baroclinic Rossby wave speed of 7.2 cm S^{-1}. It is shown that the eddies, which enter the Gulf from the Arabian Sea, owe their existence to more than one mechanism. Local Ekman pumping in the western Arabian Sea is important during the summer monsoon (June-Sept). In May and during the latter half of the summer monsoon (late July-Sept) and the fall intermonsoon (October), the dominant mechanism is the generation of eddies by the instabilities in the Somali current and the large eddies associated with it (Great whirl and socotra eddy). During the winter monsoon (Nov-April) the dominant mechanism involves the westward propagating Rossby waves generated either in the Arabian Sea by Ekman pumping or along the west coast of India by poleward propagating Kelvin waves. These Rossby waves from the Arabian Sea propagate slower on entering the Gulf of Aden because of a shallower thermocline in the gulf. Analysis shows that the sea level anomaly signal consists of low (annual and subannual) and high (100-180 days) frequencies. The low frequency signal (mainly annual) showed a discontinuity between 52^{o}E and 60^{o}E. Though the high frequency signal was seen at all longitudes, a wavelet analysis showed that it was significant only west of

60°E. An energy analysis, based on model simulations, suggested that barotropic instabilities are important during the entire year and that baroclinic instabilities are also important during summer monsoon.

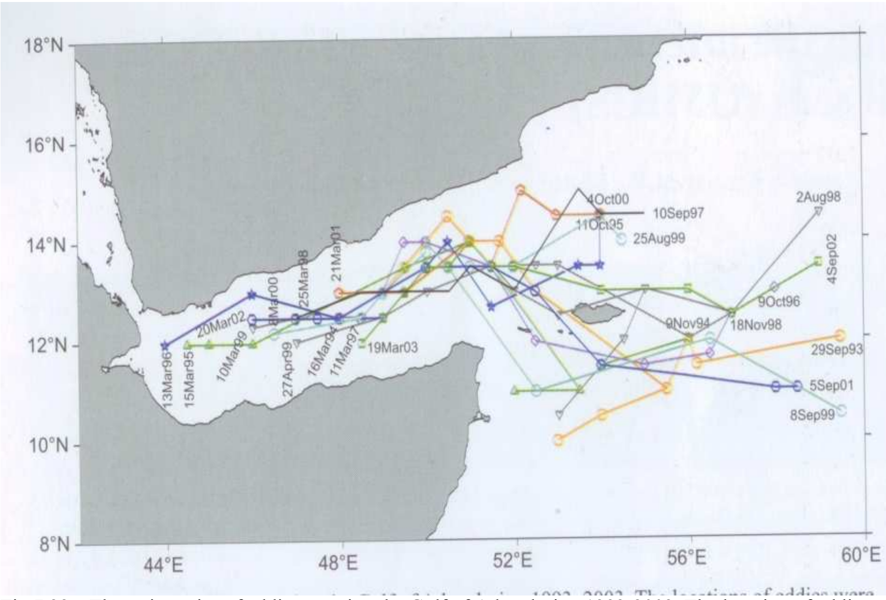

Fig.7.22c. The trajectories of eddies entering the Gulf of Aden during 1993-2003. The location of eddies were derived from the merged Topex/Poseidon and ERS-½ altimeter SLA data set.

7.5. Equatorial and southern subtropical Indian Ocean:

7.5.1. Equatorial Indian Ocean:

The equatorial Indian Ocean is driven by the wind field which is unique in the sense that its annual mean is weak and westerly and its annual cycle has strong semiannual component. Due to this unique wind field the equatorial current system in the Indian Ocean is different from the other oceans. The surface currents in the equator (Fig.7.23) reverse the direction four times a year, flowing westward during winter, weakly westward in the central and western ocean during summer and strongly eastward during spring and fall. The eastward currents were first pointed out by Wyrtki (1973) and they are known as Wyrtki Jets (WJs) or Equatorial Jets (EJs) (Fig.7.5). They appear as a narrow band, trapped in the equatorial wave guide within 2-3° of the equator mostly in the central and eastern regions and disappear in the western part where the currents have strong merdional component. The same strength was observed for the two jets, with the October – November one slightly stronger (1.0m/s) than the April-May one (0.90m/s).

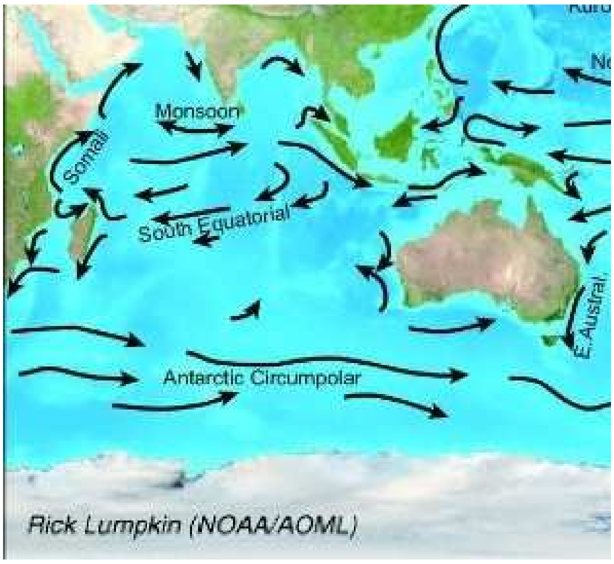

Fig.7. 23 The surface circulation in Indian ocean

The first direct current measurement carried out at the equator by Knox (1976) near Gan Island (73°10'E, 0°41'S) showed energetic eastward currents throughout the upper 100m mixed layer in phase with the zonal eastward component of local winds during this transition periods between the two monsoons. He found the fall Jet in 1973 to be stronger than either the preceding or following spring jets. The drifter climatology by Molinari et al., (1990) also shows the fall jet to be stronger than the spring jet. Equatorial current observations in the western Indian Ocean in 1975 and 1976 were carried out by Leetma et al., (1980). During both the years, a strong undercurrent was present throughout the measurement period in the vicinity of the equator. A second region of eastward flow above the thermocline was observed at 3°S. During May and June the undercurrent moved southward and merged with the southern region of the eastward flow. Hydrograpic survey made by Erikson (1979) in the equatorial section revealed high zonal pressure gradient in the near surface equatorial Indian Ocean. He pointed out that these high pressure gradients are due to intra-seasonal westerly winds prevailing at the equator. He suggested that deep fluctuations in the dynamic height found in the Indian Ocean could be related to the easterly equatorial jets of the Indian Ocean. Reverdin (1987) indicated intense variability of the equatorial currents near the surface and below the thermocline with a semiannual frequency. The eastward flowing undercurrent is detected in the thermocline during March and April. Clark and Liu (1993) concluded that the semi-annual component was largely a response for the reflection of equatorial Kelvin waves and that the annual cycle was determined by the alongshore monsoonal winds.

Reppin et al., (1999) found that the Equatorial Jet was showing large seasonal asymmetry with a monthly mean eastward transport of 3.5Sv in November 1993 and 5Sv in May 1994. The equatorial undercurrent was observed to have a maximum transport 17Sv in March to April 1994 and more than 10Sv in August 1994. They concluded that the inter-annual variability of Equatorial Jet was due to the variability of the zonal winds and southern oscillation index (SOI).

Sprintall et al., (2000) suggested that the semi-annual Kelvin waves were remotely forced by westerly wind bursts that occurred in the first week of May 1997 in the equatorial Indian Ocean during the transition from northeast to southwest monsoon. According to Unnikrishnan et al., (2001) during the southwest monsoon of 1994, an equatorial undercurrent with a transport of 5 Sv towards east was present between 2°N and 1°S.

7.5.2. Equatorial Undercurrent (EUC):

In the Indian Ocean, an eastward Equatorial Undercurrent exists only during the NE monsoon season. It was during the IIOE period; EUC was first observed and was documented by Taft (1967) at several positions along the equator between 53°E and 91°E during the months of March and April 1963 with speeds up to 0.8m/s. But it was not detected during the Southwest monsoon of 1962. Swallow (1967) reported the existence of a shallow EUC in March 1964, but by April the surface flow reversed and the EUC vanished. Then Knox (1976) reported a EUC at Gan Island (73°E) in March 1973 with velocities up to 1m/s, but no such EUC occurred in spring of 1974. Leetma and Stommel (1980) confirmed the existence of the EUC in NE monsoon of 1975 and 1976. Both these observational periods, EUC was found from January to June at 55° 30'E with observed speeds reaching 0.8m/s in February and March. They also reported a meandering of the EUC in which its core was at times displaced by more than 100Km south of the equator.

In April 1995, the 'Meteor' cruise found a well developed undercurrent at 57°E in the depth zone of 200-500m. In June, the flow at the undercurrent level reversed, and by August, all currents above 200m were directed westward on the equator (Schott et al., 1997; Walter 1997).

7.5.3. Southern Subtropical Indian Ocean:

The circulation of the southern Indian Ocean is not well understood due to paucity of hydrographic data. The dynamic topography of the Indian Ocean from the Atlas of Wyrtki (1971) shows two persistent features for the south Indian Ocean; a large, basin wide circulation and a well developed sub-gyre west of the Madagascar Ridge. For the South Java Current, he estimated a maximum eastward transport of 4 Sv during late winter monsoon and weak westward flow during the summer monsoon. Stramma (1992) investigated the distribution of the subtropical front in the southern Indian Ocean and the current associated with the front. A current band of increased zonal speed in the upper 1000m just north of the Subtropical Front (STF) in the west, north of South Africa was observed in the open Indian Ocean (Fig.7.24). He called it as the Southern Indian Ocean Current (SIOC) which separates the southern limb of the subtropical gyre of Indian Ocean from the north band of Antarctic Circumpolar Current. The estimated volume transport of southern Indian Ocean Current near Africa was 60 Sv in the upper 100m and reached to 10.1 Sv near Western Australia.

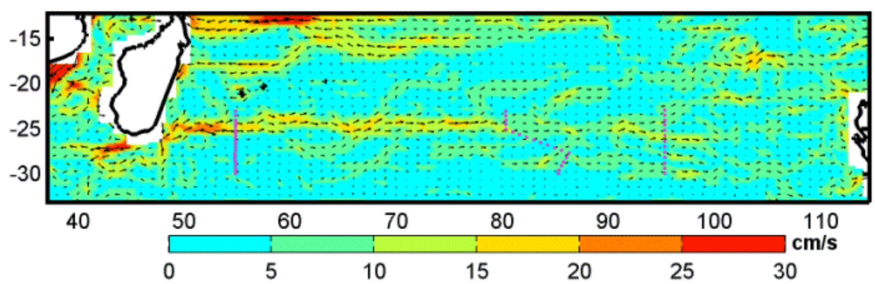

Fig.7. 24. Southern Indian Ocean current (SIOC) and Sub tropical front (STF)

Stramma et al., (1997) estimated the flow fields of the subtropical gyre and found that most of the flow fields in the subtropical gyre recirculates in the western and central part of the basin. The mean transport in the upper 100m consists of eastward transport of 60 Sv SE of south Africa, out of which about 20 Sv recirculates in the southwest Indian sub-gyre between 40°E and 50°E. Another major diversion occurred northward between 60°E and 70°E and at 90°E, the remaining 20 Sv of the eastward flow splits up, 10Sv going north to join westward flow and only 10 Sv continue in the northeastward direction to move northward near Australia.

7.5.4. Currents in the Mozambic-Madagascar basin:

The Mozambique Basin is located in the southwestern Indian Ocean and the circulation consists of the Agulhas current flowing southwestward along the coast of south Africa and in the northern part, the East Madagascar current (EMC) flowing southward along the east coast of Madagascar into the Agulhas current (Fig.7.25). Individual surveys over the past decades showed a complex structure of the flow pattern in the Mozambique Channel with the presence of energetic partially bottom trapped eddies. Grundhingh (1988) identified the appearance of strong southwesterly flow of 3×10^6 m^3/s at the Mozambique Ridge between March and April and an intense cyclonic eddy further south, east of the Ridge. They noted that between April and July the eddy had moved away and could not be located in July.

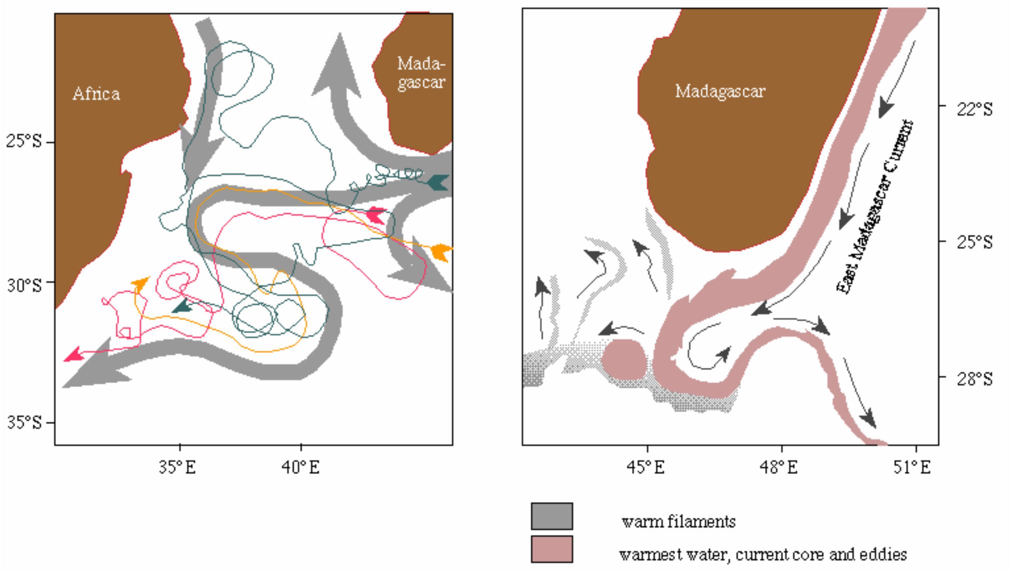

Fig.7. 25.The currents in the Mozambic channel (by courtesy from www.indianocean.free.fr/ref.2.html#tomczak)

7.5.5. Agulhas Current system:

The Agulhas Current system (Fig.7.26 a & b) may be considered to consist of four components: a source region, the northern Agulhas Current proper, the southern Agulhas Current and the Agulhas Retroflection. The sources of the Agulhas Current are the subtropical gyre of the south Indian Ocean, the region east of Madagascar and the Mozambique Channel. Of these, the subtropical gyre is the main contributor by volume. The flow through the Mozambique Channel consists largely of intense anti-cyclonic eddies that are formed in the narrows of the channel and that move poleward from there. These eddies may be 200km in diameter and extend all the way to the sea floor. Their influence on adjacent shelf regions is not known.

The Agulhas Current is, like the Gulf Stream, one of the strongest currents in the world ocean. It carries warm and salty water from the tropical Indian Ocean along South Africa's east coast. South-west of Cape Town it makes an abrupt turn back into the Indian Ocean. In this process huge rings of water with diameters of hundreds of kilometers are cut off at intervals of 3 to 4 months. These so-called "Agulhas Rings" carry extra heat and salt into the South Atlantic, making this a key region for the whole Atlantic Ocean.

Two intense cyclonic eddies of diameter 130 and 240 Km in the vicinity of Mozambique Ridge and Mozambique Basin were traced and found that the vicinity of the Madagascar Ridge seemed to represent a possible condition for equatorward transport of water extending from the mid thermocline to 1800db and originating from higher latitude. The passage of north Atlantic Deep water was constrained by the bottom topography south of the Madagascar Ridge, and this led to a reduction of its salinity and oxygen concentration. It was suggested that one of the mechanisms of Mozambique channel throughflow could be by anticyclonic eddies (Fig.7.26) that are triggered at the northern edge of the channel by Rossby waves arriving from the east. After passing through the channel, these eddies presumably even affect the Agulhas Retroflection (Agulhas Return current,Fig.7.26) and associated eddy shedding into the Atlantic. Early portrayals of the currents that feed the Agulhas current were based on the measurements of ship-drifts and SST. It is found a simple and direct inflow into the northern Agulhas current from the South Equatorial Current, one via the Mozambique Channel called Mozambique current, the other around the southern tip of Madagascar, called the East Madagascar Current. Studies suggested that the Mozambique current is not an upstream extension of the Agulhas Current; instead the circulation in the channel consists of a series of recirculation cells. Lutjeharms et al., (1981) and Lutjeharms (1988 & 2006) showed that there was no connection between the east Madagascar current and the Agulhas current, except in a sporadic way by filaments and eddies (Fig.7.26 B). Studies of Harris (1972) using hydrographic data suggested that about 35 Sv of Agulhas current comes from East Madagascar current, 10 Sv comes through the Mozambique Channel and 27 Sv is recycled in a southwest Indian Ocean sub-gyre. Fu (1986), using an inverse method solution for six hydrographic sections in the Indian Ocean indicated a southward transport of 6 Sv through the Mozambique Channel.

The West Indian Ocean region is an extensive area consisting of two large marine ecosystems (LME): the Somali Current LME and the Agulhas Current LME (Fig.7.26c).

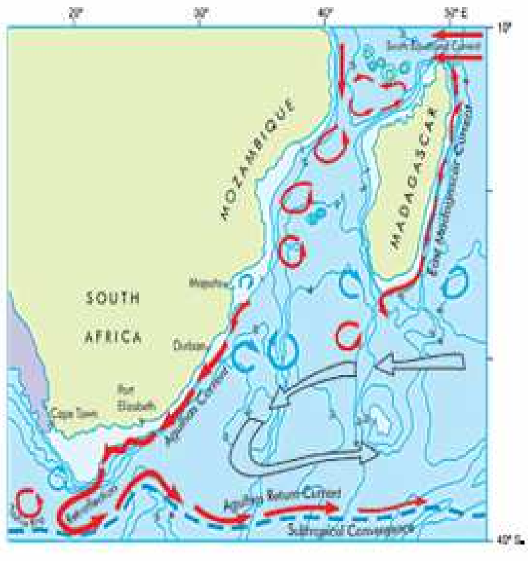

A

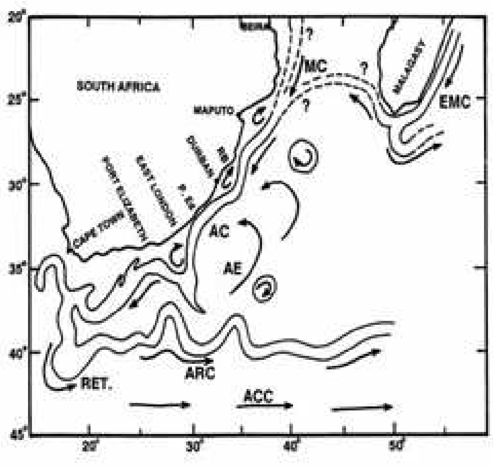

B

Fig. 7. 26 (A-Left) Agulhas current system, anti cyclonic eddies in Mozambic channel. Black arrows indicate the subtropical gyre. (B - Right) The figure in the right shows the area of coverage of Somali, Mozambic-Madagascar and Agulhas basins

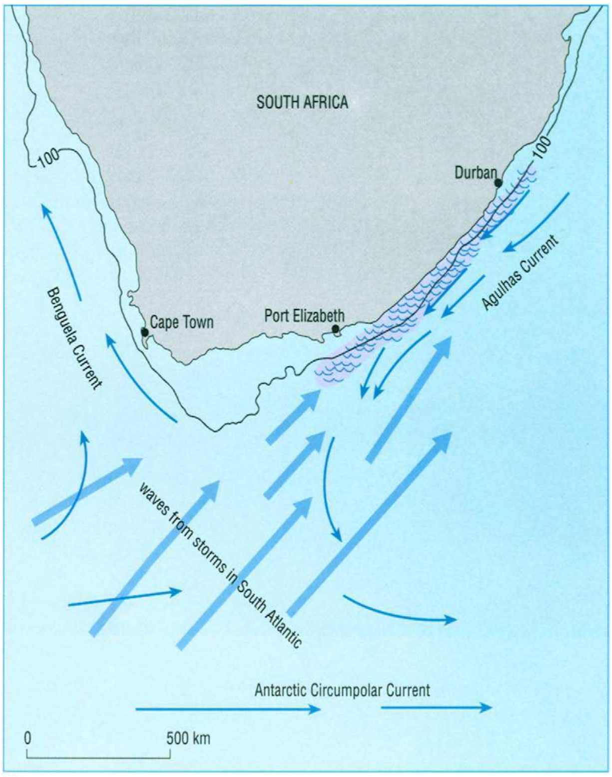

(a)

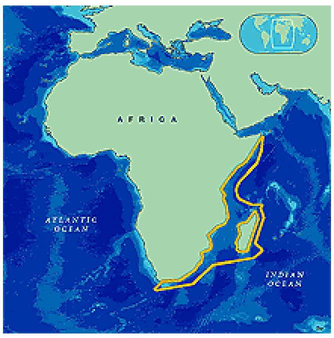

Fig. 7. 26 c) ASCLME area of investigation (www. G:\Oceanography of ASCLME Region.htm)

The Somali Current, a Western Boundary Current, runs along the northeastern coast of Africa and consists of the continental shelf adjacent to Yemen, Somalia, Kenya, and Tanzania. The ecosystem is moderately productive due to the annual reversal in the direction of flow between the summer and winter seasons. This reversal affects the nutrient-rich upwelling that occurs during the northerly summer flow. The Agulhas Current LME encompasses the continental shelf south of the Somali current and includes the area around the Seychelles, the Comoros Islands, Madagascar, Mauritius, Mozambique, and South Africa. The Agulhas Current

flows southwest along the coast and continues west past South Africa where it joins the Benguela Current. A large multidisciplinary project called Agulhas, Somali Current Large Marine Ecosystem (ASCLME) has been under the investigation by several countries of East and South Africa for a thorough study in a holistic manner (Fig.7.26c) (Lutjeharms, 2006 & 2007).

The islands that lie east of Madagascar (i.e. excluding those in the Mozambique Channel and the Comoros) all lie in the path of the South Equatorial Current. This wind-driven current is shallow and is considered not to change much in strength or direction, either seasonally or inter-annually. However, this conclusion may be the consequence of insufficient observations in the region. The effect of the passing water masses on the narrow shelf regions of most of the islands is not well known, but can be assumed to be a function of their offshore bathymetry and the absence or presence of coral reefs. The flow of the South Equatorial Current over the Mascarene Ridge that lies between Mauritius and the Seychelles has been established only recently. This shallow obstruction to the westward flow causes the current to be concentrated into a number of narrow jets through the deeper parts of the ridge. A seasonal phytoplankton bloom commences along the eastern coast of Madagascar with the onset of winter and progresses as a productivity wave eastwards as the seasonal thermocline deepens and nutrients from below are made available in the euphotic zone.

The South Equatorial Current (SEC) appears as a band of westward flow between 10°S and 20°S in Mozambic-Madagascar area. The surface current charts of Schott (1983) show the northern branch of SEC in the Indian Ocean passing around the northern extremity of Madagascar (Fig.7.6a) and continuing westward to the coast of Africa near 11°S. There it splits into the north going EACC and a branch flowing south into the Mozambique Channel to join the Agulhas current. The SEC also bifurcates along the coast of Madagascar near 17°S, generating the Northeast Madagascar Current (NEMC) to the north and the South East Madagascar Current (SEMC) to the south, which flows southward to join the Agulhas current.

The East African Coastal Current (EACC) runs northward throughout the year between latitudes 11°S and 3°S with surface speed exceeding 1m/s in northern summer. The volume transport of the EACC computed by Swallow et al., (1991) at 5 sections between 4-5 °S was 19.9 Sv northward in the upper 500db. Between 500db and 1000db, the transport was estimated to be weak of the order of 1 Sv. They found that above 300db, most of the water from the northern branch of SEC goes into the EACC and below that goes into the Mozambique Channel. During winter, the EACC meets the Somali Current to form Equatorial Counter Current (ECC) with an eastward transport of 22Sv, and in the northern summer EACC merges with the Somali Current. Studies of Duing and Schott (1978) using subsurface mooring in the Somali Current region during January-July of 1976 showed that the northward EACC and the southward Somali Current causes a confluence at 2-3°S and then flows eastward as ECC. Swallow et al., (1991) estimated the volume transport of ECC to be 22 Sv in the upper 300db during the winter season.

7.5.5. Leeuwin Current:

The Leeuwin Current is a tropical current, consisting of warm, low salinity water that affects Western Australia's coastal waters and wildlife. However, the Leeuwin Current flows southwards along the coast, before turning eastwards at Cape Leeuwin and then into the Great Australian Bight where its physical and chemical influences reach as far as Tasmania as shown in Fig.7.27.

The Leeuwin Current flows southward along the Australian coast against the prevailing winds. It is about 50 m wide, extends to a depth of 250 m and has a mean speed of about 30 cm/s with seasonal maxima of 60 cm/s. The direct observation of the Leeuwin current did not take place until 1970's, when an investigation was commissioned into the life cycle of the Western Rock Lobster. Off Australia during 1974-76 using satellite tracked buoys the flow pattern of the Leeuwin current was determined. Shipboard observations by Thompson (1984) identified poleward surface current along the west Australian shelf from 22°S t o 28°S (Fig.7.27) . The surface current was fresh, warm, low dissolved oxygen concentration and high in nutrients.

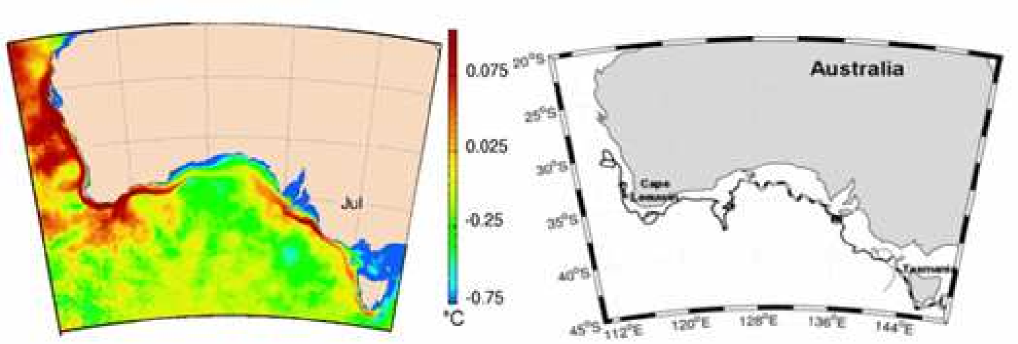

Fig. 7.27. Sea surface temperature anomalies in July: the current is visible by a narrow flow of warmer water. (Credits CSIRO Marine Research; http://www.aviso.oceanobs.com/index.php?).

Below the surface poleward flow, equatorward undercurrent was observed which was saline, high in oxygen concentration and low in nutrients. He pointed out that the winter cooling of the mixed layer allow the surface geopotential gradient to overcome the wind stress to drive the Leeuwin current against the local winds.

Godfrey and Ridgeway (1985) determined the annual mean and seasonal variability of the southward pressure gradient that existed between the warm and fresh Indonesian through-flow waters and cooler and saline water off the southwest Australia. They found that there was a southward pressure gradient throughout the year that reached maximum amplitude in May/June, when Leeuwin Current is the strongest.

The first large scale study of the Leeuwin current was undertaken during the Leeuwin Current Interdisciplinary Experiment (LUCIE). From the Current meter and CTD measurement of LUCIE, Smith et al. (1991) observed strong poleward flow between the surface and 250m within 100Km of the shelf edge with a poleward transport of 5 Sv except for January (figure B of Fig.7.28). A narrow equatorward undercurrent was also observed between 250m and 450m along the continental slope. They pointed out that the Leeuwin current depends on the alongshore pressure gradient of the eastern Indian Ocean and the seasonal variation in the strength of the current (Figure B of Fig.7.28) is due to the variation in wind stress and not due to the alongshore pressure gradient.

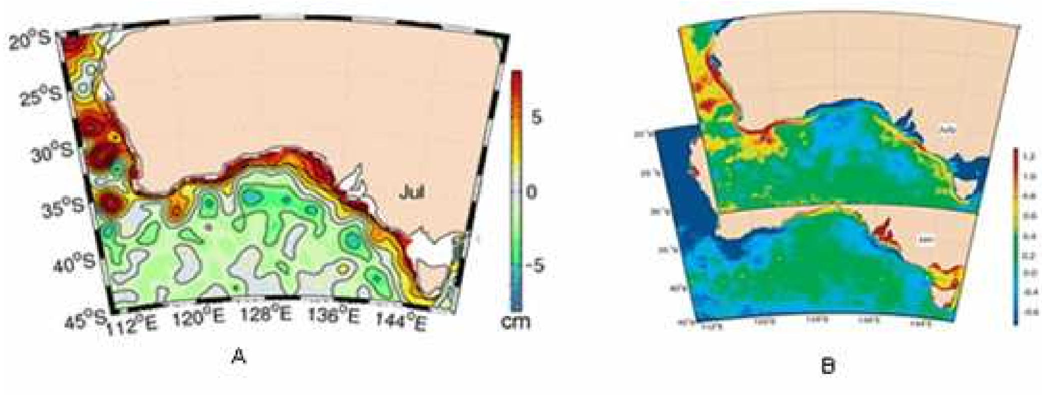

Fig.7. 28. Eddies associated with Leeuwin current (A-Left). Seasonal variation of Leeuwin current (B-right)

The Leeuwin Current was described from shipboard ADCP and moored current meter observations made during May June of 1993. The Leeuwin current was characterized by a broad (250Km), deep (440m), weak (0.2m/s) poleward flow with a transport of 4 Sv. An undercurrent of magnitude similar to poleward transport was also observed.

Using Topex/Poseidon (T/P) Altimeter data for 3 years during 1993-1995, the seasonal and inter-annual variability in the southeastern Indian Ocean was studied. The T/P data confirmed the presence of the alongshore pressure gradient maxima in May which act as the principal forcing mechanism for the Leeuwin Current that moves poleward against the prevailing equatorial winds. A secondary peak in pressure gradient was also detected in November which was not observed in the climatological data.

Fig.7.28 (Figure A) indicates that the Leeuwin current is associated with large number of eddies and it varies its strength seasonally with maximum in July and minimum in January.

7.5.6. Indonesian through-flow (ITF):

Currents flowing along the eastern boundary of the Indian Ocean are markedly different from those found in the eastern Pacific and Atlantic. The Indonesian Archipelago consisting of about 13,700 islands separate the seas of the southwest Pacific from the equatorial Indian Ocean. These islands form a 'leaky boundary' through which Pacific Ocean waters pass into the Indian Ocean (Fig.7.29). Fieux et al., (1994, 1996) carried out the first modern shipboard section observations across the exit region between Australia and Bali and reported a through-flow transport of 18.6 Sv ± 7 Sv from a ship section taken in August 1989. They also found negative transports of nearly -2.6 ± 7 Sv (Fig.7.29) from a similar section in March 1992.

In the upper 400m the transport was determined as 5 Sv with the reference level of 400m. When the reference level was extended to greater depths using climatological hydrography, the estimate increased to about 11 Sv.

Gordon and Susanto (1999) estimated a mean transport of about 5-15 Sv from annual means of moored current meter observations in the narrow Makessar strait. Little information was available on the deep structure from direct measurements.

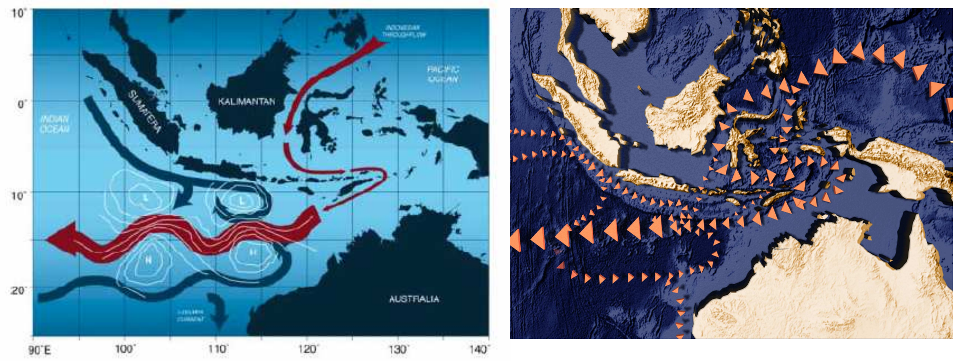

Fig.7.29. Indonesian throughflow. Large triangles depicts the positive flow path and small triangles show the negative flow path

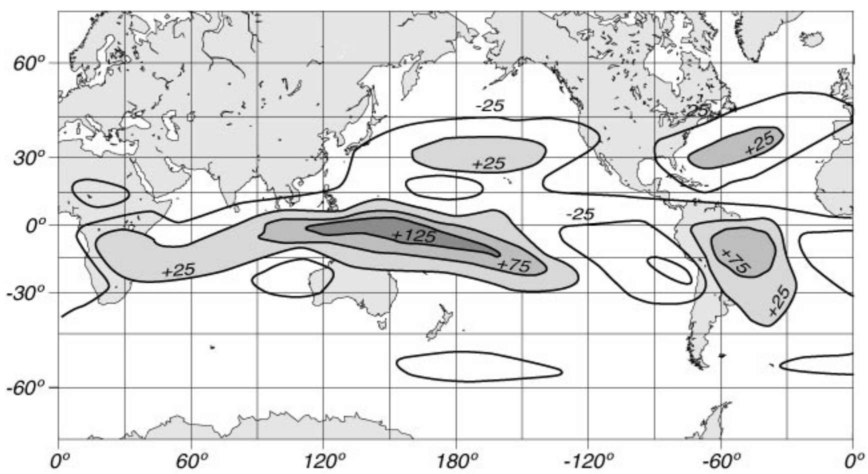

7.6. Recent developments in Indian Ocean Circulation:

The boundary of the Indian Ocean is unique in comparison to the Atlantic and Pacific, and it sets constraints on basin-wide circulation and heat-transport, giving the Indian Ocean a unique role in variability of the global climate system. If we see the geometry of the TIO, it is Closure in the north by the Asian subcontinent, opening to the Pacific through Indonesia, and a broad connection to the Southern Ocean which is the reason for a large and highly variable heat-gain by the tropical Indian Ocean. Import of heat by Indonesian Through-flow and three-dimensional, cross-equatorial export to higher latitude is the reason for the control of the heat gain in the north.

The resultant Indian Ocean heat pool is highly variable as a consequence of strongly interacting processes with time scales ranging from the intra-seasonal to the multi-decadal. At the seasonal time scale, cross-equatorial heat transport occurs in both the ocean and the atmosphere during the Asian Summer Monsoon. Ekman currents driven by south-easterlies south of the equator and south-westerlies north of the equator shift heat in the ocean-surface layer southward,

while northward flow in the thermocline feeds regional upwelling zones that cool the surface in the northern hemisphere. In the atmosphere northward propagating, seasonal to intra-seasonal variations carry latent heat northward into the zones of Monsoon rainfall. At the inter-annual time scale currents, Kelvin Waves and Rossby Waves shift the heat pool eastward and westward, changing the location of the sources of heat to the atmosphere. At the multi-decadal time scale the tropical Indian Ocean has warmed. Intra-seasonal Oscillation (ISO) events are thought to play a role in inter-annual to multi-decadal variations.

The spatial scale of Indian Ocean circulation that affects the tropical heat pool spans the width and breadth of the basin from Australia to Africa and from the Asian subcontinent to the Southern Ocean. Within this domain, key large scale processes are:

• Intraseasonal Oscillation and Madden Julien Oscillation: a weather-mode known for a long time in the atmosphere, which has a strong impact on seasonal climate in Monsoon regions. The ocean response was recently documented, but the feedback from ocean to atmosphere is still not understood, although it seems to be important in coupled models. The intra seasonal time scale has been observed throughout the Indian Ocean basin at a range of frequencies from 15 days to 60 days.

• Indian Ocean “Dipole Mode” or “Zonal Mode” a coupled ocean-atmosphere mode that develops like a “Bjerknes (1969)” feedback, during years when the seasonal Java-Sumatra upwelling is particularly strong. Oceanic, dynamical processes are clearly involved, but their role in formation of the zonal, basin-wide sea surface temperature pattern has not been adequately observed. The role of intraseasonal events in generating the mode needs a detailed study.

• Multi-decadal warming: Much of the Indian Ocean surface layer has warmed during the past 30 years, with a strong signal in the tropics. Activity at the intraseasonal time scale has become stronger during the warmer period. Historical oceanographic data is not adequate to track the trend in possibly related, subsurface, ocean dynamical properties. The ocean-atmosphere feedbacks and interactions at different time scales are not known.

• Shallow cross-equatorial exchange and upwelling: subtropical/tropical overturning cells associated with upwelling off Somalia, India, Arabia and Sri Lanka during the Asian Summer Monsoon. The overturning cell connects northern hemisphere upwelling to subduction in the southern subtropics. A reverse cell develops during Asian Winter Monsoon with upwelling (or a doming thermocline) along a broad zonal band in 5-10S. The role of these cells in the generation and maintenance of decadal to multidecadal sea surface temperature patterns is not known.

• Deep meridional overturning: circulation in the deep and abyssal ocean below 1000m extending into the tropics. The overturning cell connects subduction and mixing processes in the Southern Ocean to the deep thermocline in the tropics. A change in thermal structure may affect variability with shorter time-scales. While the heat transport of deep overturning is small, the cell is important in the estimation of future global warming because of the uptake of anthropogenic carbon in the deep and abyssal waters. Climate models predict large changes in the southern Indian Ocean in response to global warming.

The above large scale processes are all relevant in one way or the other to maintenance, variability and change in the tropical heat pool of the Indian Ocean at a range of time scales. Progress in understanding this system is critically dependent on development of the sustained

observing system. In addition to basin-scale processes, regional ocean-processes affect regional SST and, hence, probably affect regional climate.

The Indonesian Through flow (ITF) is a major choke point in heat transport of the global climate system. It is highly variable at a range of time-scales from intra-seasonal to decadal, in response to both local and remote forcing. Its variability is associated with large changes in the depth of the thermocline, mixed layer depth and SST. Located in the midst of the "maritime continent"—the most convectively active region in the world—the ITF is likely to have a profound influence on both local and global climate. The INSTANT (International Nusantrara Stratification and Transport) Experiment is a multinational process study to directly measure the ITF and understand its dynamics. The study will identify proxy-measures of ITF that can be sustained in the long term, and that will eventually become part of the Indian Ocean Observing System.

The Arabian Sea has been a focal point for regional oceanographic studies for decades because of its intrinsic oceanographic interest—strong Monsoon forcing, a strong and variable western boundary current, an upwelling zone with distinctive variability (e.g. the Great Whirl and cold water-wedges), a monsoonal equatorial current system, and circulation at intermediate depths naturally tagged by the Red Sea outflow. These features were the object of intensive observational studies and advances in dynamical understanding during WOCE (World Ocean Climate Experiment). The Arabian Sea is also a region of high evaporation and is a source of latent heat and moisture to the atmosphere. The challenge for CLIVAR (Climate Variability experiment) is to incorporate the WOCE legacy into ongoing climate research, even if the specific oceanographic phenomena are not known to be part of Monsoons. In contrast to the Arabian Sea the importance of the Bay of Bengal for Monsoon research has been recognized and has been the focus of process studies to understand regional air-sea interaction.

The south-western Indian Ocean is the primary outflow region where export of cooler waters can balance heat intake in the tropics and the mass transport of ITF. The Agulhas Current and southward flow in Mozambique Channel are the western boundary currents. Regional sea surface temperature has a statistical impact on African climate but the mechanisms of temperature variability in this region are not known.

The south-eastern Indian Ocean is unique because of the poleward flowing Leeuwin Current (Fig.7.30), which is another effect of the open boundary to the Pacific Ocean north of Australia. Heat and freshwater transports have an impact on regional climate in Australia.

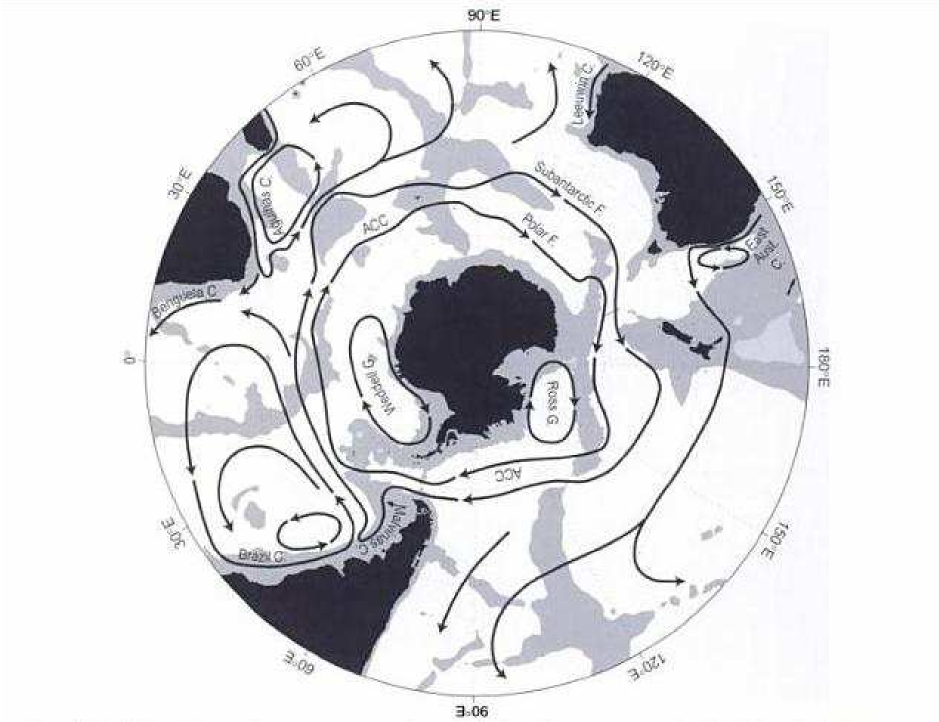

Fig.7. 30 . Currents in the southern ocean south of 20°S. The two major systems of Antarctic circum polar current (ACC), the subantarctic front (west wind drift) and the Polar front (east wind drift)are shown. F ,C and G denote respectively are front, current and Gyre. The light shading denotes the depth less than 3500m.

The above basin-scale and regional processes are research-themes all relevant to understanding how the Indian Ocean gets rid of its excess heat gain in the tropics through variability with a broad range of time scales. A sustained observing system in the Indian Ocean is needed to address this issue. Further development of the system requires a multinationally coordinated deployment of the resources identified at the Mauritius Conference. A lesson learned in WOCE is that we don't have enough resources to close the basin-scale heat budget in the face of strong variability and a complex set of basin-scale and regional processes. The challenge for developing the future observing system is to monitor a carefully selected subset of the properties of the Indian Ocean with time series long enough to see the full range of climate variability, and in sufficient detail to know if Indian Ocean models adequately represent the key processes and phenomena that affect the heat budget. Selecting the properties to be measured will be an important task for Indian Ocean oceanographers. An implementation plan agreed by all parties will be required to achieve the measurements.

7.7. Water masses of Indian Ocean:

In the Indian Ocean the information on the water mass structure has improved significantly due to the IIOE and subsequent oceanographic expeditions. The water masses of the north Indian Ocean (separated by a hydrological front near 10° S) are quite different from those in the north Atlantic and north Pacific, because of closure of the Indian Ocean on the northern side by the Asian landmass and monsoon climate and the associated changes in current pattern. A brief account of the characteristics of water masses in the upper 1000 m of the TIO is given below.

In figures below different water masses of the Indian Ocean are shown in sub surface level as 1 to 4 (Fig.7.31). They are serially as surface (upper), intermediate, Deep and bottom waters. Intermediate waters are Antarctic Intermediate water (AIW) and Red sea water (RSW), Deep waters are North Atlantic Deep water (NADW) and Indian Deep Water (IDW) and Bottom Waters are Circum Polar Bottom water (CBW) and Antarctic Bottom water (ABW). Green arrows indicate the flow from Low latitude to high latitudes and the red arrow indicate the flow from High latitude to Low latitudes. This implies that the origin of bottom water in low latitudes is from High latitudes.

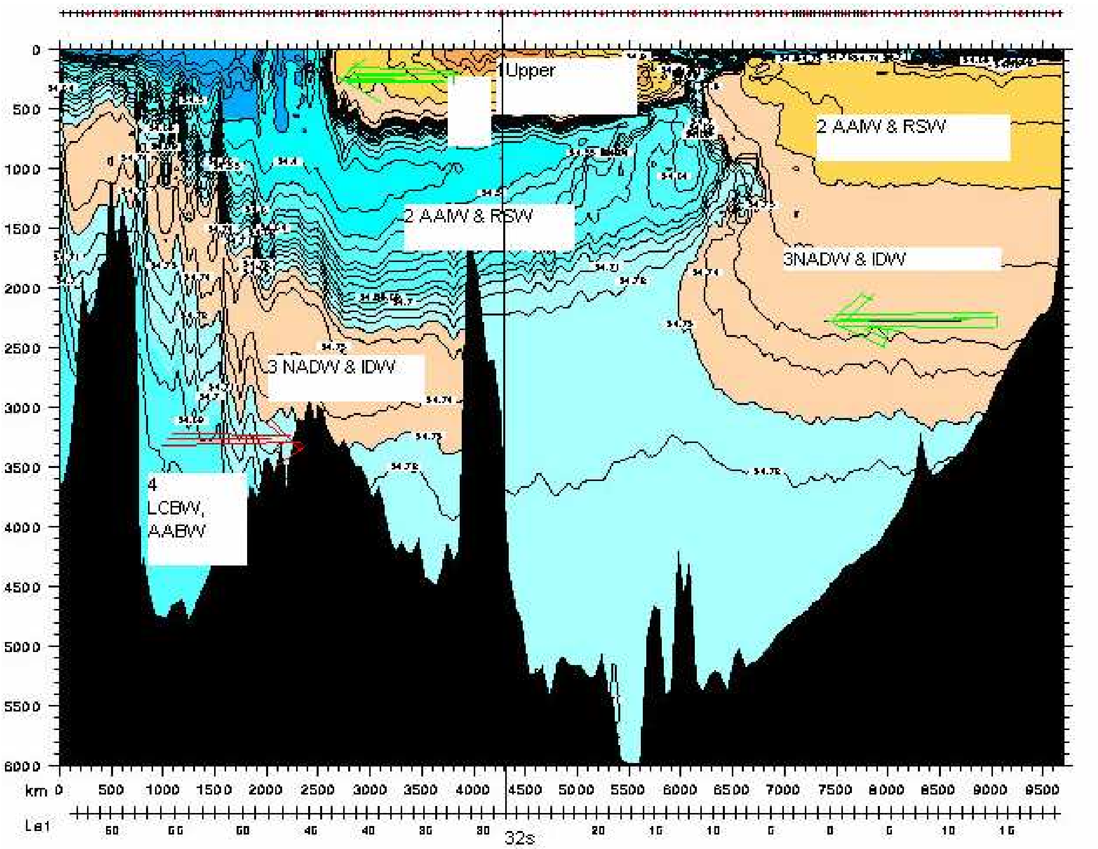

Fig.7. 31 Occurrence of different water masses in Indian Ocean.

Upper water is Indian Central & Equatorial Water (IEW), Intermediate Waters are Antarctic Intermediate Water (AIW) and Red Sea Water (RSW), Deep Waters are North Atlantic (NADW) & Indian Deep Water (IDW), and Bottom Waters are Antarctic Bottom Water and Lower Circumpolar Bottom Water (LCBW). The different water masses and their overturning principle involved in the southern Ocean are shown in Figure (7.32a) from which they spread into Indian Ocean.

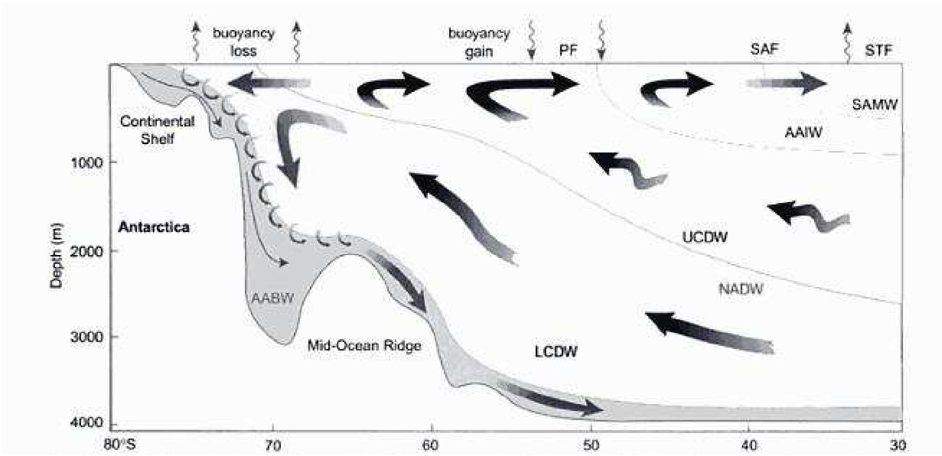

Fig.7. 32a. Meridional overturning circulation in the southern ocean. An upper cell is formed primarily by northward Ekman transport beneath the strong westerly winds and southward eddy transport in the UCDW layer. A lower cell is driven primarily by formation of dense AABW near the Antarctic continent. The abbreviations are PF- polar front, SAF-sub antantarctic front, STF-subtropical front, AAIW- Antarctic intermediate water, UCDW- upper circum polar deep water, NADW-north atlantic deep water, LCDW-Lower circumpolar deep water, AABW- Antarctic Bottom Water (From Speer et al 2000)

Water mass formation by deep convection occurs in regions with little density stratification (ie mostly in polar and subpolar regions). When the water in the mixed layer gets denser than the water below, it sinks to great depth, in some regions to the ocean floor. The density increase can be achieved by cooling or an increase in salinity (either through evaporation or through brine concentration during freezing) or both.

The driving force for the thermohaline circulation is water mass formation. Water masses with well-defined temperature and salinity characteristics are created by surface processes in specific locations; they then sink and mix slowly with other water masses as they move along. The two main processes of water mass formation are deep convection and subduction. Both are linked to the dynamics of the mixed layer at the surface of the ocean; so it is necessary to discuss thermohaline aspects of the upper ocean first.

Water mass formation by subduction occurs mainly in the subtropics. Water from the bottom of the mixed layer is pumped downward through a convergence in the Ekman transport and sinks slowly along surfaces of constant density (Fig.7.32b).

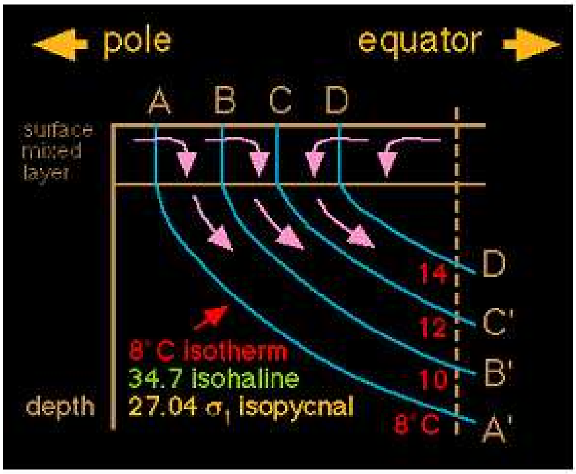

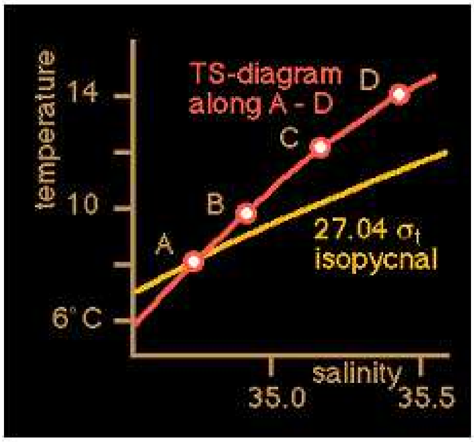

Fig.7.32b. Sketch of water mass formation by subduction.

First diagram of Fig.7.32b (A) shows the convergence in the Ekman layer (surface mixed layer) forces water downward, where it moves along surfaces of constant density. The 27.04 σ_t surface, given by the TS-combination 8°C and 34.7psu, is identified. The second diagram of Fig.7.32b (B) shows a TS- diagram along the surface through stations A - D which is identical to a TS-diagram taken vertically along depths A´ - D´.

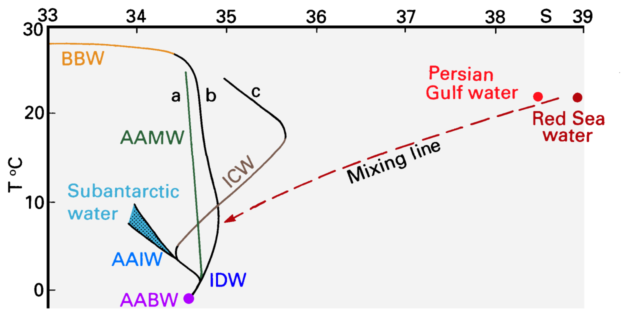

Fig.7. 33 . T-S diagram showing the source water masses for the Indian Ocean and their effect on the temperature - salinity structure in different regions.(www.indianocean.free.fr/ref.2.html # tomczak)

.

Figure 7.33 shows T-S graph describing different water masses of the Indian Ocean. Curve ***a*** is representative for the region between Australia and Indonesia (120°E), curve ***b*** for the Bay of Bengal (88°E) to 10°S, curve ***c*** for the subtropics south of 10°S. Intrusions of Red Sea and Persian Gulf Water can produce departures from the T-S curves near the isopycnal surface σ_t = 27.2 (the "mixing line").The abbreviations are AAMW: Antarctic Mode water, ICW: Indian Central water, IDW: Indian deep water the rest are as mentioned above.

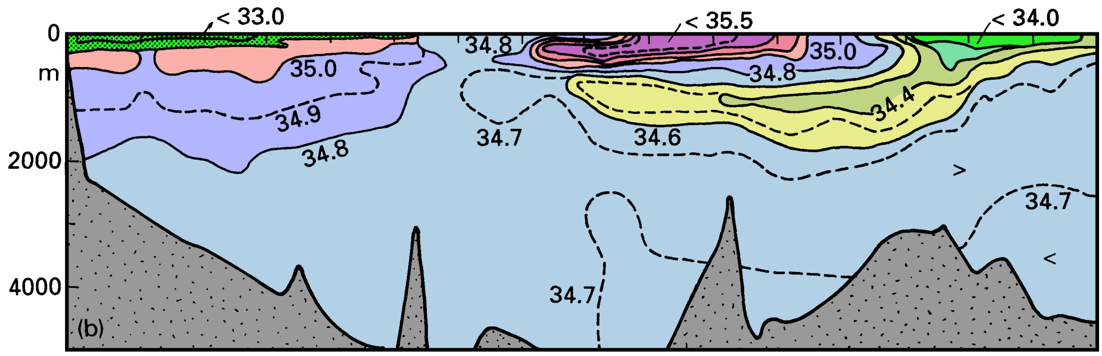

Fig.7.34. A Salinity section across the Indian Ocean along approximately 95°E. From Wyrtki (1971).

Fig.7.34 gives the salinity of different water masses as mentioned in Fig.7.33. Three distinct saline water masses namely, the Arabian Sea High Salinity Water (ASHSW), the Persian Gulf Water (PGW) and the Red Sea Water (RSW) were documented first by Rochford (1964). The thermohaline characteristics and core depths of these high salinity waters in the Arabian Sea are given in the following table (adapted from Prasanna Kumar and Prasad, 1999).

Water mass	Temp (°C)	Sal (PSU)	σ_t (Kg m^{-3})	Depth (m)
ASHSW	24-28	35.3-36.7	22.8-24.5	0-100
PGW	13-19	35.1-37.9	26.2-26.8	200-400
RSW	9-11	35.1-35.7	27.0-27.4	500-800

The Fig.7.35 indicates the approximate boundaries of the different water masses of the three major oceans of the world. The central water masses are formed and spread at the subtropical convergence which is indicated by the squares while the Antarctic Intermediate water is formed and sink at Sub Antarctic convergence and the Antarctic bottom water is formed and spread from the sills of Antarctic continent.

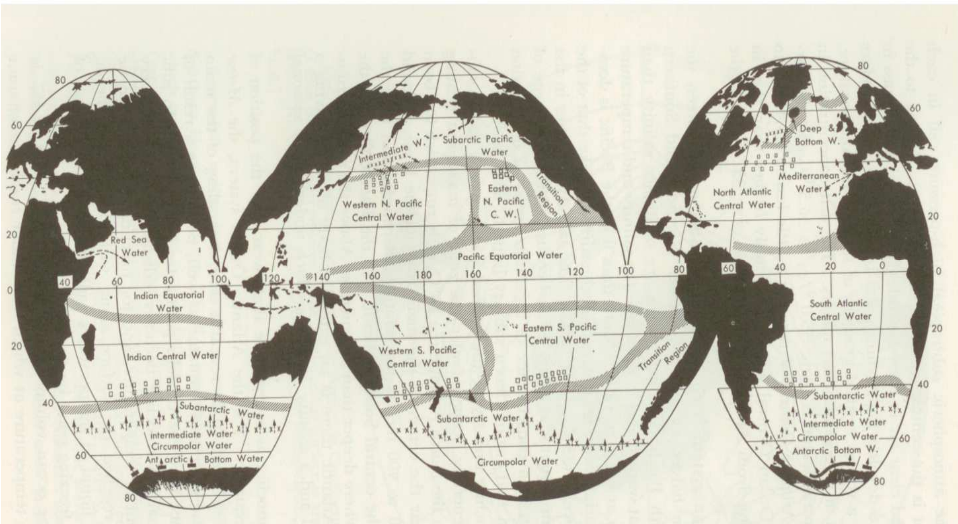

Fig.7. 35. Approximate boundaries of the upper water masses of the Oceans. Squares indicate the regions in which the central water masses are formed; crosses indicate the lines along which the Antarctic and Arctic intermediate waters sink (after Sverdrup etal., 1942)

7.7.1. Water character of equatorial Indian ocean:

Sharma (1976) said that the equatorial Indian Ocean water acts as a barrier to transequatorial movement of water masses in the Indian Ocean. He estimated the volumes of water in bivariate classes of potential temperature against salinity along 5°N, the equator and 5°S (Fig.7.36 a to c)). According to him the water south and along the equator is the most homogeneous and that of the northern side is the most heterogeneous. The influence of the Persian Gulf water is insignificant even in the northern side. There is no large flow of the Red Sea water across the equator except very near the African Coast.

The three regions can be compared with regard to the number of frequencies enclosed by the 75% and 90% boundaries.

Region	75%	90%
Northern	16	30
Equatorial	12	19
Southern	12	29
Combined	20	29

The 75% boundary reveals the northern region to be the most heterogeneous and the 90% boundary indicates the equatorial water to be the most homogeneous. It is interesting to note that the 75% boundary of the southern region constitutes only 12 frequencies while the additional 15% accounts for 17 frequencies probably because of different water masses from the east and south. In the upper layers of the northern region, high salinity water of the Arabian Sea and low salinity water of the Bay of Bengal are distinctly separated from moderately saline equatorial Indian Ocean water. One striking feature of the northern region is the bimodal distribution brought about by the 75% boundary. The primary mode at 3.5° C, 34.85‰ and 35 cl/t represents the deep water between 1,600 and 1,800 m. the secondary mode at 9.5° C, 35.15‰ and 90 cl/t is the consequence of the Red Sea water. The mode at 26.5° C, 33.35‰ and 680 cl/t within 90% boundary represents the surface water of the Bay of Bengal. In the equatorial region, the mode is the same as the primary of the northern region and in the southern region the mode at 2.5° C, 34.75‰ and 35 cl/t represents the circumpolar water.

Within the 90% boundary, there are five frequencies accounting for a total volume of 164×10^3 km^3 with salinity 35.25‰ in the northern region, while there is no frequency present within this boundary either in the equatorial or southern regions with salinity greater than 35.20‰. Of these two frequencies below 100 Cl/t with 9.0°C are essentially of the Red Sea origin and the other three are from the Arabian Sea.

In the univariate distribution of salinity at the right of the diagrams, the primary mode at 34.85‰ (Fig.7.36c) in the southern region is partly due to the equatorial Pacific Ocean water, and in the equatorial region the mode is at 34.95‰ (Fig.7.36b). But in the northern region there is no predominant primary mode and the salinityis widely scattered with almost uniform distribution between 34.80‰ and 35.20‰

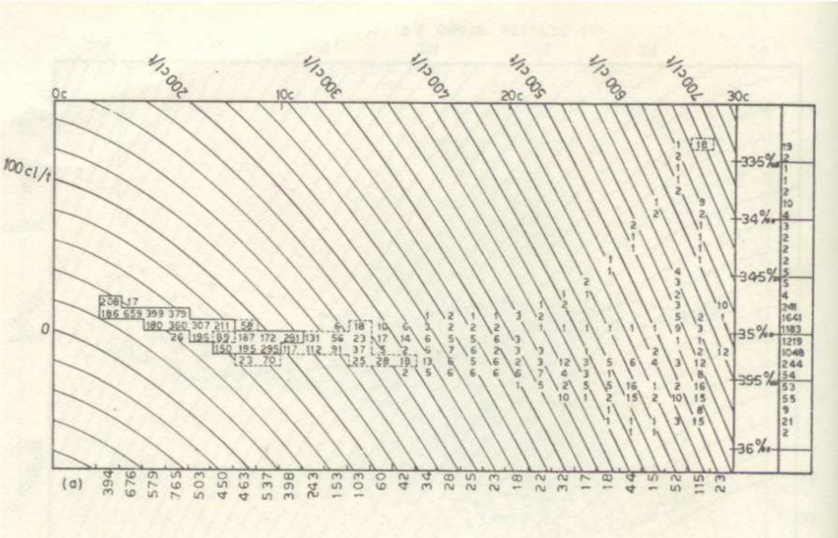
200 cl/t
300 cl/t
400 cl/t
500 cl/t
600 cl/t
700 cl/t
0c
10c
20c
30c
100 cl/t
0
33.5‰
34‰
34.5‰
35‰
35.5‰
36‰
(a)

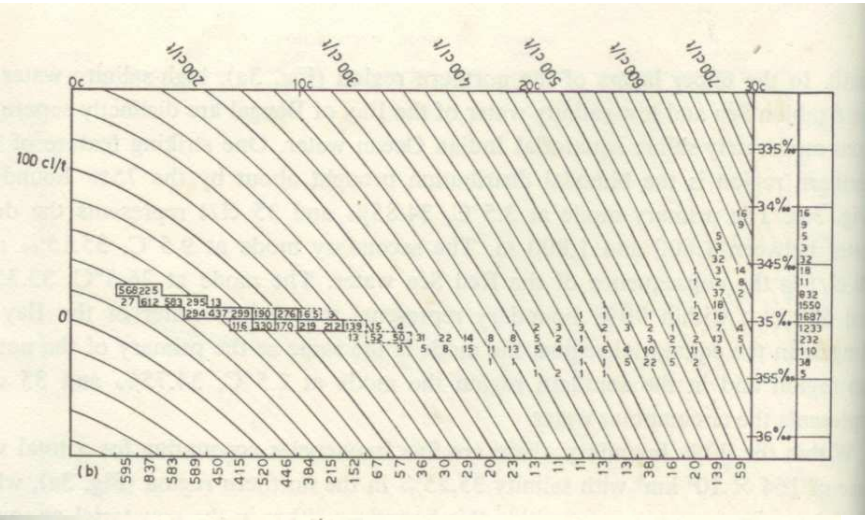
200 cl/t
300 cl/t
400 cl/t
500 cl/t
600 cl/t
700 cl/t
0c
10c
20c
30c
100 cl/t
0
33.5‰
34‰
34.5‰
35‰
35.5‰
36‰
(b)

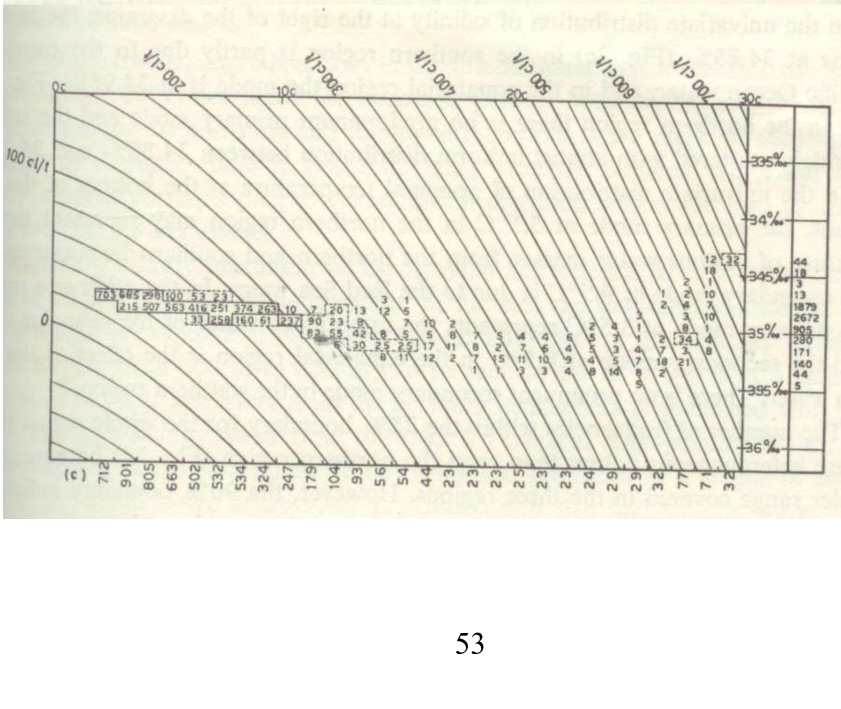
200 cl/t
300 cl/t
400 cl/t
500 cl/t
600 cl/t
700 cl/t
0c
10c
20c
30c
100 cl/t
0
33.5‰
34‰
34.5‰
35‰
35.5‰
36‰
(c)

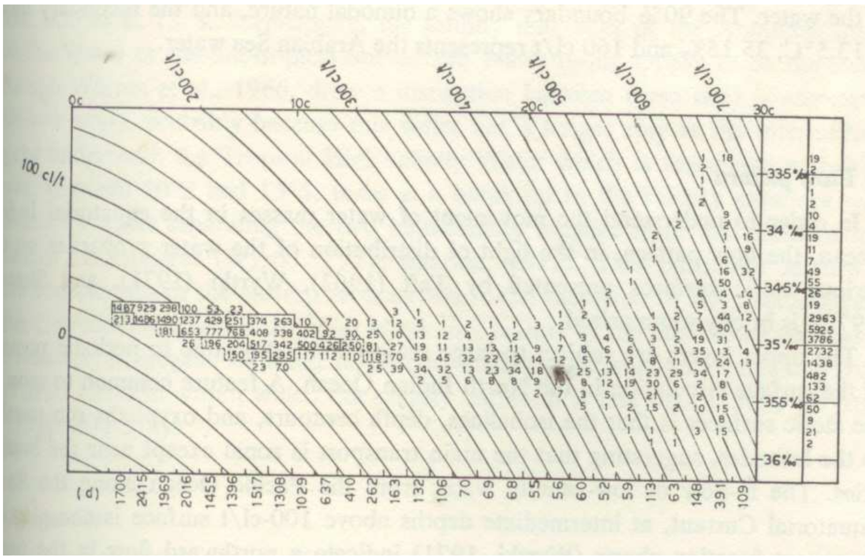

Fig.7.36. Frequency distribution in terms of 10^3 Km^3 of the upper 2000 m of water in each class of the potential temperature range of 1.0° c and with salinity range of 0.10‰. Solid line boundary encloses 75% of the total and dashed line boundary encloses 90%. Sums at bottom give the distribution by potential temperature and at right by salinity.

a) northern region between 50°E and 98°E, and 7°30'N and 2°30'N.
b) equatorial region between 50°E and 98°E, and 2°30'N and 2°30'S
c) southern region between 50°E and 98°E, and 2°30'S and 7°30'S
d) all the three regions combined between 50°E and 98°E, and 7°30'N and 7°30'S.

In the univariate distribution of potential temperature at the bottom of the diagrams, the primary mode at 5.5° C in the northern region may represent the admixture of various water masses from the northern and southern hemispheres and the secondary mode at 9.5° C is due to the Red Sea water. In the other two regions the primary mode at 3.5° C represents the upper deep water of the subpolar origin and the secondary mode at 8.5° C in the equatorial region is the effect of the Red Sea water. There is no prominent secondary mode in the southern region.

The number of frequencies within the 75% boundary for the whole region shows more heterogeneous nature than even the northern region (Fig.7.36d) because of the wider range covered in the three regions. However, the 90% boundary indicates a similar number of frequencies as those of the northern and southern regions. The mode at 4.0° C, 34.85‰ and 40 cl/t accounts for nearly 17% of the total volume of the water. The 90% boundary shows a bimodal nature, and the secondary mode at 13.5° C, 35.15‰ and 160 cl/t represents the Arabian Sea water.

7.7.2.Water masses in the Arabian Sea:

Sundararamam et al. (1968) studied water masses in the upper 500 m of the Arabian Sea using the hydrographic data collected during 1962 -1965. They traced PGW and Gulf of Oman Water in the upper 50 meters near the mouth of Persian Gulf and low saline Indus Water at 75-150 meters and RSW at 150-200 meters in the northern Arabian Sea. Arabian Sea High Salinity Water (ASHSW) shows salinity maximum at 75-150 meters in association with thermocline throughout the eastern Arabian Sea and spreads southward up to 8° N.

The ASHSW forms at the surface in the north Arabian Sea, where the evaporation exceeds precipitation. It builds up during May-July and stays more or less the same during August-October. It lies at the bottom of the Equatorial Surface Water (ESW), which forms due to high precipitation in the southern and eastern parts of the Arabian Sea (Darbyshire, 1967). Its

coverage decreases during November-January and lowest during February-April. The depth of salinity maximum associated with this water is shallowest (~ 20 m) in the northern Arabian Sea and is deepest (100 m) in the south (Shenoi et al. 1993) and generally increases from north to south and from west to east. The evaporation at surface exceeds precipitation in the Persian Gulf (average depth 25 m) by about 2 m annually. This leads to formation of a warm saline water mass namely, the PGW, which flows into the Gulf of Oman at depths of 25 to 70 m through the straits of Hormuz. In the Gulf of Oman the water sinks to 200 – 250 m depth (Shetye et al. 1994) and this water spreads in the northern Arabian Sea and the associated salinity maximum is found between 200 m and 400 m with deeper depths in the south. The area covered by the PGW is maximum during November-January and minimum during May-July (Shenoi et al. 1993). Varma et al. (1980) reported the presence of PGW at about 300 m depth and ASHSW around 60 m depth in the eastern part of northern Arabian Sea during February-April from an analysis of STD data. In the Red Sea too evaporation exceeds precipitation by over 2 m per year. The resulting RSW flows over the 110 m sill and enters the Gulf of Aden, and spreads in to the Arabian Sea. The northern extent of the salinity maximum associated with this water is approximately 18° N latitude and its depth increases from about 500 m in the north to about 800 m near the equator. These three high salinity water masses merge in the central Arabian Sea within a thick layer extending from 150 – 900 m depth to be known as the North Indian High Salinity Intermediate Water, NIHSIW (Wyrtki, 1973b). High salinity water with salinity range 35.5 - 36.8‰ and temperature range 24 - 30° C is termed as Arabian Sea Water (ASW) by Emery and Meincke (1986). The water mass between 100 m and 800 m in the western equatorial north Indian Ocean has been called the Indian Ocean Equatorial Water, IEW (Sverdrup et al., 1942). It is formed from mixture of the Indian Central Water (ICW) and the Australian Mediterranean Water, both of which form south of the equator. IEW and ICW have the same temperature range of 8.0 – 25.0° C but the Equatorial Water is some what less salty with a salinity range of 34.6 – 35.2‰, while the Central Water goes up to 35.8 ‰. IEW is a major subsurface water mass in the equatorial Indian Ocean and it extends from about 150-200 m depth to about 2000 m depth.

Waters at intermediate depths (500-1500 m) can be separated into those with a fresh water signature and those that are salty (Emery and Meincke, 1986). The salinity maximum associated with Red Sea – Persian Gulf Intermediate Water (RSPGIW) has a range of 34.8 - 35.4 ‰ and temperature range 5-14° C. The Antarctic Intermediate Water (AIW) with salinity range 33.8-34.8 psu and temperature range 2-10° C is present below the ICW in the south Indian Ocean.

7.7.3. Water Masses in the Bay Of Bengal:

LaFond (1958) grouped the surface waters of the western Bay of Bengal into three distinct classes, namely, the Northern Dilute Water (NDW), the transition water and the Southern Bay of Bengal Water (SBBW). NDW forms as a result of large quantities of fresh water influx from the Ganges and Brahmaputra rivers and has density less than 19 σ_t . The transition water is a mixture of the NDW and the SBBW in the western Bay and has a density between 19 σ_t and 21 σ_t. The SBBW is the major source of surface water in the Bay with density between 21 σ_t and 22 σ_t. Varkey et al. 1996 identified the low salinity surface water as the Bay of Bengal Low Salinity Water (BBLSW), which appears in the northern Bay and Andaman Sea and is formed as a result of great dilution. He assigned thermohaline indices for the BBLSW as T=27° C, S=33 ‰ and $\sigma_t \sim 21.2$ in the northern Bay. The surface layer with freshwater component having salinity range from 35.0‰ down to 28.0‰ and temperature range 29-25° C is termed as Bay of Bengal Water (BBW) by Emery and Meincke (1986).

Rao and Jayaraman (1968b) have identified two water masses in the upper 100 m of the central and southern Bay of Bengal during the transition period between winter and summer namely, (i) A low salinity water mass characterized by salinity < 33.0‰ and σ_t < 21.0 in the upper 50 m of the eastern Bay and the Andaman Sea named as the Eastern Dilute Water of Indo-Pacific origin, considered to be formed by the admixture of the runoff from the Burmese coast with the less saline waters of Pacific region entering the southeastern Bay through the Straits of Malacca, (ii) Another water mass which resembles the SBBW with salinity range 33.0-34.0‰ and σ_t range 21.0-22.0 in the upper 100 meters of the southern Bay and the western and middle parts of the Central Bay. Below 100-150 m depth, they encountered the IEW as the major subsurface water mass in this region.

The subsurface saline (> 35.0‰) layer was identified as Intermediate High Salinity Water (IHSW) of the Bay of Bengal (Varkey et al. 1996), which represents the Indian Equatorial Intermediate Water (IEIW) identified by Gallagher (1966) to have been formed as a result of mixing between high salinity waters from the Arabian Sea present in the central and southern Bay at depths grater than 100-150 m up to 1000 m with temperature range 15-5° C and salinity nearly constant (35.02 – 35.1‰). ASHSW was identified at subsurface depths (50-100 m) in the southern Bay towards equator (Suryanarayana et al., 1993). The presence of PGW around 26.81 σ_t, RSW around 27.19 σ_t and ESW around 22.5 σ_t in the Bay of Bengal was reported by Varkey and Sastry (1992).

The tropospheric water masses in the Bay of Bengal according to Varkey and sastry (1992) are i) Bay Bengal Low salinity water (BBLSW) around σ_t = 20.8 ii) Arabian Sea High salinity Water (ASHSW) around σ_t = 23.92 iii) Water mass E around σ_t = 23.94 iv) Persian Gulf Water (PGW) around σ_t = 26.81 v) red Sea Water (RSW) around σ_t = 27.19 and vi) Equatorial Surface Water (ESW) around σ_t = 22.5

Detailed studies of water masses of the Bay of Bengal were non-existent before the IIOE. La Fond (1958) grouped the surface waters of the western Bay of Bengal into three distinct classes, viz., the Northern Dilute Water (NDW), a Transition Water (TW) and the Southern Bay of Bengal Water (SBBW). The NDW was considered to have been formed as a result of large quantities of fresh water influx from the rivers Ganges and Brahmaputra. In terms of σ_t, the density of the water is less than 19 σ_t. The transition water (TW) is a mixture of the NDW and the SBBW in the western Bay and has a density between 19 σ_t and 21 σ_t. The SBBW is the major source of surface water in the Bay of Bengal with its density between 21 σ_t and 22 σ_t. However, it can be observed along the east coast of India as it is carried north by the northeast coastal current. It is apparent that these results are limited to the Bay alone. Gallagher (1966) pointed out that the subsurface waters of the Bay of Bengal are very uniform in all parts north of 5°N and can be identified as the Indian Equatorial Intermediate Water (IEIW). Furthermore, he stated that this water penetrates into the Bay at depths greater than 100-150m. In the central and southern Bay of Bengal, this water mass is present up to 1000m with its temperature decreasing from 15°C to 5°C and the salinity remaining nearly constant (35-35.1psu). He suggested that IEIW is formed as a result of mixing between high salinity waters from the Arabian Sea and the North Indian Ocean Deep Water (NIODW). Rao and Jayaraman (1968b) identified Eastern low salinity waters of Indo-Pacific origin in the upper 100m and Indian Ocean Equatorial Water (T = 4°C- 16°C, S = 34.8-35.2 psu) below 100-150m in the southern Bay of Bengal during Feb-March. Scherbinin (1969) studied the structure of water masses in the equatorial Indian Ocean. Sharma (1972) showed a salinity of 35.0psu on 200 cl/t surface appearing at 250m in the south central Bay of Bengal during summer season. This corresponds to the IEIW. Maslennikov (1973) noted that the surface waters of the Bay of Bengal and the Andaman Sea could be regarded as a single

type due to identical conditions of formation. He identified the penetration of waters from the Arabian Sea into the Bay characterized by high salinity. It was found also that the vertical water structures in the Bay of Bengal and Andaman Sea are similar up to 700-800.

Varkey (1986) studied in detail the water masses in the Bay during the winter. Figure (7.37)below shows some typical T-S diagrams in selected areas like a) south western Bay (5-10°N, and 81°-89°E), b) East Equatorial Indian Ocean (92°-97°E), c) S = 34.6 psu is envisaged as a mixture of BBLSW at the surface and IHSW at intermediate depths.

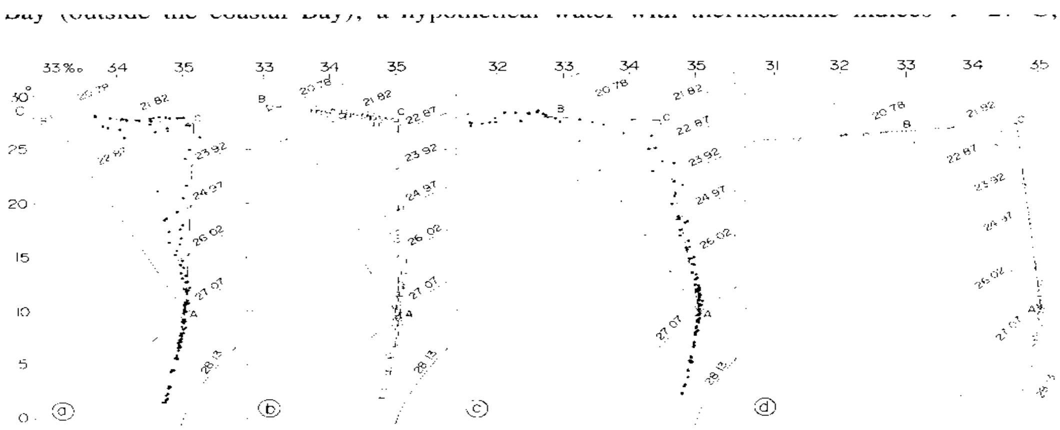

Fig.7.37. Typical T-S diagrams for areas (a) Southwestern Bay of Bengal (b) East Equatorial Indian Ocean (c) Andaman Sea and (d) North Western Bay of Bengal (adapted from Varkey, M.J.(1986)

Wyrtki(1961), Rochford (1964) and Suryanarayana et al.(1993) have identified the ASHSW at subsurface depths (50-100m)in the southern Bay towards the equator. It is also understood that ASHSW does not appear in the central Bay (15°N) and eastern Bay (91°E) during the winter monsoon. However, its penetration in the depth range of 75-425m can be seen between 12-14°N and 87-89°E during the summer monsoon and can be influenced by the surface divergences and gyres. Wyrtki (1961, 1971), Rochford (1964), Rao & Jayaraman (1968a) and Varadachari et al., (1968b) also noticed a high salinity (>35.0‰) water mass in the intermediate depth range of the Bay of Bengal and attributed this to the penetration of saline PGW and RSW at different depths greater than 200m during different seasons. Murty etal.(1992) and Suryanarayana et al.(1993) observed a layer of high salinity water (35.0-35.1‰) in the depth interval of 200-900m between 26.0 σ_t and 27.4 σ_t isopycnals with its salinity decreasing marginally towards the northern Bay. It has been suggested that this intermediate nearly isohaline layer was the result of penetration of a similar isohaline layer (35.7 ‰) in the depth interval 250-800m, which formed along the Arabian Coast in the Arabian Sea and was itself the result of high salinity mixing of PGW and RSW (Premchand 1981, Sastry et al. 1985, Premchand et al. 1986). The salinity of the isohaline layer in the Arabian Sea gradually decreases as it moves away into the eastern Indian Ocean (Premchand et al. 1986). The thickness of the Intermediate High Salinity Water (IHSW) layer fluctuates in the western Bay of Bengal. During the summer monsoon, the salinity of the IHSW is high and reaches up to 35.1‰ at 8°N, 87°E and appears as large number of cells in the western and eastern Bay of Bengal (Fig.7.38) which indicates the seasonal variation of thickness and salinity of this layer. The IHSW is also noticed in the Andaman Sea during the winter monsoon. The maximum salinity of this layer is found to be 35.06‰ in the southern region.

At depths greater than 1500m, north Indian deep water (NIDW) spreads into the Bay of Bengal. This water mass is formed by mixing Arabian sea Intermediate Water (ASIW) with Indian Ocean Bottom Water (IOBW) which has temperature between 1.6-2.8°C,salinity between 34.68-34.78‰ and oxygen between 3.18-4.17ml l^{-1} (Gallagher 1966). While the deep water - temperature (4.8°C) and salinity (34.9‰) are nearly uniform in the Andaman Sea, the salinity in Bay of Bengal decreases to 34.74‰.

Sewell (1932) showed that the eastern drift of the Antarctic Bottom Water (ABW) was first towards northwards between Carpenter's Ridge and the Andaman-Nicobar ridge then it established a cyclonic flow in the Central Bay of Bengal. The western branch of the bottom drift moves towards the east coast of India and then northeastward up to the head of the Bay and form a clockwise flow in the eastern Bay of Bengal.

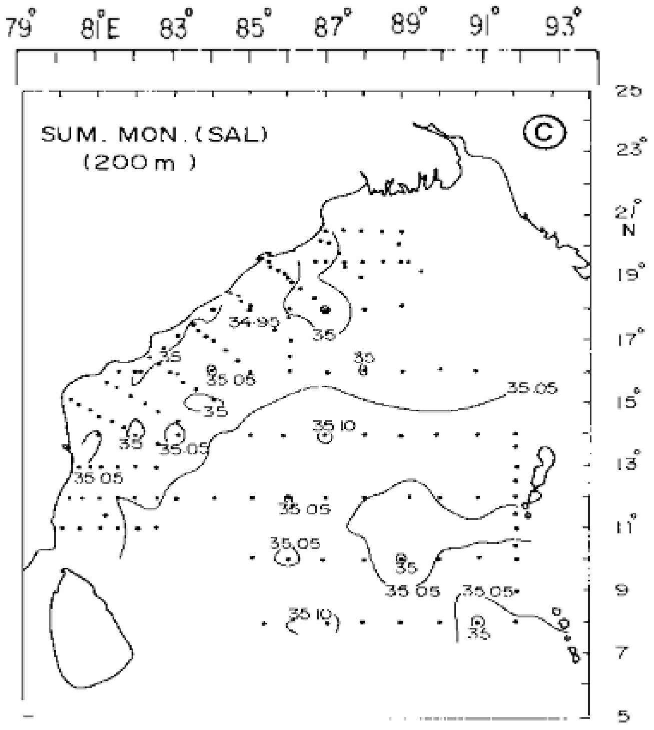

Fig.7.38. IHSW in Bay of Bengal during summer monsoon

Fig.7.39.shows the T-S plot for the Bay of Bengal during the southwest monsoon season of 1984.Region wise T-S plots for the Northern Bay (north of 15°N), the Central Bay (between 15°N and 9°N) and the Southern Bay (south of 9°N) together with the climatological T-S plot are shown in the inset map.

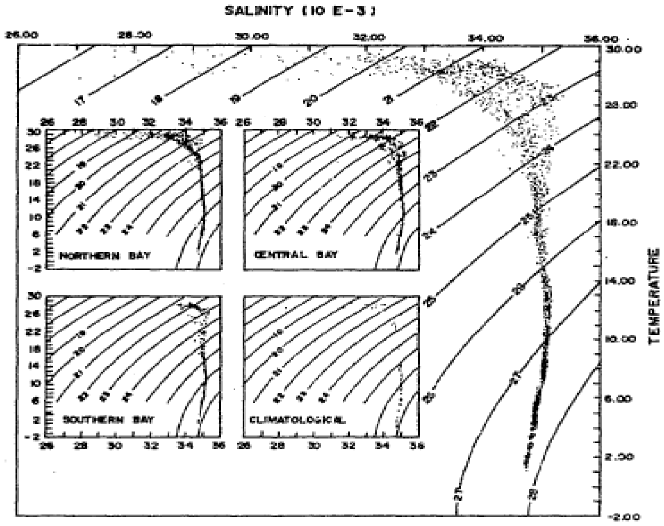

Fig.7.39. The T-S plot for the Bay of Bengal during the southwest monsoon season of 1984 (wyrtki 1971).

7.7.4.Water masses in the Gulf of Aden:

Based on the θ-S characteristics, four water masses have been identified in the Gulf of Aden (Fig.7.40). The Red Sea Water (RSW) that flows from the Red Sea is the most prominent water in the Gulf of Aden. This occupies about 37% of the total volume of the Gulf of Aden. The Gulf of Aden surface water (GASW) (3%) forms as a mixture of local water and the water from the western Arabian Sea during winter and Red Sea surface water during summer. The intermediate water, identified as Gulf of Aden Intermediate water (GAIW), occupies about 9% of the total volume of Gulf of Aden. A characteristic salinity minimum is associated it at $\sigma_\theta = 26.50$ kg m^{-3}. The northward spread of subtropical subsurface water from the south appears to be the major source of GAIW. The bottom water, named Gulf of Aden Bottom water (GABW), showed the least variability. It was formed due to the mixing of Red sea water and water of southern origin.

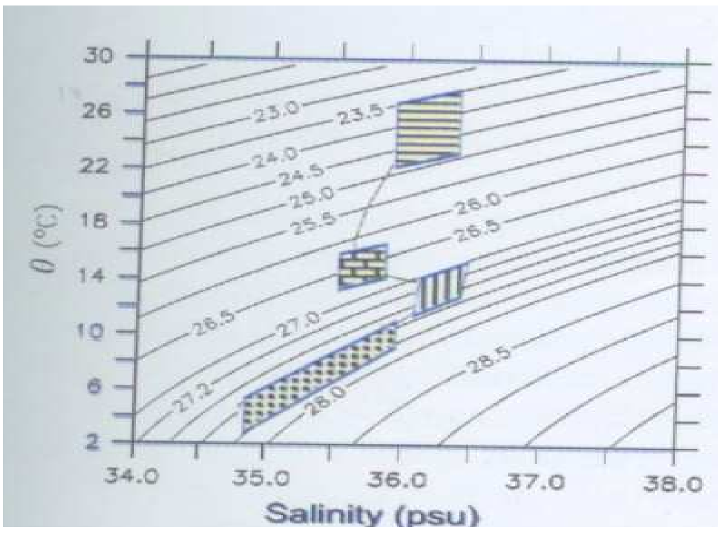

Fig.7.40. Typical θ-S curve of Gulf of Aden. Four water masses, RSW,GASW,GAIW and GABW are shown in hatching.

7.8. Global Ocean circulation:

There are two major processes in our description of ocean circulation: one is wind driven ocean circulation – this constitutes largely horizontal gyres in the upper ocean including main thermocline and the other is thermo-haline circulation driven by "small horizontal differences in density" – the main component of it is the vertical overturning of the whole ocean.

7.8.1 Global Thermohaline Circulation (THC) or the Global Conveyor Circulation:

The global thermohaline circulation, driven by fluxes of heat and fresh water at the ocean surface, is an important mechanism for the global redistribution of heat and salt and is known to be intimately involved in the major changes in earth's climate.

The thermohaline circulation is a very important process for heat transport within the ocean. Of the 5 PW of meridional heat transport required by the global energy budget, the ocean is estimated to carry 20 to 50% (and the atmosphere the remainder). At low and mid-latitudes most all of this heat transport is carried by the THC or the Meridional Overturning Circulation (MOC), whereby warm, surface waters replace cold, deep waters.

The literal meaning of thermohaline circulation (THC) is the circulation driven by temperature and salinity. Thus the THC is driven by cooling, evaporation and salinization caused by ice formation. While salinization increases density, heating and precipitation decreases density. The THC is much weaker than the wind driven circulation and so it is difficult to see its effect on currents in the upper ocean where the wind driven circulation is vigorous. In the deep ocean, the permanent circulation is dominated by thermohaline forcing. Because the THC is weaker than the wind driven circulation and because it inherently involves overturning, a common way to quantify it is to compute how much water in different layers is transported into and out of given areas. Thermohaline circulation links the Earth's oceans. Cold, dense, salty water from the North Atlantic sinks into the deep and drives the circulation like a giant plunger (Fig.7.41a).

Recently it has been coined as "the global conveyor circulation". There are (1) equator to pole differences in density and (2) pole to pole differences in density which drive the thermo-haline circulation. However this circulation is responsible for the observed vertical stratification of the ocean. Thus thermohaline Circulation is driven by horizontal density gradients. These differences in density in the deep ocean are very small (sigma-t varies by less than 0.1 kg/m^3 in deep ocean below 1 km.). The thermohaline circulation is a very slow circulation with average velocities about 1 mm/s, and overturning circulation of about $20\times 10^6\, m^3/s$ or 20 Sverdrups.

The driving of "present day" THC are due to:(i) Deep open ocean convection arising from intense cooling in limited areas of North Atlantic and Southern Ocean (especially Weddell Sea and Ross Sea). (ii) Overflow waters from Antarctic. These regions are very small in area when compared with global ocean. Production of "deep water masses" means that volume is displaced. Hence "all other water masses" are therefore displaced upwards. It takes 3000 years to fill the ocean with these deep water masses. Circulation time scale may be about 100-1000 years. We have downward motion in the N Atlantic 60^{o}N and Antarctica where the deep waters are formed, and upward motion in the remainder of the ocean. Diffusion of heat especially at low latitudes also is responsible to balance the production of deep water masses. Cooling at polar latitudes will produce dense water deep water masses (NADW) which will flow to lower latitudes, and compensated by a return flow towards polar latitudes of warmer less dense water.

In reality it is complicated by: (i) asymmetries in density between northern and southern hemispheres (ii) Most deep water production takes place in Atlantic Ocean and Lack of deep water production in the Pacific Ocean. These factors give rise to a global conveyor circulation, where the North Atlantic is the main source of dense water and a return flow of lighter thermocline waters towards North Atlantic.

A complex of globally interconnected ocean currents, collectively known as the Conveyor (Fig.7.41a), governs our climate by transporting heat and moisture around the planet. Broecker (1991) wrote "the Conveyor is the achilles heel of the climate system".

While the wind driven western boundary currents carry about 50-100 Sv, the global THC carry about 15-20 Sv. Though the THC is considerably less than the wind driven circulation, it is important because it connects all regions of the globe.

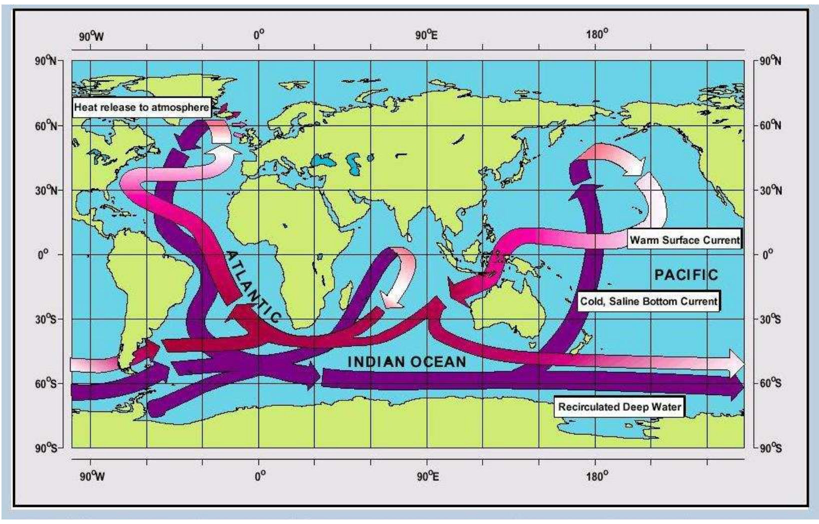

Fig.7.41 a. The conveyor belt- global ocean circulation pathways (after Broecker, 1991)

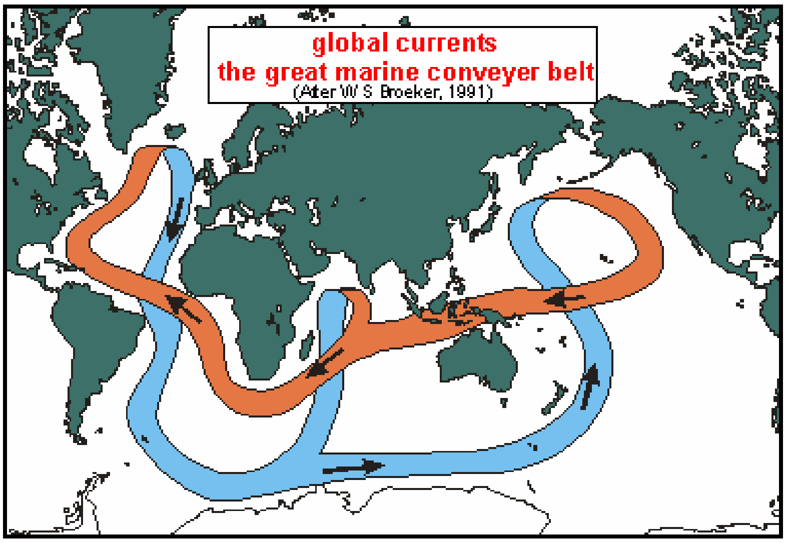

Fig.7.41b The Ocean plays a major role in the distribution of the planet's heat through deep sea circulation. This simplified illustration shows the conveyor belt circulation, which is driven by differences in heat and salinity. Records of past climate suggest that there is some chance that this circulation could be altered by the changes projected in many climate models, with impacts to climate throughout lands bordering the North Atlantic (Redrawn from Broecker, 1991) (www. Columbia.edu/cu/record/23/11/25c.gif)

Somehow the deep circulation and surface circulations must join up, a puzzle that plagued scientists for many years, leading to several hypotheses. The Figure 7.41b shows how the great marine conveyor belt is thought to work now. The orange part is the surface component, which fits into the surface currents shown above. Only in one place does the surface component dip down into the cold depths of the deep sea: south of Greenland, as also shown in the deep sea circulation diagram above. The cold bottom water then flows above the ocean floor to Antarctica, where some of it comes to surface (not shown), but most of the cold, nutrient-rich water will come to surface in two places: in the northern Indian Ocean and northern Pacific Ocean. Although this ocean conveyor belt moves slowly, it is massive, and plays a major role in the heat transfer of the planet. It certainly plays a major role in the circulation of nutrients from the depths of the oceans, back to the surface. It is speculated, that during ice ages, the belt is interrupted over Indonesia, due to ocean levels dipping more than 100 metres.

The global scale thermohaline circulation of the world ocean has been termed as the ocean conveyor belt (Fig.7.41 a & b), because it forms a continuous loop carrying water and its properties around the world (Gordon, 1986). A description may conveniently begin in the North Atlantic where the well known Gulf Stream carry warm and salty waters to the north. There the Arctic cold winds cause chilling. The resulting cold, salty and therefore dense water sinks to become immense southward flowing stream of North Atlantic deep water. Because of the earth's rotation, this deep ocean current hugs to the western edge of the Atlantic basin, running southward into the South Atlantic, where it joins with even colder, dense, and oxygen rich water sinking from the seas bordering Antarctica to form a pool of circumpolar deep water.

Two branches of the global circulation emerge from this Antarctic abyss (Fig.7.41b). One branch flows northward along the eastern coast of Africa to mix with

the waters of the Indian Ocean. The other continues around the eastern coast of Australia and then northward, eventually mixing upward with surface waters in the tropical and North Pacific. The surface waters in the pacific ocean then move equatorward, then westward, driven by the trade winds through the Indonesian archipelago, across the South Indian Ocean, around the Cape of Good Hope, and ultimately back into the equatorial Atlantic where the waters are taken up by the Gulf stream and begin another round trip of the world for a thousand year tour.

Today we know, the driving force of the Conveyor is the cold, salty water of the North Atlantic Ocean (Fig.7.41c). Such water is denser than warm, fresh water and hence sinks to the ocean bottom, pushing water through the world's oceans like a great plunger. The volume of this deep undersea current is 16 times greater than the flow of all the world's rivers combined, and it runs southward all the way to the southern tip of Africa, where it joins a watery raceway that circles Antarctica. Here the Conveyor is recharged by cold, salty water created by the formation of sea ice, which leaves salt behind when it freezes. This renewed sinking shoves water back northward, where it gradually warms again and rises to the surface in the Pacific and Indian oceans.

There are two global THC cells involving deep convection at high latitudes. They are the North Atlantic Deep Water (NADW) and the Antacrctic Bottom Water (AABW) cells in the (Fig.7.41c). The source regions are shown as yellow spots in fig.7.41c. These two global overturning circulations are interconnected.

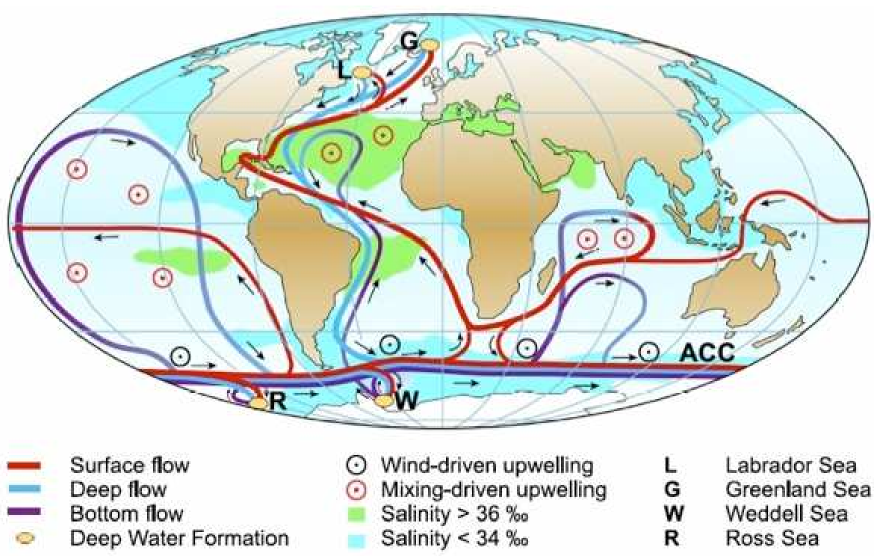

Fig.7.41 c. Global thermohaline circulation through two global over turning systems of the conveyor .

NADW and AABW are particular types of waters that can be recognized by their special properties such as salinity maximum (NADW) or extreme cold temperature (AABW). Besides

these two water masses there are several other water masses associated with overturning in different oceans.

The deep water in the NADW cell is formed in the northern North Atlantic. There are three northern North Atlantic sources. First is localized deep convection in the Nordic Seas, which lie north of the sills connecting Greenland, Iceland and Scotland.

This dense Nordic Sea overflow water (NSOW) reaches the bottom of the northern North Atlantic through Denmark Straight and flows westward and later southward following the continental slope. The second source is localized intermediate depth convection in the Labrador Sea Water (LSW).Together the LSW and NSOW form the deep western boundary current in the North Atlantic. At mid latitudes these waters are joined by those from the third source, which is the Mediterranean Sea.

The NADW in the South Atlantic joins the Antarctic Circumpolar Current (ACC) and flows eastward towards the Indian Ocean. As the NADW is carried eastward in the ACC, its high salinity gradually becomes fresher through mixing with other waters, but it remains recognizable as a high salinity water through the Indian and Pacific Oceans. Some of this high salinity water flows northward into the Indian and Pacific oceans, and is one of the two major components of the deep water for these oceans. In the Indian Ocean, the northward flow of deep water occurs in three regions, separated by mid ocean ridges. In the southwestern Indian Ocean, a branch of NADW flows northward into the region east of the Agulhas. In the Pacific Ocean, the main northward flow is just east of New Zealand, in the deep western boundary current described in the section on tropical circulation. This deep flow fills the South Pacific and moves northward through the Samoan Passage into the tropics and then into the North Atlantic.

Where does NADW upwell to eventually complete the circuit back to the North Atlantic? The NADW and the Antarctic Bottom Water after mixing and flowing into the deep Indian and Pacific Oceans form as Indian Deep Water and Pacific Deep Water. These both upwell into older deep water layers between 1500 and 3000 m depth in those oceans. The IDW and PDW re-enter the Antarctic Circumpolar current to dilute the fresh flowing NADW.

Some of the upwelled deep waters take part in the formation of the thick mixed layer waters just north of the ACC. This thick mixed layer is called Sub Antarctic Mode Water (SAMW) which is cold and fresh. This SAMW is modified by intermediate depth convection just west of Chile and becomes Antarctic Intermediate Water (AAIW). AAIW thus occupies all of the Southern Hemisphere oceans north of the ACC.

The second major over turning circulation is that of the AABW. The two primary sources of AABW are Ross and Weddell Seas. The formation of AABW is through brine rejection, which occurs during formation of sea ice. AABW also spreads northwards through the gyre circulations.

What is the warm water return path to the AABW source? As mentioned above, the water that is found at the surface in the Antarctic regions where AABW is formed is upwelled deep water from the ACC.

The magnitude of the currents associated with the NADW and AABW overturning circulations is about 5cm s^{-1}. The total transport of NADW out of the North Atlantic is about 15-20 Sv. The transport of AABW into the ACC is about 10-30 Sv.

The Fig.7.41d gives a complete description of flow paths of different water masses in different oceans at different levels. One can see from this description that the circulation is complete in each leg of the water masses in each ocean. For example, in the Indian leg at different layers starting from Circumpolar Deep Water (CDW) in the bottom serially lie one over the other are North Atlantic Deep Water (NADW), Indain Ocean Deep Water (IODW), Banda Intermediate Water (BIW) and Red Sea Water (RSW), Northwest Indain Intermediate Water (NIIW), Indian Surface Layer Water (ISLW). You may note all the deep and intermediate waters raise and goes back to the Antarctic Circum polar Current system (ACCS) at the specified depths as denoted by their densities or their T-S characteristics.

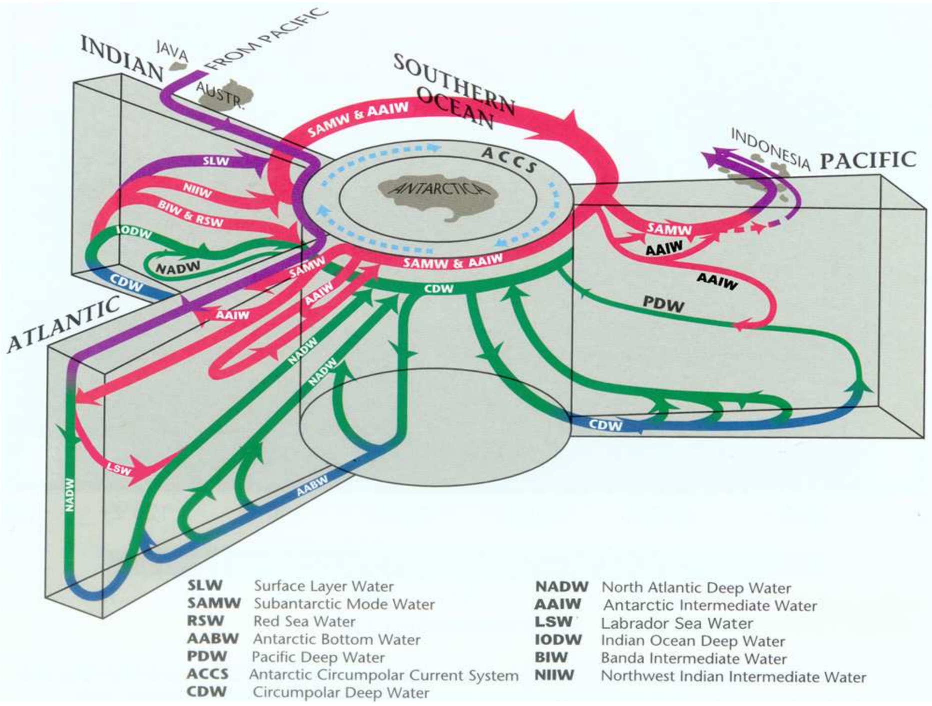

Fig.7.41 d. Flow paths of different water masses in different oceans at different levels.

That the thermohaline circulation has changed in the past has raised questions about how it might change in the future. Many of the coupled ocean-atmosphere model simulations of potential climate change during the 21st century project a slow down of the thermohaline circulation, with some indication that the likelihood and magnitude of the reduction in strength increase as the rate of change in CO_2 concentration increases. Such a slow down would reduce the amount of warming over Europe and the North Atlantic.

The idealized model of global bottom water circulation developed by Stommel (1958) is shown in Figure7.41e. He predicted an abyssal circulation driven by a uniform upwelling of deep water into the thermocline. As he perceived it, the upwelling is such that it balances the downward diffusion of heat through the thermocline. The Figure7.41e shows the abyssal circulation based on their simple theory. Notice that the interior flow is everywhere towards the sources of deep water. The Deep Western Boundary Currents which carry the deep waters equatorward, away from their source represented by thick curves. He said that because in low latitudes there is a net annual inflow of heat through

the surface into the water, the upper warm layer, and its boundary the thermocline, should deepen with time. As this deepening does not happen, some mechanism must be opposing. He suggested that this mechanism is slow upward flow of cool deep water. This means due to continuity requirements the sinking water in the North and South polar latitudes must be balanced by rising and spreading over most of the low and middle latitudes. He was also successful in getting the southward return Western Boundary Currents (WBCs) of the north ward bound WBCs at the surface as shown by thick curves in the Figure 7.41e.

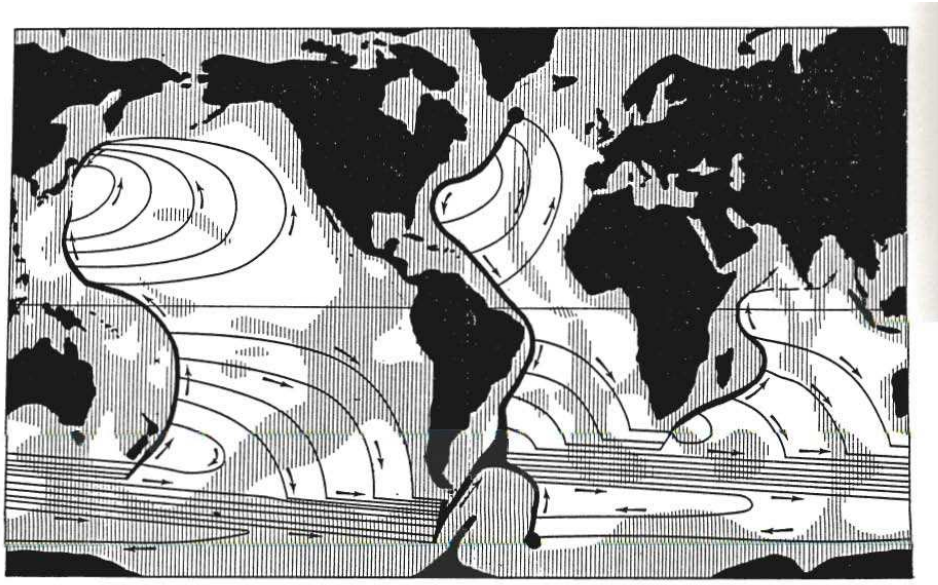

Fig.7.41e Stommel-Arons theoretical abyssal circulation (1958-1960)

7.9. GLOBAL SURFACE CIRCULATION

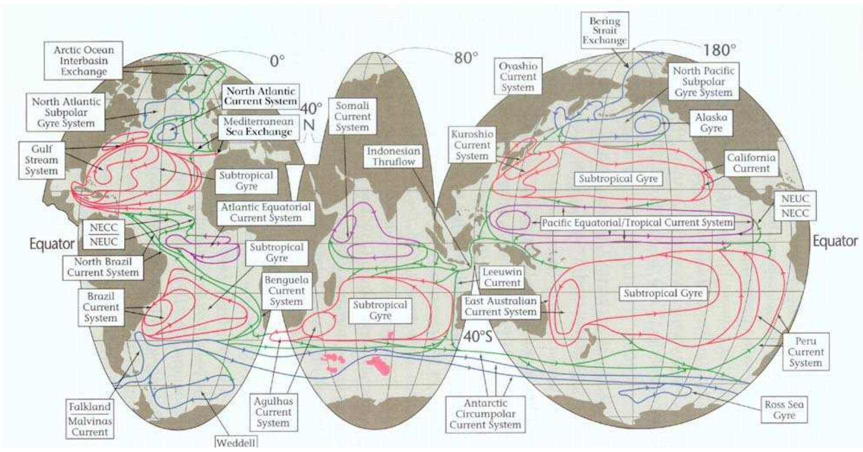

Fig.7.42. Surface circulation of global oceans

By seeing Figure 7.42 one can easily note the different current systems and the associated gyres or circulations. While generally equatorial and tropical circulations are warm the subpolar and polar circulations are colder. In every ocean we can consider three different current systems that make to form the circulations. They are i) equatorial current system, ii) western boundary currents and iii) the eastern boundary currents. All these three join to form the gyres. Thus a clock wise gyre in the Northern oceans and an anticlockwise gyre in the southern oceans form. These two gyres are known as the back bone of the circulation of the major oceans. The equatorial current system comprises of three main currents. They are the westward flowing North Equatorial Current (NEC), eastward flowing Equatorial Counter Current (ECC) and the westward flowing South Equatorial Current (SEC) and the eastward flowing Equatorial Under Current (EUC) at the depth of thermocline. While the NEC is always in north of the equator, the SEC is always south of the equator. However, all these currents migrate a few latitudes north and south between summer and winter.The western boundery currents are swifter than the eastern boundary currents due to increase of Coriolis force with increase of latitude.

As the low latitudes are the sources of heat and the subpolar and polar latitudes are the sources of sinks. The accumulated heat is to be transported quickly to the deficit latitudes. Thus the ocean and atmosphere together act as a big thermodynamic engine. So through currents and circulation in the oceans this heat is transported at the sea surface. As from low latitudes to high latitudes heat is to be transported, the tendency of currents will be towards north from the equator on either side of the hemisphere. So northward tending currents are warm currents and equatorward tending currents are cold currents.

The resultant currents formed in the oceans are driven by two forces one is density and the other is wind. The circulations will complete as closed loops at various places at various latitudinal belts depending on several factors. Mostly these are governed by surface wind and pressure belts at different latitudinal zones. As for example low latitude easterlies, mid-latitude westerlies and Polar easterlies. For example the equatorial gyres, the subtropical gyres and the sub polar gyres are common in all the oceans with some local sub gyres like Alaskan gyre etc. But the Indian Ocean is little exception to this general system. While the subtropical gyre is permanently present in the south Indian Ocean, it is not present in the north Indian Ocean as it has no subtropical latitudes and also North Indian circulation is controlled by the two monsoons and so reversal of circulation takes place semi annually as was discussed earlier.